

Lithostratigraphy and physical properties of the Chalk Group from Danish North Sea wells

A contribution to the Chalk Background
Velocity project

Peter Japsen, Finn Jacobsen & Torben Bidstrup



Lithostratigraphy and physical properties of the Chalk Group from Danish North Sea wells

A contribution to the Chalk Background
Velocity project

The Chalk Background Velocity project
is funded by the South Arne Group

Peter Japsen, Finn Jacobsen & Torben Bidstrup

Contents

1. Introduction	3
2. Lithostratigraphic subdivision	4
Introduction	4
Database	4
Lithostratigraphy	4
Intra-Chalk Unconformity.....	5
3. Formation pressure	12
Overpressure due to compaction disequilibrium.....	12
Effective depth for $\beta=1$	12
Chalk pressure data	14
4. Temperature	19
5. Acoustic properties	24
Comments to the cross plots for the individual wells	26
6. Data CD	36
Lithostratigraphic subdivision	36
Excel file with depth to individual boundaries in the wells.....	36
CGM files with cross correlation of log data.....	36
Acoustic properties	38
Power Point files with cross plots of log data	38
MatLab files with log data for the chalk sections in each well.....	39
7. References	40
Appendix 1: The main lithostratigraphic formations	42
Appendix 2: Cross plots of log data	46
Vp plots.....	47
Vp-Vs plots	104

1. Introduction

The present report is a contribution to the project "Variability of the chalk background velocity in the South Arne area". The project is funded by the South Arne Group (Amerada Hess Aps, Dong E&P, Denerco Oil) and the partners in the project are GEUS, DTU E&R, Ødegaard A/S and Gary Mavko (Stanford University).

The aims of the project are the following

- Quantification of how the chalk background velocity (the low-frequent velocity variations which define the absolute level of the chalk velocity) in the South Arne area is affected by effective stress, presence of hydrocarbons as well as porosity, composition, texture and cementation of chalk.
- Estimation of upper and lower bounds on chalk porosity estimated from seismic inversion based on the analysis of these factors.
- Evaluation of the usefulness of velocities estimated from seismic processing as a supplement to well log data for establishing chalk background velocity.

The present report documents various aspects of the Chalk Group in wells in the Danish North Sea: the lithostratigraphic subdivision of the chalk (29 wells), the temperature at the top and the base of the chalk, the formation pressure and the acoustic properties estimated from well logs (28 wells). Most of the wells are located in the northern part of the Danish Central Graben. Stratigraphic correlation diagrams, log data in MatLab format and PowerPoint files with cross plots of the log data are included on a CD.

2. Lithostratigraphic subdivision

Introduction

The Chalk Group in 29 wells has been divided into lithostratigraphic units (Figure 2.1). The subdivision follows the formal lithostratigraphic nomenclature for the Chalk Group (Isakson & Tonstad 1989; Surlyk *et al.* 2003) and includes the Ekofisk, Tor, Hod, Blødøks and Hidra Formations (Figure 2.2).

The basis for the subdivision is the bio- and log-stratigraphy provided by the drilling operators. There are, however, some inconsistencies connected with the identification of the top and base of the various formations due to inadequate biostratigraphical information. Inconsistencies are often related with the determination of the top Hod Formation. In this study a consistent definition of the top of the Hod Formation is attempted by referring the surface to the major regional unconformity (the Intra-Chalk Unconformity) associated with the Late Campanian inversion in the Central Graben area.

The thickness of the chalk formations varies according to depositional basin setting and a number of hiatus are found within the different formations. In addition to the Upper Campanian Intra-Chalk Unconformity, two unconformities are encountered in the Cenomanian to Santonian succession (within the Lower and Middle Hod). These unconformities are identified from seismic interpretation and are generally overlooked in well interpretation unless detailed biostratigraphy in that section is available (among others Robertson Research International Ltd 1984). The thickness variation within the various formations is illustrated in the enclosed correlation panels (Enclosure 1-3). Hiatus identified within the various wells are indicated in Appendix 1.

Database

29 wells have been selected for the study (Table 2.1, Figure 2.1). Wire-line logs and biostratigraphic data from these wells are used for the lithostratigraphical subdivision. The stratigraphical data available for this study are primarily from final completion well reports provided by the drilling operator. When available, additional biostratigraphical reports have been included.

Lithostratigraphy

Different lithostratigraphic subdivisions of the Chalk Group are shown in Figure 2.2. The definition of the top Hod formation varies between authors and may range from being an internal Upper Campanian surface (Vejbæk & Andersen 1987) to represent the Campanian

/Maastrichtian boundary (Surlyk *et al.* 2003; Figure 2.2). In this study the lithostratigraphy given in the Millennium Atlas (Surlyk *et al.* 2003) is applied and consequently the Upper Campanian deposits are included in the Hod formation. A hiatus (the Intra-Chalk Unconformity) is found between the Hod and Tor formations. The hiatus is associated with a regional sea level fall and inversion of varying intensity within the Danish Central Graben area.

For illustration of the hiatus and thickness variations within the Tor and Hod Formations a correlation between the internal horizons/unit tops has been carried out (Enclosure 1-3). The division of the Chalk sequence into subunits is based on the log motif and biostratigraphy. The horizons/unit tops used for this correlation are listed in Table 2.2 and a correlation is shown in Figure 2.3 using the Gwen-2 and Sine-1 as reference wells. Both wells comprise a thick and a nearly complete stratigraphic section of the post-Cenomanian sequence, but are located in two different geological provinces with different subsidence history during the Late Cretaceous. The surface picks from the examined wells are listed in Appendix 1.

Intra-Chalk Unconformity

A major hiatus characterises the boundary between the Hod and the overlying Tor formations and is associated with the major sea level fall and inversion during Late Campanian (Oakman & Partington, 1998). On seismic data the top of the Hod formation is connected with an unconformity (the Intra-Chalk Unconformity). The unconformity is significant in the southern part of the Danish Central Graben and is associated with severe erosion and non-deposition. The unconformity locally represents a hiatus ranging in age from Santonian to Maastrichtian, but occasionally the hiatus represents a minor time gap ranging in age from the latest Campanian to earliest Maastrichtian (e.g. Sine-1 and Skjold Flanke-1).

Contrary to Vejbæk & Andersen (1987), the unconformity is here considered as isochronous with significant variations in the time span of the missing section in the different wells. The time gap related to the hiatus in the various wells is indicated in Appendix 1.

The Intra-Chalk Unconformity mirrors a significant change in the depositional environment and represents the boundary between two generally different lithofacies. The rock properties related to the lithofacies are controlled by the geological setting, which again is controlled by the tectonic regime. For illustration of the variation in thickness and lithotypes in the Danish Central Graben the geological setting is summarised below.

A compressional tectonic regime with inversion prevailed during the deposition of the Hydra and Hod Formations. The inversion activity ceased through the Late Upper Cretaceous and the Intra-Chalk Unconformity represents the end of the main inversion activity during Late Campanian. Contemporaneously with the tectonic activity the global sea level continued to rise throughout the Santonian and into the Campanian, reaching a high stand maximum in the late Campanian. In the Danish Central Graben the high stand is locally masked by the compressive event resulting in inversion structures (Figure 2.4). Significant parts of the

Campanian succession are absent over inversion swells suggesting considerable local erosion and redeposition in adjacent deeper sub-basins

Large thickness variations developed, as the post-inversion topography was infilled during the Maastrichtian and Danian. Deeper subbasins were filled with considerable thicknesses of mass-flow and turbiditic chalk. Thick basinal chinks, often of remarkable purity, can be mapped adjacent to the inversion area e.g. to the east of the inversion axis on the Ringkøbing Fyn High (represented by the Sine-1 well).

The difference between inversion swells with erosion and/or non-deposition and basins gives rise to significant variation in the lithofacies and thickness especially for the Hod and Tor formations; which is demonstrated by this study.

Table 2.1. *Wells used in this study*

Baron-2	Falk-1	Jette-1	Ravn-1	Skjold Flank-1
Bertel-1A	Gert-1	Nora-1	Ravn-2	T-1
Diamant-1	Gwen-2	NW Adda-1	Rigs-1	T-3
Elin-1	I-1x	Otto-1	Rigs-2	W-1
Elly-1	Iris-1	P-1x	SA-1	W. Lulu-1
Elly-2	Isak-1	Q-1	Sine-1	

Table 2.2. Correlation surfaces used in the study. The formal lithostratigraphic boundaries are marked in bold blue and unit tops are in black.

Chronostratigraphy		Correlation horizons Formation and unit tops	Abbreviations
Danian		Top Chalk Ekofisk 3 Ekofisk 2 Ekofisk 1	Top Chalk Eko3 Eko2 Eko1
Maastrichtian	Latest Maastrichtian	Top Tor Upper Tor 2 Upper Tor 1	Top Tor UT2 UT1
	Late Maastrichtian	Middle Tor 2 Middle Tor 1	MT2 MT1
	Early Maastrichtian	Lower Tor 3 Lower Tor 2 Lower Tor 1	LT3 LT2 LT1
Campanian	Late Campanian	Top Hod Upper Hod 4 Upper Hod 3	Top Hod UH4 UH3
	Early Campanian	Upper Hod 2 Upper Hod 1	UH2 UH1
Santonian		Middle Hod 4 Middle Hod 3	MH4 MH3
Coniacian		Middle Hod 2 Middle Hod 1	MH2 MH1
Turonian		Lower Hod 4 Lower Hod 3 Lower Hod 2 Lower Hod 1	LH4 LH3 LH2 LH1
Cenomanian		Top Plenus Marl	
		Top Hydra	Top Hydra
Albian		Base Chalk	Base Chalk

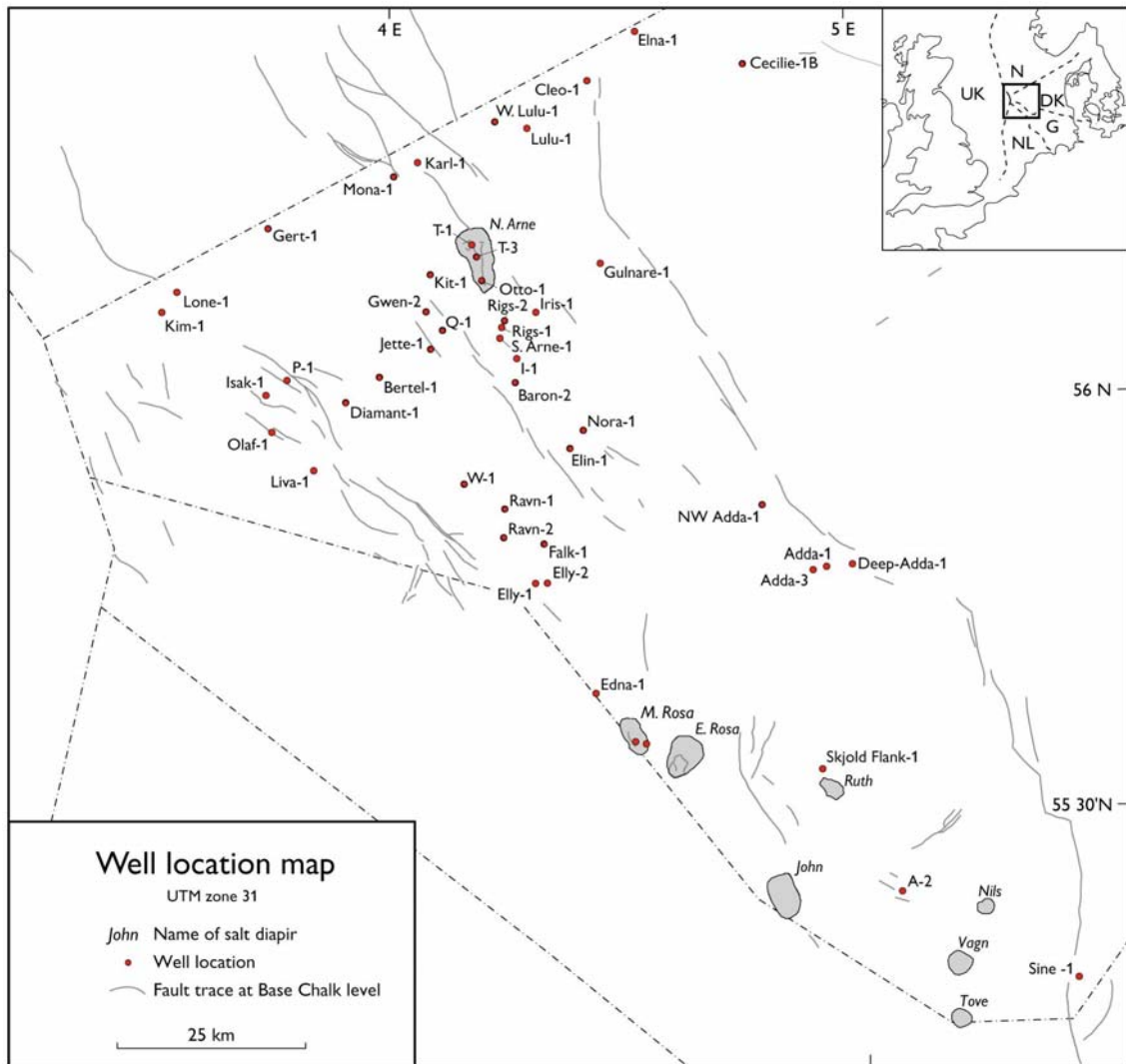


Figure 2.1. Location map for wells in this report. Fault pattern after Britze et al. 1995.

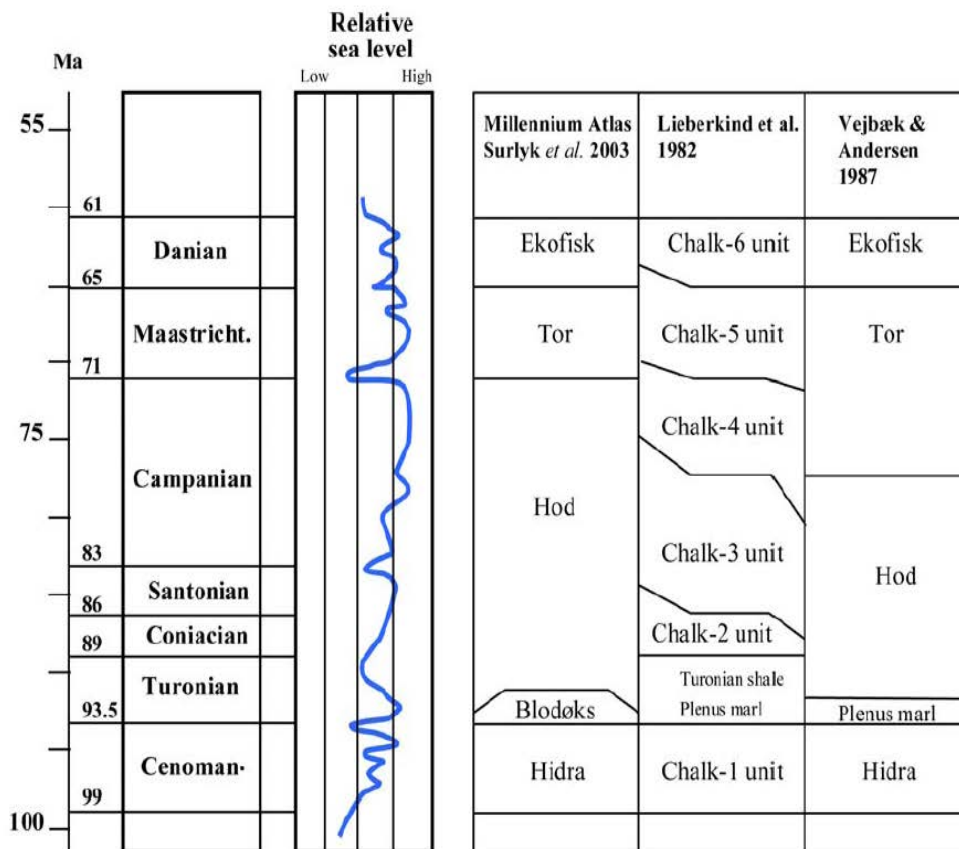


Figure 2.2. Lithostratigraphic nomenclature for the Chalk Group in Danish Central Graben. From Surlyk *et al.* 2003; Vejbæk & Andersen 1987 and Lieberkind *et al.* 1982. Time scale according to Gradstein *et al.* 1995.

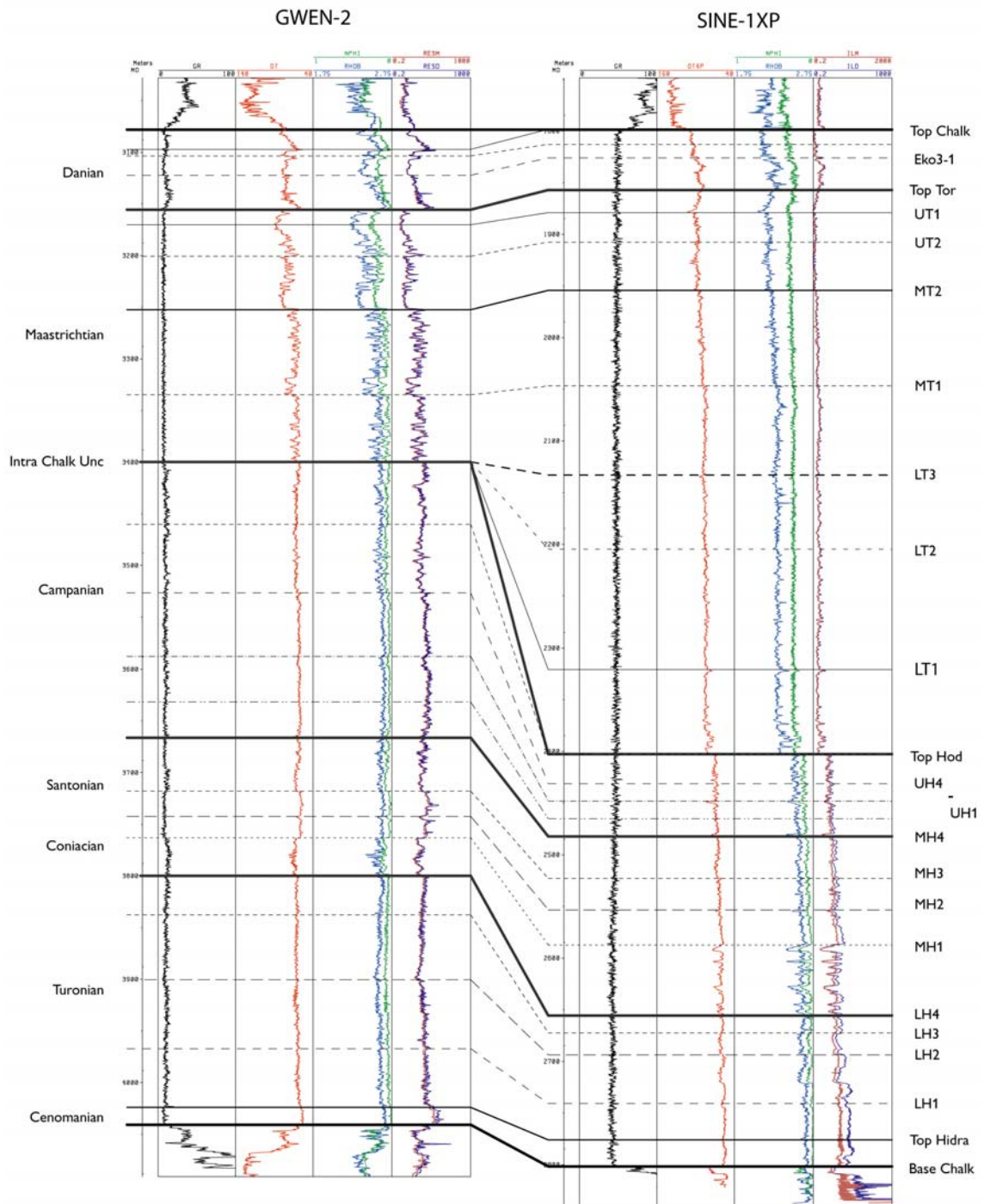


Figure 2.3. Log correlation between the Gwen-2 and Sine-1 wells. In the Sine-1 well the uppermost Hod formation is condensed or even missing. In the Gwen-2 well the lowermost Tor formation is missing.

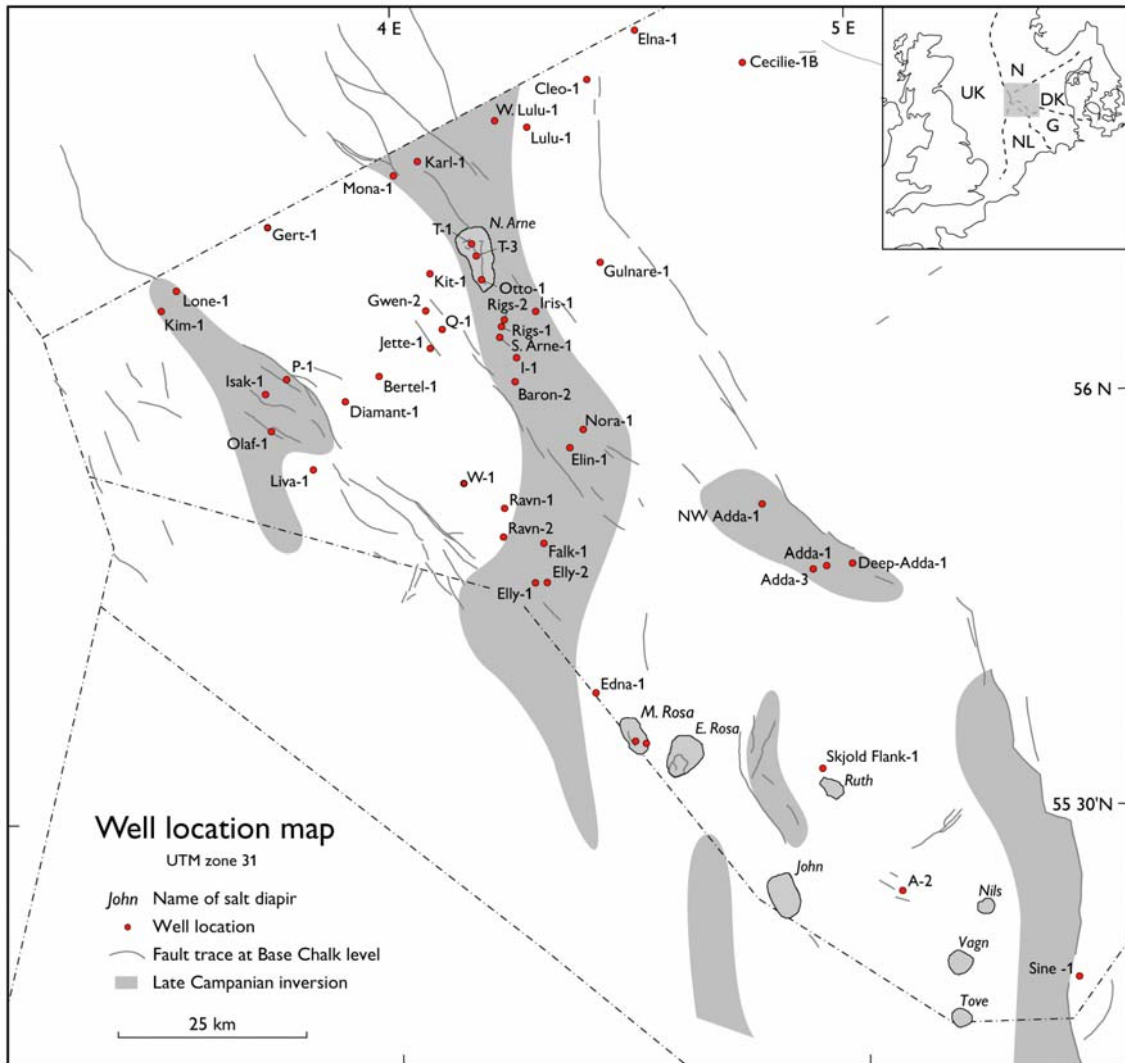


Figure 2.4. Danish Central Graben structural elements with faults at Base Chalk level. Hatching indicates areas of positive Late Campanian inversion. (From Vejrbæk & Andersen 2002). Associated with the main inversion phase during Late Campanian erosion on the swells and redeposition in adjacent deeper sub-basins took place.

3. Formation pressure

Overpressure due to compaction disequilibrium

Overpressure, ΔP (Pa; 1 MPa=145 psi) is the difference between the measured formation pressure, P , and the calculated hydrostatic pressure, P_H , at depth Z :

$$\Delta P = P - P_H = P - \rho_f \cdot g \cdot Z ,$$

where ρ_f (kg/m^3) is the mean pore fluid density of the overburden, and g is the gravitational acceleration (9.807 m/s^2). According to Japsen (1998), $\rho_f = 1.02 \text{ g/cm}^3$ at depth in the central North Sea. Overpressure is frequently given in mud weight equivalents (mwe):

$$1 \cdot 10^3 \text{ kg/m}^3 \text{ mwe} = 1 \text{ g/cm}^3 \text{ mwe} = 9.807 \text{ MPa/km} = 0.4335 \text{ psi/foot}.$$

A pore fluid density of 1.02 g/cm^3 thus corresponds to a water gradient of 10 MPa/km or 0.44 psi/f. The lithostatic pressure, S (Pa), at depth z is the stress exerted by the weight of the overburden: $S = \rho_b \cdot g \cdot z$ where ρ_b is the mean bulk density (wet). Terzaghi's principle states that the weight of the overburden per unit area, S , is borne partly by the rock matrix and partly by the pore fluid:

$$S = S_{eff} + \beta \cdot P ,$$

where S_{eff} (Pa) is the effective stress that is transmitted through the matrix (Terzaghi & Peck 1968). β is the Biot factor – or the effective stress coefficient (see Prasad & Manghnani 1997) – of the sediment and it ranges between 0 and 1 (assumed to equal 1 for high-porosity rocks). The principle implies that if a rock is more deeply buried without change in effective stress, the added load is carried by an increase in pore pressure, ΔP (for $\beta=1$).

Overpressure is generated by disequilibrium compaction when the weight of the overburden is increased by addition of sediments at the surface, and the pore fluid in the formation is sealed in the formation (Dickinson 1953; Rubey & Hubbert 1959; Osborne & Swarbrick 1997). The rock is unable to compact because the pore fluid cannot escape at the same rate as load is added to the overburden of the rock. Consequently, the additional load is carried by pore fluids, and higher than hydrostatic pressures result. The rock is said to be undercompacted, because porosity becomes high relative to depth.

Effective depth for $\beta=1$

The chalk in the central North Sea is buried below a normally compacted upper overburden and an undercompacted, sealing lower overburden. Here we will apply Terzaghi's principle to the case when a normally compacted rock is shifted to greater burial without change in porosity (nor velocity) and thus without change in effective stress. In such a case the added

load is carried by an increase in pore pressure. This may take place because the loading is so rapid compared to the low permeability of the sealing shales that no pore fluid can escape from the rock and hence no compaction can take place (Fig. 3.1). The effective stress on the rock is identical before and after overpressuring, and we refer to the initial depth as the effective depth of the rock: the depth corresponding to normal compaction of the rock for the given effective stress (reflected in a given sonic velocity).

Prior to the additional burial the rock was at its maximum burial, Z_{eff} (m below sea bed) and the formation pressure prior was hydrostatic (i.e. the rock was normally compacted) and we can write

$$S_{eff} = S - P = \rho_{low} \cdot g \cdot Z_{eff} - \rho_{fl} \cdot g \cdot Z_{eff} \quad (1)$$

where ρ is the average bulk density of the overburden,

If the rock is more deeply buried by the burial anomaly, $dZ_B = Z - Z_{eff}$, relative to the depth of normal compaction, without change in porosity or velocity of the chalk, the effective stress, S_{eff} , is unchanged because the overpressure, ΔP , carries the effective stress of the additional overburden entirely. The unchanged effective stress in the rock and the overpressure equals the effective stress of the overburden:

$$S_{eff} = S' - P' = (\rho \cdot g \cdot Z_{eff} + \rho_{up} \cdot g \cdot dZ_B) - (\rho_w \cdot g \cdot Z_{eff} + \rho_w \cdot g \cdot dZ_B + \Delta P) \quad (2)$$

where ρ_{up} is the bulk density of the added upper part of the overburden (below the later added upper overburden). We can combine the two above expressions:

$$\begin{aligned} \rho \cdot g \cdot Z_{eff} - \rho_{fl} \cdot g \cdot Z_{eff} &= (\rho_{low} \cdot g \cdot Z_{eff} + \rho_{up} \cdot g \cdot dZ_B) - (\rho_{fl} \cdot g \cdot Z_{eff} + \rho_{fl} \cdot g \cdot dZ_B + \Delta P) \\ \rho_{fl} \cdot g \cdot dZ_B + \Delta P &= \rho_{up} \cdot g \cdot dZ_B \\ \Delta P &= g \cdot dZ_B \cdot (\rho_{up} - \rho_{fl}) \end{aligned} \quad (3)$$

if $\rho_{up}=2.06 \cdot 10^3 \text{ kg/m}^3$ and $\rho_w=1.02 \cdot 10^3 \text{ kg/m}^3$ we get:

$$\begin{aligned} \Delta P &= 9.807 \cdot dZ_B \cdot (2.06 - 1.02) \cdot 10^3 \\ \Delta P &\approx dZ_B / 100 \text{ MPa} \quad (dZ_B \text{ in m}) \end{aligned} \quad (4)$$

This means that a burial anomaly of 1000 m relative to the depth of normal compaction reflects overpressure due to undercompaction of c. 10 MPa. In this simple case the load of the added kilometre (20 MPa) is carried by the formation pressure – partly by increased hydrostatic pressure (10 MPa) and partly by the overpressure (10 MPa): The effective stress exerted by the added overburden is carried by the overpressure. Reformulating the last two expressions we can estimate the effective depth in terms of the actual depth of the rock with overpressure, ΔP , due to undercompaction:

$$\begin{aligned} Z_{eff} &= Z - \Delta P \frac{1}{g \cdot (\rho_{up} - \rho_{fl})} \\ Z_{eff} &= Z - \Delta P \cdot 100 \text{ m} \quad (\Delta P \text{ in MPa}) \end{aligned} \quad (5)$$

This means that if the overpressure is 10 MPa, the effective stress at depth Z is the same as for a normally compacted rock c. 1000 m less deeply buried.

Chalk pressure data

Chalk formation pressure data from Danish central North Sea are available for the study from a number of sources (Table 3.1):

- pressure data published by Japsen (1998)
- pressure data from in-house reports
- pressure data in various completion reports

The pressure evaluations are based on drill stem and repeat formation tests, and are generally from the uppermost part of the Chalk. A few tests indicating very high pressure near the base of the Chalk are probably related to the Jurassic-Lower Cretaceous pressure regimes in the Central Graben, and are not included in the study. Mud weights have only been used to give an upper limit for the overpressure where indicated.

The general trend revealed by the chalk overpressure data given in Table 3.1 agrees with the map of chalk overpressure in the central North Sea (Fig. 3.2): Maximum overpressure is found in the Ekofisk area below the late Cenozoic depocentre. The rapid loading of sediments over the last c. 15 million years has generated undercompaction in the chalk because the sealing lower Cenozoic shales prevent the chalk from compacting at the same speed as sediments are added at sea bed. Overpressure declines away from this centre towards NNW and SSE along the depocentre axis. In Danish waters overpressure exceeding 15 MPa occurs in the northern part of the Central Graben area (e.g. the South Arne field) and decreases towards the south where 8 MPa is estimated for Skjold Flank-1 and 6.2 MPa for Sine-1. There is however some uncertainty about the decline of overpressure towards the west and east where few data are available for the chalk; e.g. west of the South Arne field and the Kit-1 well (Isak-1) and along the eastern flank of the graben.

Comments to selected overpressure estimates:

Baron-2/2a, 17.5 MPa: This value exceeds the regional level by c. 2 MPa.

Very few good estimates of the chalk formation pressure are available for the area west of the South Arne Field.

Kit-1; 14.6 MPa: This well (just north of Jette-1) provides one of the few good data points based on several pressure tests in the Maastrichtian reservoir (Tor Fm).

Gert-1; 16.4 MPa: This value based on formation tests indicates increasing pressure in the direction of the Ekofisk Field.

Olaf-1; 16.9 MPa: A very high overpressure based on an unsuccessful test in that well. Overpressure estimates based on mud weights in near-by wells indicate a more moderate level: Isak-1 (12.6 MPa), Diamant-1 (13.9 MPa), Liva-1 (14.0 MPa) and a very low value for P-1 (9.0 MPa). The data from Olaf-1 has thus not been used in the estimation, and the values for Diamant-1 and Bertel-1 (14.0 MPa) are taken as intermediate value between the estimate in Isak-1 and the test result in Kit-1. Likewise, the estimate for Jette-1 (14.6 MPa) is copied from the test result in Kit-1.

Skjold Flank-1; 8.1 MPa: This value is based an estimate of the initial pressure at the location of the well based on regional data. RFT data for the Ekofisk Formation in the well is c. 8 MPa, but RFT data for the Tor Formation give an overpressure of only c. 7 MPa. According to the completion report this drop of about 1 MPa is to be expected due to pressure depletion related to the production of the Skjold Field. The higher overpressure in the Ekofisk Formation than in the Tor Formation suggests differential depletion between these two formations.

Table 3.1. Chalk formation pressure

Well	Core *	Vs *	DP (MPa)	P (MPa)	Z (m bsl)	Source	Comment
Baron-2/2a	x		17.5	45.8	2845	RFT	Completion report
Bertel-1A			14.0			-ch	Regional estimate, Kit-1
Cecilie-1B	x	(x)	3.5		2223	-ch	Estimate from Elna-1
Diamant-1			14.0			-ch	Regional estimate, Kit-1
Elin-1			15.9			-ch	Estimate from Nora-1
Elly-1			13.4			-ch	Estimate from Elly-2
Elly-2			13.4	42.8	2941	PJ	
Falk-1			15.0	44.9	3010	Erico	
Gert-1	x		16.4	49.0	3262	PJ	
Gwen-2			14.6			-ch	Estimate from Kit-1
I-1	x		14.9	42.6	2765	PJ	
Iris-1			15.1	46.0	3111	Erico	
Isak-1		x	12.6		3200	mud weight	Completion report
Jette-1		x	14.6			-ch, mud	Estimate from Kit-1
Kit-1		x	14.6	46.3	3170	RFT	Completion report
Nora-1			15.9	41.2	2574	PJ	
NW Adda-1		x	10.0	33.0	2300	-ch	Regional estimate, Adda-1 + Bo-1
Otto-1	x		14.6	39.8	2521	PJ	
P-1			12.6			-ch	Isak-1, possibly less (cf. Erico)
Q-1	x		14.6			-ch	Regional estimate, Kit-1
Ravn-1			14.2			-ch	Regional estimate, Falk-1 + Elly-2
Ravn-2			14.2			-ch	Regional estimate, Falk-1 + Elly-2
Rigs-2	x	x	15.4	43.4	2800	Tests	Amerada
SA-1	x	x	15.4	43.4	2800	Tests	Amerada
Sine-1		x	6.5	27.4	2100	RFT	Completion report
Skjold Flank-1		x	8.1	29.0	2100	-ch	Regional estimate, Skjold-1 (Erico)
T-1			15.0	37.5	2251	PJ	
T-3	x		14.5	39.3	2494	Erico	
W. Lulu-1	x		13.8	42.8	2910	Erico	
W-1			14.2			-ch	Regional estimate, Falk-1+ Elly-2

* Availability of chalk cores and S-wave sonic log.

** Data courtesy of Amerada Hess (personal communication, Jørgen Jensenius 2003)

P Formation pressure.

ΔP Overpressure relative to water gradient of 10 MPa/km.

Z Vertical depth below sea level.

RFT Repeat formation tester.

-ch No chalk pressure data.

PJ Japsen (1998).

Erico Petroleum Information (Erico) (1995).

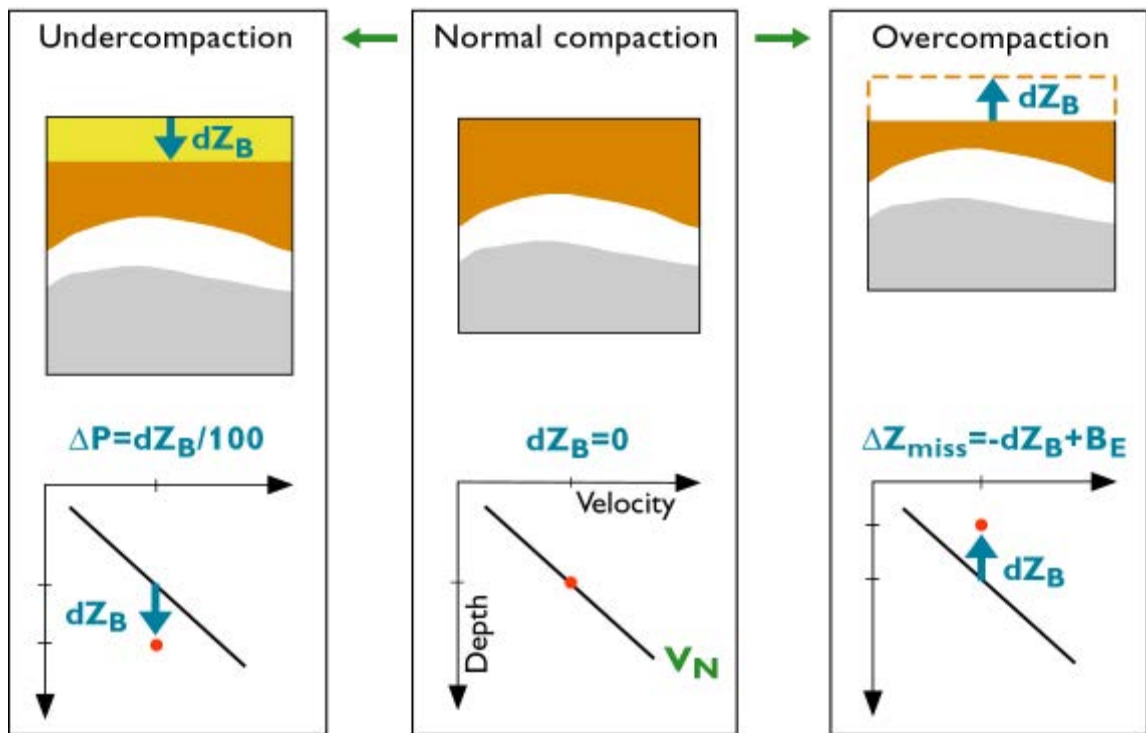


Figure 3.1. Burial anomaly, dZ_B (m), relative to a normal velocity-depth trend, V_N . Undercompaction due to rapid burial and low permeability causes overpressure, ΔP_{comp} (MPa), and low velocities relative to depth (positive dZ_B). Uplift and erosion reduce the overburden thickness and result in overcompaction expressed as anomalously high velocities relative to present-day depth (negative dZ_B). However, post-exhumational burial, B_E , will mask the magnitude of the missing section, ΔZ_{miss} . The effective depth, Z_{eff} , is the depth corresponding to normal compaction as predicted by the normal velocity-depth trend for the measured velocity. Modified after Japsen (1998).

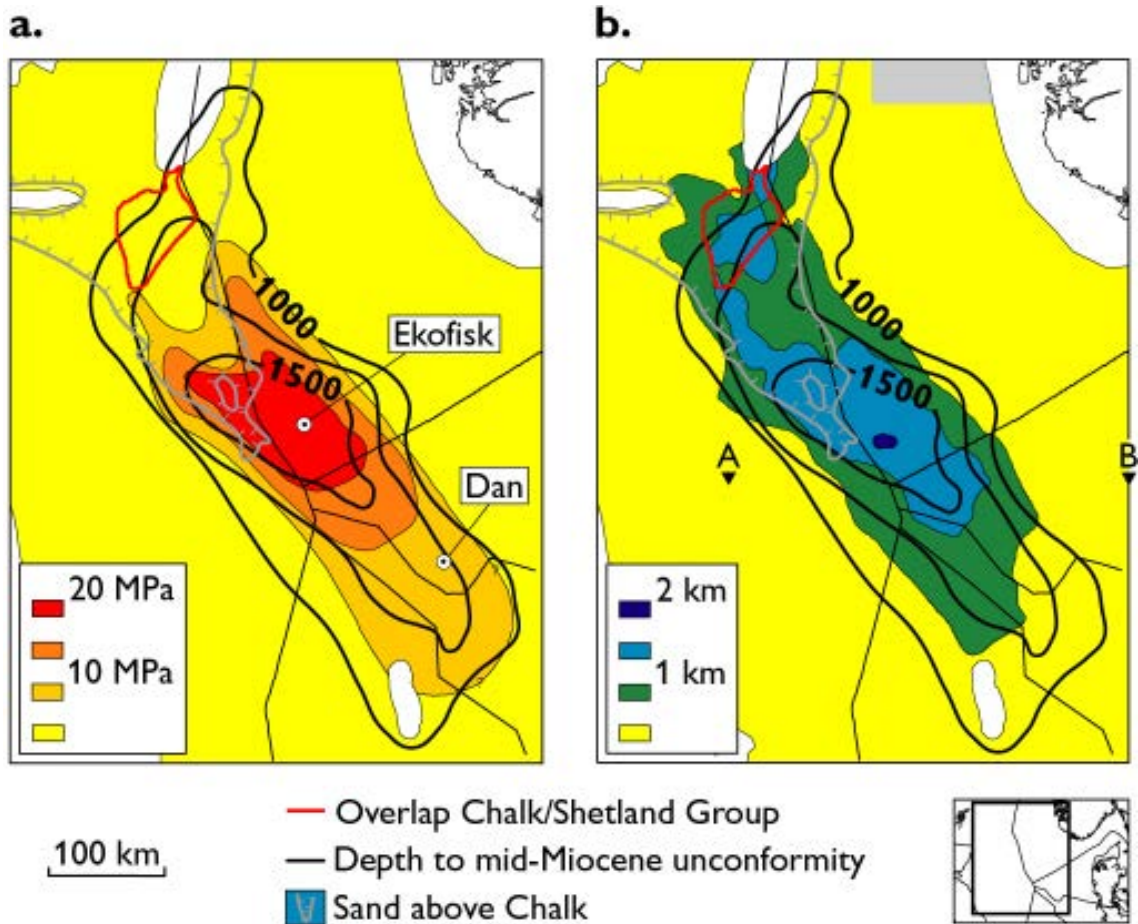


Figure 3.2. Corresponding areas of overpressured Chalk outlined from pressure measurements and from Chalk burial anomalies coincident with the late Cenozoic depocenter.

a. Chalk formation overpressure.

b. Chalk burial anomalies relative to a normal velocity-depth trend (Japsen 1998).

The overpressured zone corresponds to maximum thickness of the late Cenozoic deposits, whereas Paleocene sands overlying the Chalk to the northwest cause bleed-off of overpressure. South of the Viking Graben, shaly Chalk causes positive velocity anomalies even where the Chalk is normally compacted. Modified after Japsen (1998).

4. Temperature

The temperature at the top and the base of the chalk has been estimated for a number of wells (Table 4.1) and mapped (Figs 4.1 – 4.2). The temperatures were calculated based on the following considerations:

The temperature gradient was estimated for each well (Fig. 4.3) as the average gradient based on available down-hole temperature measurements in the well using an assumption of a surface temperature of 5°C. However, data from near-by wells were used for some wells (Jette-1, Bertel-1, Baron-2 and Rigs-1). The estimated temperature gradients are thus based on temperatures measured in different depths and in different formations depending on the TD of each well.

The temperature at Base Chalk was calculated from its depth in the well, the temperature gradient and a surface temperature of 5°C. The temperature at Top Chalk was calculated from the thickness of the chalk in the well, the temperature at Base Chalk and a temperature gradient only 77% of the estimated average gradient in the well. The factor of 77% is found from comparison of the average measured gradients and estimated gradients in the chalk based on basin modeling.

Table 4.1. *Temperature estimated at top and base chalk.*

Well	Top Chalk temp. (°C)	Base Chalk temp. (°C)	Temp. gradient (°C/km)	Top Chalk depth (m TVD)	Base Chalk depth (m TD)
A-2	71	82	35	1778	2171
Adda-1	71	76	31	2058	2256
Adda-3	68	73	30	2071	2303
Baron-2	98	101	33	2803	2928
Bertel-1	100	124	28	3107	4222
Cleo-1	91	102	30	2791	3277
Deep Adda-1	78	85	34	2128	2384
Diamant-1	94	108	28	3013	3660
Edna-1	101	109	35	2678	2966
Elin-1	98	103	34	2679	2897
Elna	88	95	35	2438	2723
Gulnare-1	95	115	28	2942	3899
Gwen-2	102	124	30	3039	4004
I-1X	95	97	33	2727	2814
Iris-1	87	94	28	2867	3171
Jette-1	92	99	29	2889	3182
Karl-1	102	127	30	3023	4147
Kim-1	105	123	30	3119	3871
Liva-1	92	112	28	2910	3793
Lone-1	94	101	30	2949	3255
Lulu-1	97	109	32	2722	3214
Nora-1	98	106	35	2560	2861
Otto-1	99	106	38	2441	2689
P-1	87	92	28	2882	3117
Q-1	100	120	29	3033	3925
Ravn-1	105	122	31	3013	3745
Rigs-1	82	84	28	2748	2812
Skjold Flank-1	78	95	32	2169	2795
T-3	95	102	36	2438	2699
W-1	97	112	29	3054	3726

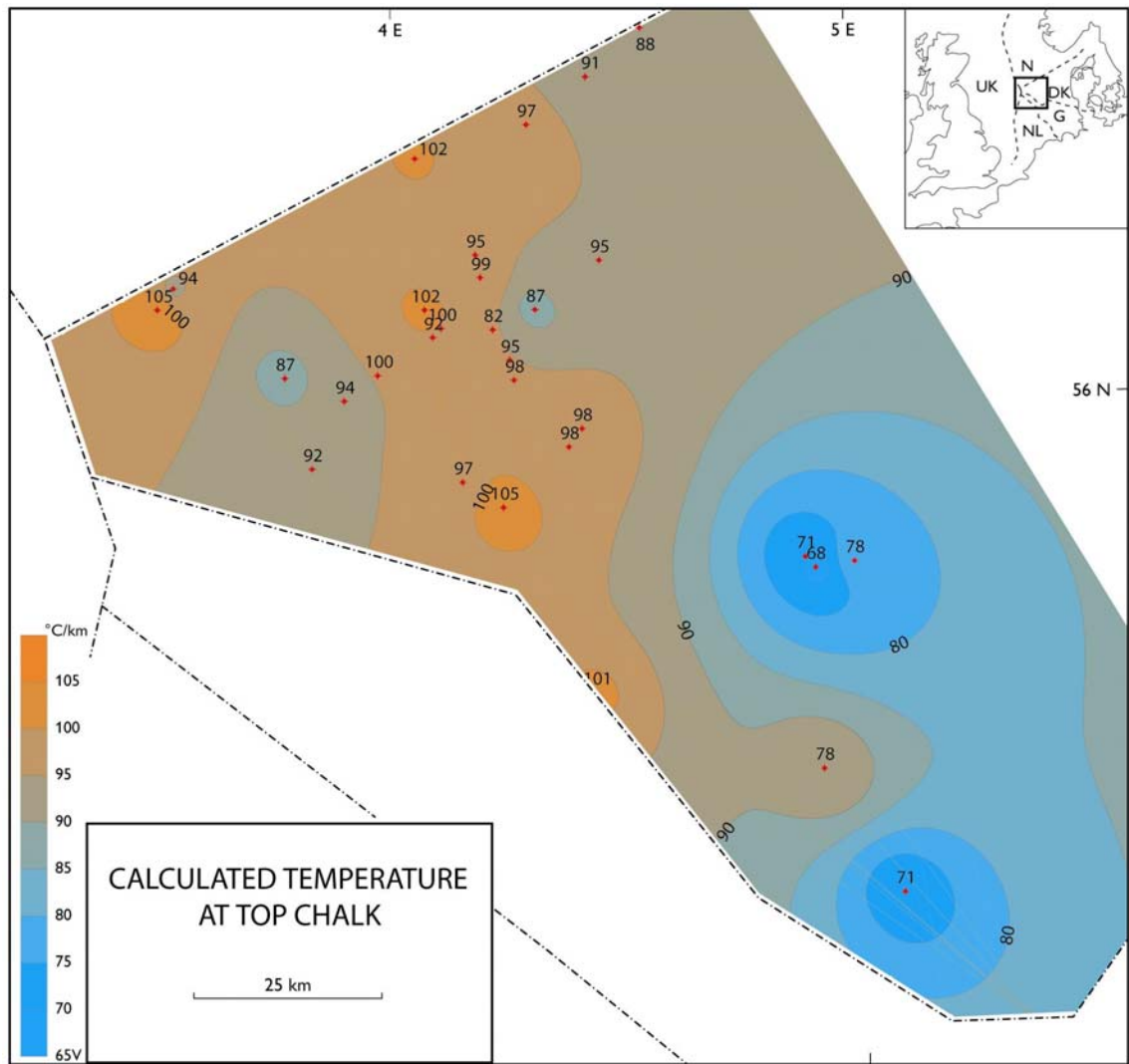


Figure 4.1. Temperature at Top Chalk estimated in wells (Table 4.1). Contours represent interpolation of the temperatures in the wells.

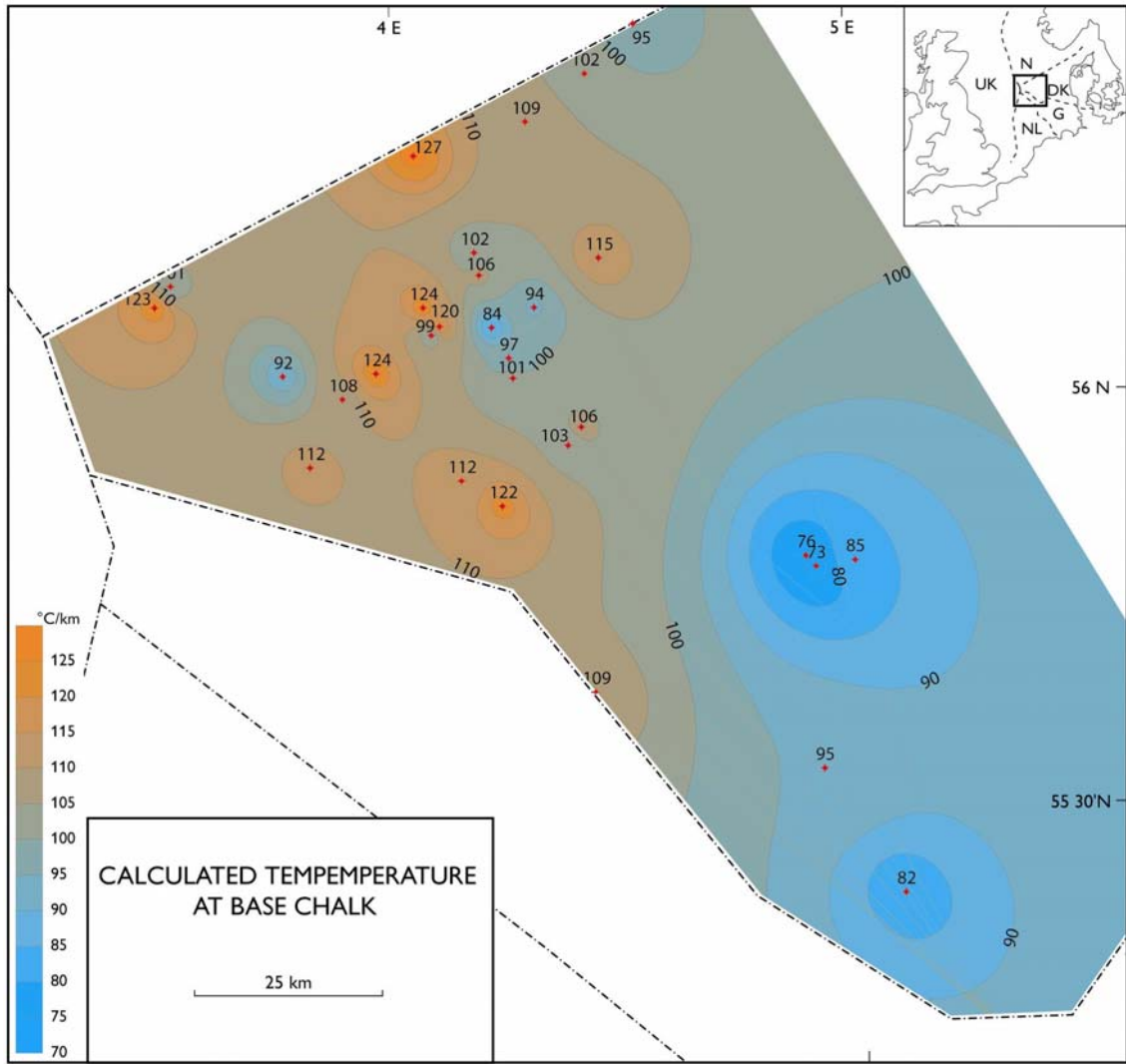
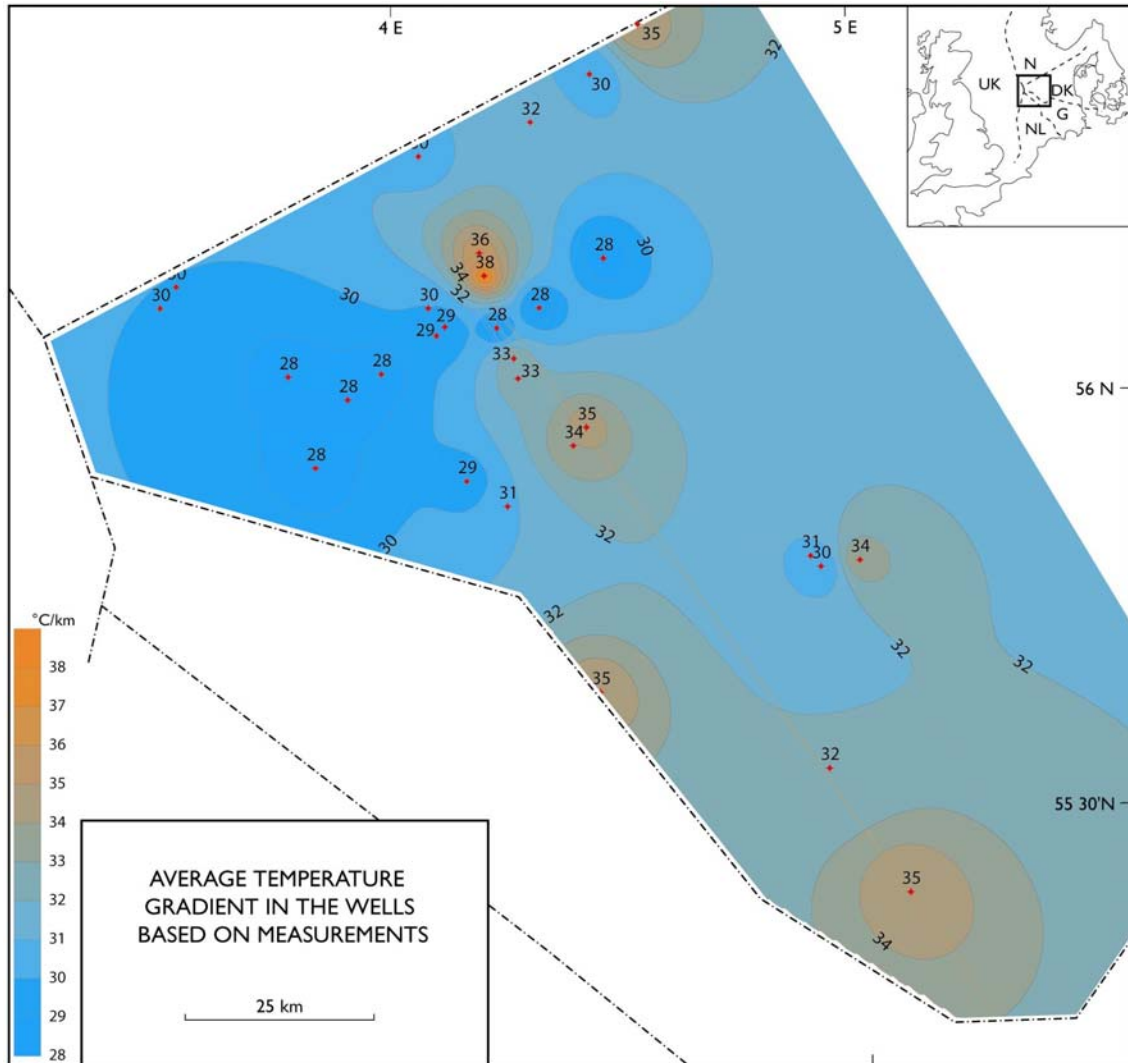


Figure 4.2. Temperature at Base Chalk estimated in wells (Table 4.1). Contours represent interpolation of the temperatures in the wells.



5. Acoustic properties

Log data from the Chalk Group in 28 wells were quality controlled and used as input for estimation of porosity and water saturation (Ødegaard 2005). The porosity and brine saturation interpretation was done simultaneously using the bulk density, deep and micro/shallow resistivity well log curves together with Archie's equation assuming $(a, n, m) = (1, 2, 2)$. Parameters such as R_w , R_{mf} and RHO_{mf} was used as input (if available) together with fixed matrix density and clay properties.

Main aspects of the chalk data are shown in cross plots of the physical parameters in Appendix 2. A larger selection of cross plots is presented in PowerPoint files on the enclosed CD together with the data files in MatLab format. Various aspects of the data for each of the wells is discussed in the section below.

Typical examples of the variation of the acoustic properties of the chalk are revealed by the plots of the thick chalk sections in the Gwen-2 and the near-by Jette-1 well (plots shown in Appendix 2):

- The plot of V_p versus porosity indicates a clear separation between the formations in these wells: Tor plots along a long and narrow trend whereas Hod plots as a cluster of points with low porosity and Ekofisk either plots along the Tor trend (Ekofisk porous) or as data points with low velocity-porosity values (Ekofisk tight). This distinction corresponds to the differences in the gamma log: low gamma ray (GR) in Tor and parts of Ekofisk and higher values for most of Hod and Ekofisk (see also cross plots colorcoded by GR values in the PowerPoint files on the enclosed CD).
- There is an overall drop in porosity with depth in the Tor Formation and corresponding increase in velocity for these wells. When the log data are plotted against depth and effective depth with compressed depth scales it is apparent that there is a drastic change in these parameters over a narrow interval in effective depth (corrected for overpressure): c. 1700 – 1800 m. We refer to this sharp drop in porosity and an increase in velocity as the 'Cementation front'. The front is where (minimum) velocity cross c. 4.5 km/s and (maximum) porosity cross c. 15%. It is only possible to judge the match between the normal trends and the data versus effective depth for chalk sections of substantial thickness.
- The plots of velocity versus porosity reveals that velocity increases as porosity is lost during greater burial; cf. the plots for the Gwen-2 and Isak-1 wells. For these wells data for the Hod Formation moves towards the upper left of the diagram when we compare the more deeply buried chalk in the Gwen-2 well (c. 3400 – 4000 m) with the Isak-1 well (c. 3100 – 3200 m). The data are moving along the MLHS trend. A similar shift of the data points can be seen for the Tor and Hod formations when comparing the Sine-1 well with the more deeply buried Skjold Flank-1 well.
- The level of V_p versus porosity is quite different for the Gwen-2 and the Jette-1 well: Jette-1 has considerably higher P-velocities for the same porosity than the Gwen-2 well. This difference would probably have been even clearer if a shear ve-

locity log had been available for the Gwen-2 well, because Jette-1 has very high S-velocities compared to porosity and a corresponding low Vp-Vs ratio (also compared to other wells with Vs data).

The analysis reveals that the gamma ray gives information that are important for evaluating the acoustic properties of the chalk. The typical level for the GR readings for the chalk is just below 10 API for the pure chalk in the Tor Formation with maxima up to c. 20 API in the less pure formations (e.g. Jette-1). Bad calibration of the gamma tool may be the reason why the same relative variations are found for chalk in other wells – only with a much higher base level (e.g. Baron-2). The true variations of the gamma radiation in the chalk may also be obscured by potassium content of the drilling mud (compare the low and systematic GR variations in the T-1 well with high and constant level in the near-by T-3 well or P-1 relative to Isak-1 or Elin-1 relative to Nora-1). The high and monotonous GR reading (c. 45 API) for the Sine-1 well could be mistaken as an erroneous measurement, but the log data from the near-by Per-1 well (not included in this report) show the same uniform GR level for the chalk – only very close to a base level of 10 API.

Plots of velocity versus porosity or Vp versus Vs show two reference curves: The modified upper and lower Hashin-Shtrikman curves (MUHS, MLHS) defined from log data for chalk on the Ekofisk Field (Walls et al. 1998; see also Japsen et al. 2004).

Plots of velocity and porosity versus depth show two other reference curves: The normal-velocity depth trend for North Sea Chalk defined by Japsen (2000) (a revision of the trend defined by Japsen 1998). The normal velocity-depth trend was based on an analysis of data from 845 wells throughout the North Sea Basin and data from outside the North Sea (Ocean Drilling Project). Normally compacted Chalk is rare in the North Sea Basin (no overpressure and no erosion of the overburden). However, in the southern, central part of the Basin, the chalk is deeply buried and overpressure is low and decreasing towards the south. Here, – in Dutch and British waters – it is thus possible to identify wells where the chalk is normally compacted in the interval with velocities ranging from c. 2.5 to 4 km/s. For smaller velocities the trend is based on ODP data and for velocities greater than 4 km/s, data representing normal compaction were identified along the upper bound in a velocity-depth plot where the effect of undercompaction due to overpressuring is a minimum. The trend is formulated as a segmented, linear function:

$$\begin{aligned}
 V_N^{Ch} &= 1550 + 1.3 \cdot z, & z < 900 \text{ m} \\
 V_N^{Ch} &= 920 + 2 \cdot z, & 900 < z < 1471 \text{ m} \\
 V_N^{Ch} &= 1950 + 1.3 \cdot z, & 1471 < z < 2250 \text{ m} \\
 V_N^{Ch} &= 2625 + z, & 2250 < z < 2875 \text{ m}
 \end{aligned}
 \tag{2}$$

The velocity increase with depth, k [m/s/m = 1/s], ranges from 1 to 2 s⁻¹ with a maximum between a depth of 1 and 1.5 km (Fig. 1b).

The normal porosity-depth trend for North Sea chalk was estimated by Sclater & Christie (1980) also by combining shallow data from outside the North Sea (Deep Sea Drilling Proj-

ect) with deep data from two normally pressured bore holes in the North Sea. The trend is formulated as exponential porosity decay (Fig. 2a):

$$\phi_N^{Ch} = 0.7 \cdot e^{-z/1408} \quad (3)$$

The porosity decay with depth, $kphi$ [$m^{-1} = 10^5$ pu/km], ranges from -50 pu/km ($=0.0005$ m^{-1}) near the surface to c. -5 pu/km at a depth of 3 km (Fig. 2b).

There is an overall agreement between the normal trends for velocity-depth and for porosity-depth of Japsen (1998, 2000) and Sclater & Christie (1980), even though they are not completely compatible. The agreement is evident from these plots for the Gwen-2 well: at shallow depths (c. 1.7 km) the minimum velocities and the maximum porosities are in agreement with normal trends when plotted against effective depth. However, at the base of the chalk velocity data match the velocity-depth trend, whereas the porosity data are much smaller than predicted by the porosity-depth trend.

Comments to the cross plots for the individual wells

Baron-2

- Thin chalk section (c. 100 m) with no GR separation between Ekofisk porous and Hod (Tor missing). Some HC in Ekofisk. Log pattern comparable to I-1. (log plot)
- Max phi c. 30% in Ekofisk (large scatter). (V-phi plot)
- Estimate of overpressure results in a poor match between normal trend and sonic data vs effective depth. Overpressure may be overestimated. Section just above 'Cementation front'. (V-Z plot)

Bertel-1

- Very thick chalk section (c. 1100 m) where GR is relatively high in Ekofisk and Hod and relatively low in Tor. Thick Tor with shift in character between Tor and Hod (GR, V and phi). No clear porosity-depth trend in Hod, but velocity variations reflect GR log. Similar log pattern as in Diamant-1, Gwen-2, Q-1 and Jette-1. Bertel more deeply buried than near-by Diamant-1 and thick chalk section down to c 4300 m. (log plot)
- Max phi c. 25% in Ekofisk and Tor. Ekofisk tight separated from clean Ekofisk and Tor. Very high Vp-values (up to 6 km/s) reflecting deep burial. Tor plot on a clearly 'stiffer' V-phi trend than Diamant-1. High GR plot in the lower left corner of the V-phi data (low V). Large phi-range for Tor and low range for Hod. (V-phi plot)
- Estimate of overpressure results in a fair match between normal trend and sonic data vs effective depth. Overpressure may be underestimated. 'Cementation front' within Tor Fm (V-Z plot)

Diamant-1

- Fairly thick chalk section (c. 600 m) where GR is relatively high in Ekofisk and Hod and relatively low in Tor. A high-porosity interval in Hod (3575 m kb) is reflected in low Vp. Similar log pattern as in W-1 and Jette-1. (log plot)
- Max phi c. 20% in Ekofisk and Tor. Ekofisk tight separated from clean Ekofisk and Tor. High GR plot in the lower left corner of the V-phi data (low V). (V-phi plot)
- Estimate of overpressure results in a good match between normal trend and sonic data vs effective depth. 'Cementation front' within Tor. (V-Z plot)

Elin-1

- Fairly thin chalk section (c. 200 m) with no GR difference between Ekofisk, Hod and Hidra (untypical high GR level – compare with near-by Nora-1 well) (Tor almost absent). Log pattern comparable to Nora-1 (and Isak-1). (log plot)
- Max phi around 20% for few recordings in Tor and Ekofisk. Rather scattered data points. (V-phi plot)
- Estimate of overpressure results in a poor match between normal trend and sonic data vs effective depth (maybe overestimated overpressure). 'Cementation front' within Hod. (V-Z plot)

Elly-1

- Fairly thick chalk section (c. 400 m) where GR is relatively high in Ekofisk and in Hod and particularly in the deepest part of Hod and in Hidra, but generally small variations. Small phi-contrast between Tor and Hod. Gradual decrease of phi corresponds to marked increase of V with depth in Hod (high porosity near base chalk). Similar to Falk-1 (and Elly-1, Ravn-1, -2) – but no high-porosity interval in Hod. (log plot)
- Max phi c. 20% in Tor. Narrow V-phi trend for Hod (near MLHS trend). Hidra reveal high GR and phi around 10-15%. High GR plot in the lower left corner of the V-phi data (low V). The deepest data points plot (Hidra) plot in the middle of the V-phi trend. (V-phi plot)
- Estimate of overpressure results in a good match between normal trend and sonic data vs effective depth. 'Cementation front' represented by gradual increase of velocity below effective depth of 1500 m within Hod Fm (similar to the changes seen in Hod in Sine-1). (V-Z plot)

Elly-2

- Fairly thick chalk section (c. 600 m) where GR is higher in Hod than in Tor, but small GR range. Small phi-contrast between Tor and Hod. Gradual decrease of phi and increase of V with depth in Tor and Hod. Hidra reveal high GR and phi around 10-15%. Similar to Elly-1 – but with high-porosity interval in Hod as in Falk-1. (log plot)
- Max phi c. 20% in Tor. Broader V-phi trend for Hod than in Elly-1. High GR plot in

the lower left corner of the V-phi data (low V). The deepest data points plot (Hidra) plot in the middle of the V-phi trend. (V-phi plot)

- Estimate of overpressure results in a good match between normal trend and sonic data vs effective depth. 'Cementation front' represented by gradual increase of velocity below effective depth of 1500 m within Hod (cf. Sine-1). (V-Z plot)

Falk-1

- Thick chalk section (c. 700 m) where GR is relatively high in Ekofisk and relatively low in the thin Tor. Sharp drop of phi (increase in V) from Tor to Hod. Gradual decrease of phi with depth in Hod. Very similar to Ravn-1 and W-1 (and Elly-1, -2) – also a high-porosity interval in Hod (3450 m kb) is reflected in low Vp. Less deeply buried than Ravn-1. (log plot)
- Max phi c. 25% in Tor and Ekofisk. Slightly higher minimum phi than in the Ravn-1 and corresponding higher max. Vp. Hidra reveals high GR and low phi. High GR plot in the lower left corner of the V-phi data (low V). (V-phi plot)
- Estimate of overpressure results in a good match between normal trend and sonic data vs effective depth. Slightly overestimated overpressure? 'Cementation front' represented by gradual increase of velocity below effective depth of 1500 m within Hod. (V-Z plot)

Gert-1

- Thick chalk section (c. 800 m) where GR is relatively high in Ekofisk and Hod and relatively low in Tor (but also low in the upper part of Hod). Thick Ekofisk and Tor. Rather gradual shift in character between Tor and Hod – e.g. decline of porosity (GR, V and phi). No clear porosity-depth trend in Hod, but velocity variations reflect variations in GR and porosity logs. Similar log pattern as in Diamant-1, Bertel-1, Gwen-2 and Jette-1. (log plot)
- Max phi c. 25% in Tor and Ekofisk. Rather scattered data, but difference between Tor and Hod. Tor plot on a rather low V-phi trend. Hod has fairly high minimum porosities (>5%) – cf. Gwen-2 (greater effective depth, more compacted Hod). High GR plot in the lower left corner of the V-phi data (low V). (V-phi plot)
- Estimate of overpressure results in a match between normal trend and sonic data vs effective depth. Velocity increase in upper Tor matches normal trend. 'Cementation front' within Tor. (V-Z plot)

Gwen-2

- Very thick chalk section (c. 1000 m) where GR is relatively high in Ekofisk and Hod and relatively low in Tor. Thick Tor with shift in character between Tor and Hod (GR, V and phi). No clear porosity-depth trend in Hod, but velocity variations reflect porosity and GR log. Similar log pattern as in Diamant-1, Bertel-1, Q-1 and Jette-1. (log plot)
- Max phi c. 25-30% in Tor. Very nice example of separation of the chalk formations

in a plot of V-phi. Ekofisk tight separated from clean Ekofisk and Tor. Tor plot on a very narrow V-phi but not as 'stiff' as in Bertel-1 (but a higher trend than in Diamant-1). Hod has low phi and high V. Hydra represent max velocities for the chalk. High GR plot in the lower left corner of the V-phi data (low V). Large phi-range for Tor and low range for Hod. (V-phi plot)

- Estimate of overpressure results in good match between normal trend and sonic data vs effective depth. 'Cementation front' within Tor. (V-Z plot)

I-1

- Thin chalk section (c. 100 m) with no GR separation between Ekofisk and Hod (Tor almost missing). Some HC in Ekofisk and thin Tor. Log pattern comparable to Baron-2. (log plot)
- Max phi c. 30% in Ekofisk (large scatter). (V-phi plot)
- Estimate of overpressure results in a match between normal trend and sonic data vs effective depth. Section above 'Cementation front'. (V-Z plot)

Iris-1

- Fairly thin chalk section (c. 300 m) with no clear GR separation between Ekofisk, Tor (thin) and Hod. High GR and low Vp for most of Hydra. Log pattern comparable to Isak-1. (log plot)
- Max phi c. 20-25% in Ekofisk. High GR plot in the lower left corner of the V-phi data (low V). (V-phi plot)
- Estimate of overpressure results in a fair match between normal trend and sonic data vs effective depth. Overpressure may be overestimated. No clear 'Cementation front' (section mainly below the front). (V-Z plot)

Isak-1

- Fairly thin chalk section (c. 300 m) without clear GR difference between Ekofisk, Tor and Hod. The clear GR difference seen for the near-by P-1 well may suggest that the GR data for Isak-1 may be of bad quality. A clear separation between the formations is seen on the Vp/Vs log. A consistent depth trend is seen for phi and Vp in the Hod formation. Log pattern comparable to e.g. P-1, Nora-1 and Elin-1. (log plot)
- Max phi c. 25% in Tor. The V-phi plot reveals a clear separation of the Ekofisk, Tor and Hod formations: Ekofisk tight separated from clean Tor, which has a well-defined trend. Hod plots towards lower phi-V and this is probably related to higher clay content (not revealed by the GR data). The data plot quite similarly to the data from the near-by Diamant-1 well, but significantly lower V-phi compared to the Jette-1 well. (V-phi plot)
- Estimate of overpressure results in a good match between normal trend and sonic data vs effective depth (maybe slightly underestimated overpressure). 'Cementation front' within Tor and Hod. (V-Z plot)

- High Vp/Vs for Ekofisk and Tor tight and elevated level for most of Hod (compared to Tor) – probably related to clay content. Vp/Vs(Tor) c. 1.9 in contrast to c. 1.8 for Jette-1. (Vp/Vs-phi plot)

Jette-1

- Thick chalk section (c. 900 m) with clear GR difference between Ekofisk, Tor and Hod. This separation is also seen on the Vp/Vs log. An overall depth trend is seen for phi and Vp in the Tor formation. High GR correlates with low Vp and Vs in the Hod Formation (c. 3720 and 3820 m) and consequently not with high Vp/Vs. Very similar to the logs from the near-by Gwen-2 well (log plot)
- Max phi c. 25-30% in Ekofisk and Tor. The V-phi plot reveals a clear separation of the Ekofisk, Tor and Hod formations: Ekofisk tight separated from clean Tor, which has a well-defined trend with a very large phi-range (over a limited depth range). High-GR Ekofisk and Hod plot towards lower phi-V. The data plot quite similarly to the data from the near-by Gwen-2 well, but along a higher V-phi trend. (V-phi plot)
- Estimate of overpressure results in a good match between normal trend and sonic data vs effective depth. 'Cementation front' within Tor. (V-Z plot)
- Low Vp/Vs for Tor and Hod – marked 'smile' with minimum for phi = 15%. Vp/Vs(Tor) c. 1.8 in contrast to c. 1.9 for Isak-1. No high Vp/Vs values for high GR (as in Isak-1), whereas high GR deviates from V-phi trend. (Vp/Vs-phi plot)

Nora-1

- Fairly thin chalk section (c. 300 m) with higher GR in Hidra than in most of Hod (Tor absent). General depth trend in Hod for phi and Vp. Log pattern comparable with Elin-1 (and Isak-1). (log plot)
- Max phi around 25% for few recordings in Ekofisk and Hod. General V-phi trend for Hod. Very low velocities for most Hidra data (but normal porosities). Could be related to transference of overpressure from deeper source rocks: $V > 3.5$ km/s for phi = 10% (original data $V > 3$ km/s). (V-phi plot)
- Estimate of overpressure results in a poor match between normal trend and sonic data vs effective depth (maybe overestimated overpressure or transference of overpressure from pre-chalk strata). 'Cementation front' near Hod. (V-Z plot)

NW Adda-1

- Fairly thin chalk section (c. 300 m) without clear GR difference between Ekofisk, Tor and Hod. The GR level is high (50 API), but it is unclear whether it represents a uniform level as that for the uniform chalk in Sine-1 or an erroneous reading. That the GR log is erroneous is indicated because a high Vp/Vs ratio in the uppermost Ekofisk is not reflected in high GR readings. Both GR and Vp/Vs-log has a very broad range. Large porosity variations are seen along the depth axis. Fairly long distance between this well and the other wells in the study, but the log pattern corresponds to Ein-1 and Nora-1 – only with higher porosities. (log plot)

- Max phi c. 30-35% in Ekofisk and Tor – a large scatter is seen in the data set. (V-phi plot)
- Estimate of overpressure results in a good match between normal trend and sonic data vs effective depth (maybe slightly underestimated overpressure). ‘Cementation front’ just below the section. (V-Z plot)
- Huge scatter in Vp/Vs – centred around a value of 1.9. (Vp/Vs-phi plot)

Otto-1

- Fairly thin chalk section (c. 200 m) with no GR separation (high API level). HC in Tor. Comparable to T-3. (log plot)
- Max phi c. 40% in Tor reservoir (low Sw and low Vp). No GR separation of the data. (V-phi plot)
- Estimate of overpressure results in a poor match between normal trend and sonic data vs effective depth. Overpressure may be overestimated or maybe salt diapirism has moved the chalk to a more shallow depth or overpressure is increased by transfer from more deeply buried chalk. Section above ‘Cementation front’. (V-Z plot)

P-1

- Fairly thin chalk section (c. 200 m) with clear GR difference between Ekofisk and Tor (thin) (similar to upper part of Hod). High GR in the lower part of Hod is reflected in low Vp. Thin Hydra has low GR and high Vp. Log pattern comparable to Isak-1 and Elin-1. (log plot)
- Max phi c. 25% in Tor and Ekofisk (few points). The V-phi plot indicates the typical separation of the Ekofisk, Tor and Hod formations (cf. Isak-1). High-GR Ekofisk and Hod plot towards lower phi-V. (V-phi plot)
- Estimate of overpressure results in a fair match between normal trend and sonic data vs effective depth (section too thin to make any further assessments). ‘Cementation front’ within Hod. (V-Z plot)

Q-1

- Thick chalk section (c. 900 m, but no data for lower part) where GR is relatively high in Ekofisk and Hod and relatively low in Tor. Thick Tor with shift in character between Tor and Hod (GR, V and phi). No clear porosity-depth trend in Hod. Similar log pattern as in Diamant-1, Bertel-1, Gwen-2 and Jette-1. (log plot)
- Max phi c. 20-25% in Tor and Ekofisk. Ekofisk tight separated from clean Ekofisk and Tor. Tor plot on a well-defined V-phi but, fairly ‘stiff’, but not as ‘stiff’ as in Bertel-1. Hod has very low phi (lower than Gwen-2). High GR plot in the lower left corner of the V-phi data (low V). (V-phi plot)
- Estimate of overpressure results in a match between normal trend and sonic data vs effective depth. ‘Cementation front’ within Tor. (V-Z plot)

Ravn-1

- Thick chalk section (c. 700 m) where GR is relatively high in Ekofisk and relatively low in Tor. Very similar to Ravn-2 and W-1 – also a high-porosity interval in Hod (3630 m kb) is reflected in low Vp. Extends deeper than Ravn-2. (log plot)
- Max phi c. 20% in Ekofisk and Tor. Slightly lower phi and higher Vp than in W-1 matches deeper burial of chalk in Ravn-1. Hidra reveal high GR and low phi, plot similarly as Hod. High GR plot in the lower left corner of the V-phi data (low V). (V-phi plot)
- Estimate of overpressure results in a good match between normal trend and sonic data vs effective depth. 'Cementation front' represented by gradual increase of velocity below effective depth of 1500 m within Hod (cf. Sine-1). (V-Z plot)

Ravn-2

- Thick chalk section (c. 700 m) where GR is relatively high in Ekofisk and relatively low in Tor. Sharp drop of phi from Tor to Hod (increase in V). Hidra reveal high GR and low phi. Very similar to Ravn-1 and W-1 – also a high-porosity interval in Hod (3600 m kb) is reflected in low Vp. (log plot)
- Max phi c. 20-25% in Tor. Lower minimum phi than in Ravn-1 even though the Ravn-1 chalk section extends to greater burial – differences in porosity estimation? High GR plot in the lower left corner of the V-phi data (low V). (V-phi plot)
- Estimate of overpressure results in a good match between normal trend and sonic data vs effective depth. 'Cementation front' represented by gradual increase of velocity below effective depth of 1500 m. (V-Z plot)

Rigs-2

- Very thin chalk section (c. 50 m) with no GR difference between Ekofisk and Tor. Clear peak in Vp and Vs at top Tor. High oil saturation in Tor. Low Vp-Vs ratio – maybe related to invasion of mud filtrate and problematic estimation of Vs in very high-porosity chalk (see Japsen et al. 2004). (log plot)
- Max phi c. 40-45% in Tor and Ekofisk. The V-phi plot reveals a separation of the Ekofisk and Tor formations with the pure Tor formation shifted towards higher porosities. No clear GR separation of the data. (V-phi plot)
- Estimate of overpressure results in a poor match between normal trend and sonic data vs effective depth. Possibly due to high porosities caused by porosity preservation due to early hydrocarbon entry. Section above 'Cementation front'. (V-Z plot)
- Vs plot above the MUHS trend – maybe data problems. (Vs-phi plot)
- Low Vp/Vs for Tor and Hod – see above. (Vp/Vs-phi plot)

SA-1 TVD ??

- Fairly thin chalk section (c. 200 m) with GR difference between Ekofisk and Tor. This separation is not seen on the Vp/Vs log because of the high oil saturation in the Tor formation (low Vp). (log plot)

- Max phi c. 30-35% in Tor. The V-phi plot reveals a clear separation of the Ekofisk and Tor formations with the pure Tor formation shifted towards higher porosities. Fluid substitution of the Tor data would shift them up towards the MUHS trend – and thus a higher trend than seen in most wells (apart from Jette-1). This argument assumes that there are no problems with invasion of mud filtrate in the well (as in the high-porosity Rigs-2 well). No clear GR separation of the data. (V-phi plot)
- Estimate of overpressure results in good match between normal trend and sonic data vs effective depth. This indicates that the porosities in SA-1 are agreement with the present effective stress (in contrast to Rigs-2 where porosities are relatively high). Section above 'Cementation front'. (V-Z plot)
- Vs plot along MUHS trend as for Jette-1 data (in sharp contrast to Isak-1). Bad Vs data for Ekofisk. (Vs-phi plot)
- Low Vp/Vs for Ekofisk and Tor – probably due to low density of hydrocarbons. Fluid substitution would result in a high Vp/Vs ratio (probably close to the MUHS trend and quite different from Jette-1). (Vp/Vs-phi plot)

Sine-1

- Very thick chalk section (c. 1000 m) without clear GR difference between Ekofisk, Tor and Hod. The GR level is high (40 to 50 API) and fairly scattered. The uniform level may correspond to that seen in Skjold Flank-1 and thus simply reflect very uniform chalk. This interpretation is also supported by the symmetry between the GR and the Vp/Vs logs. The Vp/Vs-log has a very broad range. Consistent depth trends are seen for phi and Vp in the upper part of Tor (above c 2100 m MD) and in Hod. The lower part of Tor reveals remarkably stable values of ϕ and Vp over c. 300 m. The log pattern is similar to Skjold Flank-1, but with a more clearly developed intra-chalk unconformity in Sine-1 – probably due to differences in the physical parameters across the unconformity in Sine-1. The hiatus is very small at this unconformity for both wells (see Appendix 1). (log plot)
- Max phi up to 40% in Tor – large range of both phi and Vp, and a fairly narrow trend in the data set. Apparently a slight shift in the V-phi trends for Tor and Hod, but few data points for ϕ between 15 and 20%. However, the chalk is probably very uniform and the general trend related to depth-dependent 'compaction' (cf. the Skjold Flank-1 well). (V-phi plot)
- Estimate of overpressure results in a good match between normal trend and sonic data vs effective depth (maybe slightly underestimated overpressure – or slightly to high normal velocity-depth trend). Note the relatively low P-velocities in the lower part of Tor. 'Cementation front' in uppermost part of Hod. (V-Z plot)
- Rather high Vp/Vs for Tor and Hod: plots as a smile versus phi with a range from 1.85 to 2.05 (similar to Skjold Flank-1). Data between 5 and 25% plot near the MUHS/MLHS trends. Whereas Vp plots close to the MLHS trends (Vp-phi), Vs plots slightly below the MLHS trend for the upper part of Tor (Vs-phi plot not shown). Lowest part of Hod and Hidra show relatively low Vp/Vs. (Vp/Vs plots)

Skjold Flank-1

- Fairly thick chalk section (c. 600 m) without clear GR difference between Ekofisk, Tor and Hod. The GR level is high (30 API), but the uniform level may correspond to that seen in Sine-1 and thus simply reflect very uniform chalk. This interpretation is also supported by the symmetry between the GR and the Vp/Vs logs. The Vp/Vs-log has a fairly broad range and even a cyclicity in the Tor Formation with a wavelength of about 10 m. This cyclicity is not seen on the porosity-log and may well be an artefact. A consistent depth trend is seen for phi and Vp in the Tor and especially the Hod. The log pattern is similar to Sine-1, but with a less clearly developed intra-chalk unconformity. The hiatus is very small at this unconformity for both wells (see Appendix 1). (log plot)
- Max phi c. 30% in Tor – large range of both phi and Vp, but also a large scatter in the data set. No V-phi separation between Tor and Hod in agreement with the uniform GR log for both formations: The chalk is probably very uniform and the general trend related to depth-dependent ‘compaction’ (cf. the Sine-1 well). (V-phi plot)
- Estimate of overpressure results in a good match between normal trend and sonic data vs effective depth (maybe slightly to high normal velocity-depth trend). ‘Cementation front’ in uppermost part of Hod. (V-Z plot)
- Rather high Vp/Vs for Tor and Hod: plots as a smile versus phi with a range from 1.9 to 2, but large scatter (and unlikely variations in Vs seen in plot of Vp vs Vs). Whereas Vp plots in between the MUHS and MLHS trends (Vp-phi), Vs plots towards the MLHS trend (Vs-phi plot not shown). (Vp/Vs plots)

T-1

- Thin chalk section (c. 100 m) with GR separation between Ekofisk, Tor (thin) and most of Hod. Low Sw in Tor. Log pattern a condensed version of T-3. (log plot)
- Max phi c. 30% in Ekofisk and Tor. Low Vp in Tor due to HC. High GR plot in the lower left corner of the V-phi data (low V, Ekofisk tight). (V-phi plot)
- Estimate of overpressure results in a very poor match between normal trend and sonic data vs effective depth. Maybe salt diapirism has moved the chalk to a more shallow depth or overpressure is increased by transfer from more deeply buried chalk. Section above ‘Cementation front’. (V-Z plot)

T-3

- Fairly thin chalk section (c. 300 m) with slightly higher GR for Ekofisk. Some HC in upper part of Tor. General depth trend for Vp and phi. Comparable to T-3. (log plot)
- Max phi c. 30% in Tor and Ekofisk. Separation of Ekofisk, Tor and Hod similar to Isak-1 (but higher V-phi level for T-3). No clear GR separation of the data. (V-phi plot)
- Estimate of overpressure results in a poor match between normal trend and sonic data vs effective depth. Maybe salt diapirism has moved the chalk to a more shallow depth or overpressure is increased by transfer from more deeply buried chalk. Section above ‘Cementation front’. (V-Z plot)

W-1

- Thick chalk section (c. 700 m) where GR is relatively high in Ekofisk and relatively low in Tor. A high-porosity interval in Hod (3650 m kb) is reflected in low Vp. Log pattern comparable to Diamant-1 and Jette-1. (log plot)
- Max phi c. 25% in Ekofisk and Tor. Uppermost part of Ekofisk plot outside normal V-phi chalk area, Ekofisk tight clearly separated from clean Ekofisk and Tor. (V-phi plot)
- Estimate of overpressure results in a good match between normal trend and sonic data vs effective depth. 'Cementation front' within Tor. (V-Z plot)

West Lulu-1

- Fairly thick chalk section (c. 600 m) with clear GR difference between Ekofisk, Tor and Hod. An overall depth trend is seen for phi and Vp in the thick Tor formation. High GR in the thick Ekofisk formation correlates with low phi. Similar to the logs from the Jette-1 well (log plot)
- Max phi c. 25-30% in Tor. The V-phi plot reveals a clear separation of the Ekofisk, Tor and Hod formations: Ekofisk tight separated from clean Tor, which has a well-defined trend with a very large phi-range. High-GR Ekofisk and Hod plot towards lower phi-V. The data plot quite similarly to the data from the Jette-1 well, also along a high V-phi trend. (V-phi plot)
- Estimate of overpressure results in a good match between normal trend and sonic data vs effective depth. 'Cementation front' within Tor. (V-Z plot)

6. Data CD

Lithostratigraphic subdivision

Excel file with depth to individual boundaries in the wells

Filename: lithological subdivision.xls

CGM files with cross correlation of log data

Filenames:

correl1.cgm: Arne-Elin Graben – NW Adda-1 – Sine-1

correl2.cgm: Mandal High – Svend Field – Gertrud and Feda Grabens

correl3.cgm: Inge High – Heno Plateau

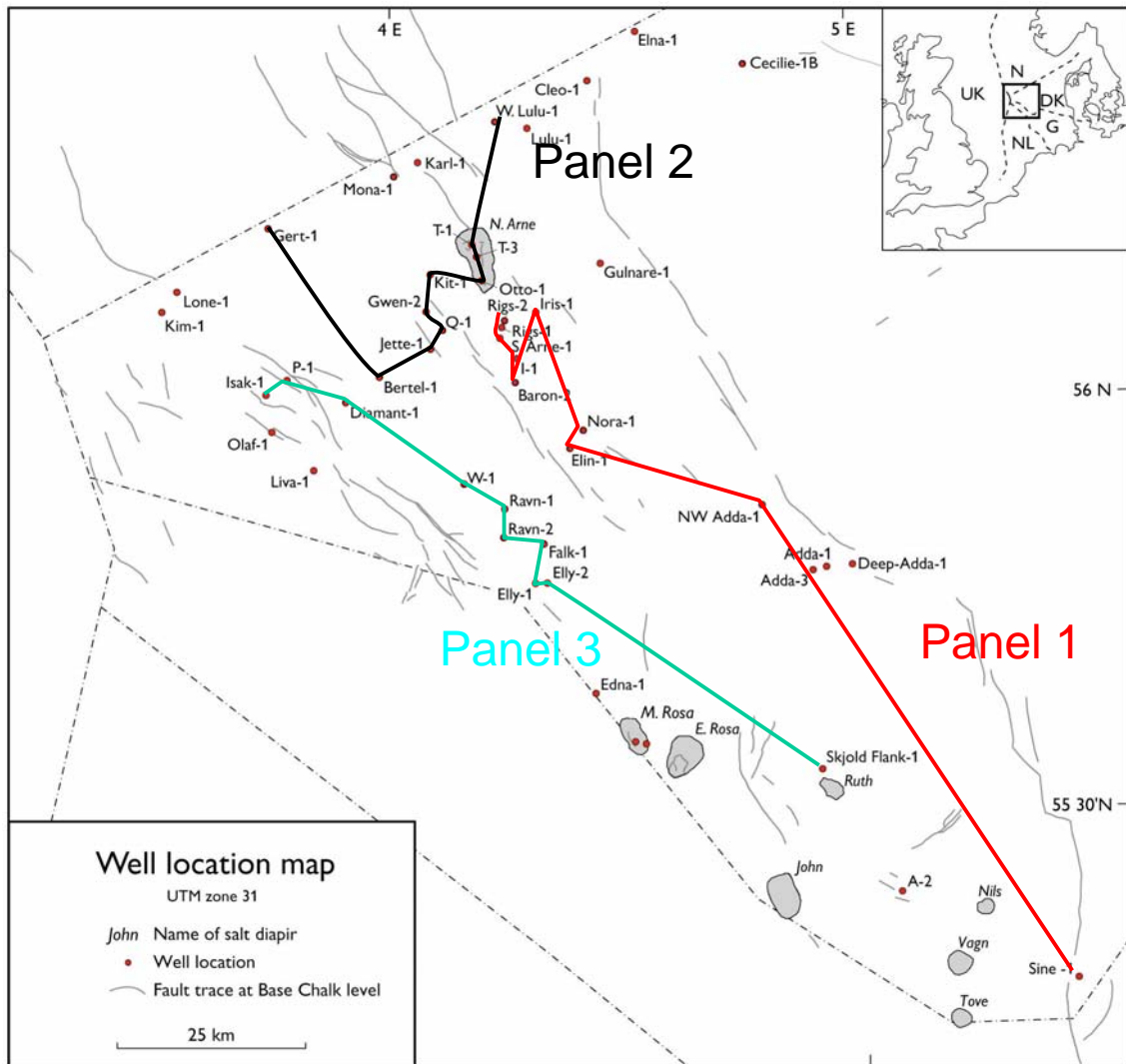


Figure 6.1. Location of the stratigraphic correlation panels

Acoustic properties

Power Point files with cross plots of log data

Filenames: <wellname<.ppt:

Baron-2
Bertel-1A
Diamant-1
Elin-1
Elly-1
Elly-2
Falk-1
Gert-1
Gwen-2
I-1
Iris-1
Isak-1
Jette-1
Nora-1
NW Adda-1
Otto-1
P-1
Q-1
Ravn-1
Ravn-2
Rigs-2
SA-1
Sine-1
Skjold Flank-1
T-1
T-3
W. Lulu-1
W-1

MatLab files with log data for the chalk sections in each well

Filenames:

v6_<wellname>.m (MatLab version 6)

v7_<wellname>.m (MatLab version 7)

Parameters:

d	depth, m below kb (array)
d1, d2,	depth to top and base chalk, m below kb (scalar)
dmax, dmin	min and max depths used in log plots (scalar)
dp	chalk formation overpressure, 100xMPa (scalar)
dref	distance between kb and sea bed, m (scalar)
dtp, dts	transit time for P- and S-waves, micro sec/foot (array)
g = g_i	shear modulus, GPa (array)
gr	gamma ray (scalar)
i, j	indices (scalar)
k_w=k_w_i	bulk modulus, GPa (array)
litho	lithology code*, - (array)
m_w	P-wave modulus, GPa (array)
nu_w	poisson's ratio. – (array)
phi	porosity, - (array)
rho	density, g/cm ³ (array)
sw	water saturation, - (array)
vp, vs	P- and S-wave velocity, m/s (array)
zb_eko, zb_hdr, zb_hod, zb_plm, zb_tor, zt_eko, zt_hdr, zt_hod, zt_plm, zt_tor	depth to top and base Ekofisk/Hidra/Hod/Plenus Marl/Tor formations

*) lithology code:

- 1 – Ekofisk Fm
- 2 – Tor Fm
- 3 – Hod Fm
- 4 – Plenus Marl
- 5 – Hidra Fm

If the thickness of any of these units is less than 1 m the unit is not present in the well but only included in the data set in this way to avoid problems with the legends in the cross plots.

7. References

- Britze, P., Japsen, P. & Andersen, C. 1995. Geological map of Denmark 1:200,000. The Danish Central Graben. "Base Chalk" and the Chalk Group (two-way travelttime and depth, interval velocity and isochore). Geological Survey of Denmark Map Series **48**.
- Chiarelli, A. and F. Duffaud, 1980, Pressure origin and distribution in Jurassic of Viking Basin (United Kingdom-Norway): AAPG Bulletin **64**, 1245–1250.
- Dickinson, G. 1953. Geological aspects of abnormal reservoir pressures in Gulf Coast Louisiana. AAPG Bulletin **37**, 410–432.
- Foged, N., A. Krogsbøll, C.F. Hansen, K. Zinck-Jørgensen, H.F. Christensen and J.-E. Jepsen, 1995, EFP-93. Modelling of stresses and fractures in a reservoir. Final report. Copenhagen, DGU/DGI, 68 pp.
- Gradstein F.M., Agterberg, F. P., Ogg, J. G., Hardenbol, J., Veen, P.v., Thierry, J. & Huang, Z. 1995: A Triassic, Jurassic and Cretaceous time scale. Geochronology time scales and global stratigraphic correlation. SEPM Special Publication **54**, 95–126.
- Isaksen, D. and Tonstad, K. (Eds.) 1989. A revised Cretaceous and Tertiary lithostratigraphic nomenclature for the Norwegian North Sea. NPD-Bulletin **5**, Oljedirektoratet, Stavanger, 59 pp.
- Japsen, P., 1994, Retarded compaction due to overpressure deduced from a seismic velocity/depth conversion study in the Danish Central Trough, North Sea: Marine and Petroleum Geology **11**, 715–733.
- Japsen, P. 1998. Regional velocity-depth anomalies, North Sea Chalk: a record of overpressure and Neogene uplift and erosion. AAPG Bulletin **82**, 2031–2074.
- Japsen, P. 2000. Investigation of multi-phase erosion using reconstructed shale trends based on sonic data. Sole Pit axis, North Sea. Global and Planetary Change **24**, 189–210.
- Japsen, P., Bruun, A., Fabricius, I.L., Rasmussen, R., Vejbæk, O.V., Pedersen, J.M., Mavko, G., Mogensen, C. & Høier, C. 2004. Influence of porosity and pore fluid on acoustic properties of chalk: AVO-response from oil, South Arne Field, North Sea. Petroleum Geoscience **10**, 319–330.
- Lieberkind, K., Bang, I., Mikkelsen, N. & Nygaard, E. 1982: Late Cretaceous and Danian Limestones. *In* Michelsen, O. (ed) Geology of the Danish Central Graben. Danmarks Geologiske Undersøgelse **B8**, 45–49.
- Knudsen, P., 1993, Integrated inversion of gravity data: National Survey and cadastre - Denmark, Geodetic Division, technical report **7**, 52 pp.
- Nielsen, L.H. and P. Japsen, 1991, Deep wells in Denmark, 1935-1990; lithostratigraphic subdivision: Geological Survey of Denmark, Series A **31**, 179 pp.
- Oakman, C. D. & Partington, M. A. 1998. Cretaceous. *In* K.W. Glennie, (ed.) Petroleum geology of the North Sea, basic concepts and recent advances, 4th edition: London, Blackwell Science Limited, 294–349.
- Ødegaard A/S 2005. Quality control and petrophysical evaluation of Danish North Sea wells. Report.
- Osborne, M.J. & Swarbrick, R.E. 1997. Mechanisms for generating overpressure in sedi-

- mentary basins: A reevaluation. AAPG Bulletin **81**, 1023–1041.
- Petroleum Information (Erico) 1995. Danish Central Trough. Formation pressure database and regional evaluation. 47 pp.
- Robertson Research International 1984: The Danish North Sea Area: The stratigraphy and petroleum Geochemistry of the Jurassic to Tertiary sediment. Robertson Report
- Prasad, M. & Manghnani 1997. Effects of pore and differential pressure on compressional wave velocity and quality factor in Berea and Michigan sandstones. *Geophysics* **62**, 1163–1176.
- Rubey, W.W. & Hubbert, M.K. 1959. Role of fluid pressure in mechanics of overthrust faulting, II. Geological Society of America Bulletin **70**, 167–206.
- Sclater, J.G. & Christie, P.A.F. 1980. Continental stretching; an explanation of the post-Mid-Cretaceous subsidence of the central North Sea basin. *Journal of Geophysical Research* **85**, 3711–3739.
- Surlyk, F., Dons, T., Clausen, C.K. & Highan, J. 2003: Upper Cretaceous. In: D.Evans, C. Graham, A. Armour & P. Bathurst (eds), 2003. The Millennium Atlas. Petroleum geology of the Central and Northern North Sea.
- Terzaghi, K. & Peck, R.P. 1968. Soil mechanics in engineering practice, John Wiley and Sons, New York.
- The Millennium Atlas. Petroleum geology of the Central and Northern North Sea. (Eds.) D.Evans, C. Graham, A. Armour & P. Bathurst, 2003. Geol.Soc. London.
- Vejbæk, O.V., Rasmussen, R., Japsen, P., Pedersen, J.M., Fabricius, I.L. & Marsden, G. *in press*. Modelling seismic response from North Sea Chalk reservoirs resulting from changes in burial depth and fluid saturation. In: Doré, A.G. & Vining, B. (eds) Petroleum Geology: NW Europe and Global Perspectives: Proceedings of the 6th Conference. Geological Society, London.
- Vejbæk, O. V. & Andersen, C. 1987: Cretaceous-Early Tertiary inversion tectonism in the Danish Central Trough. In: Ziegler, P. A. (ed.) Compressional intra-plate deformations on the Alpine foreland. *Tectonophysics* **137**, 221–238.
- Vejbæk, O. V. & Andersen, C. 2002: Post mid-Cretaceous inversion tectonics in the Danish Central Graben – regional synchronous tectonic events? *Bulletin of Geological Society of Denmark* **49**, 129–144
- Walls J.D., Dvorkin J. & Smith B.A. 1998. Modeling seismic velocity in Ekofisk Chalk. *In: 1998*, SEG, Tulsa, 1016–1019.

Appendix 1: Lithostratigraphic subdivision

Formation tops in 29 wells. Bold numbers refer to the main lithostratigraphic formations. Normal font numbers refer to subunits. Grey pattern indicate a hiatus identified in the wells. The data indicate a regional hiatus (the Intra-Chalk Unconformity) associated with the top of the Hod formation. The time span related to with the Intra-Chalk Unconformity varies according to basin setting.

Chronostratigraphy		Correlations horizons	Short	Baron-2	Bertel-1	Diamant-1	Elin-1	Elly-1	Elly-2	Falk-1	Gert-1	Gwen-2	I-1
				m MD	m MD	m MD	m MD	m MD	m MD	m MD	m MD	m MD	m MD
Danian		Top Chalk	Top Chalk	2826	3147,5	3050	2733,5	2855	2857	2901	3150,5	3078	2764,5
		Ekofisk 3	Eko3	2841	3174	3063		2857	2858,5	2922	3179,5	3097	
		Ekofisk 2	Eko 2	2860	3196	3073	2733,5	2864	2866	2940,5	3205	3103,5	2764,5
		Ekofisk 1	Eko 1	2880	3221	3097	2746	2867,5	2874	2955	3229	3122,5	2779
Maastrichtian	Latest	Top Tor	Top Tor	2905	3259	3139	2751	2883	2900	2991,5	3277,5	3155,5	2798
		Upper Tor 2	UT2		3281	3182	2753	2891	2918,5	3012,3	3276,5	3170,5	
		Upper Tor 1	UT1		3336	3207,5	2779	2925	2947,5	3029,7	3304	3201	2798
	Late	Middle Tor 2	MT2		3401	3229	2806		2994	3054	3348,5	3252,5	2805
		Middle Tor 1	MT1		3522	3257					3406	3335	
	Early	Lower Tor 3	LT3		3460,5	3308					3453	3400	
		Lower Tor 2	LT2		3521								
Lower Tor 1		LT1											
Campanian	Late	Top Hod	Top Hod	2905	3521	3308	2806	2925	2994	3054	3453	3400	2805
		Upper Hod 4	UH4		3575	3344,5		2963	3018	3116,5		3460	
		Upper Hod 3	UH3		3646	3412,5		3006	3050	3163		3526,5	
	Early	Upper Hod 2	UH2		3694	3454		3037	3082	3224	3453	3587,5	
		Upper Hod 1	UH1		3731	3485		3055,5	3120	3280,5	3479,5	3631,5	
Santonian		Middle Hod 4	MH4		3799	3533	2806	3105,5	3137	3332	3528	3666	
		Middle Hod 3	MH3		3837	3533	2821	3179	3209	3378,5	3591,5	3718	
Coniacian		Middle Hod 2	MH2	2905	3866,5	3554	2848,5	3214	3253	3410	3626	3742	2805
		Middle Hod 1	MH1	2930	3908	3579	2868	3263	3291	3449	3671	3763	2821,5
Turonian		Lower Hod 4	LH4	2949	3949	3631	2915		3323,5	3483	3730	3800	2852
		Lower Hod 3	LH3		4010,5				3365	3495	3781	3837,5	
		Lower Hod 2	LH2		4077				3397	3516,5	3832	3900,5	
		Lower Hod 1	LH1		4181	3631			3432	3556	3870	3967	
Cenomanian		Top Plenus Marl			4238								
		Top Hydra			4248	3660	2915	3263	3467	3580,5	3906	4024	
Albian		Base Chalk	Base Chalk	2949	4264	3693,5	2943,5	3790	3486	3603,5	3930,5	4041	2852

Chronostratigraphy		Correlations horizons	Short	Iris-1	Isak-1	Jette-1	Nora-1	NW-Adda-1	Otto-1	P-1	Q-1	Ravn-1	Ravn-2
				m MD	m MD	m MD	m MD	m MD	m MD	m MD	m MD	m MD	m MD
Danian		Top Chalk	Top Chalk	2902	2925,5	3076,5	2597	2296	2477	2919,5	3070	3054	3052
		Ekofisk 3	Eko3	2907	2932	3097	2606	2312,5	2481	2931,5	3098	3054	3062
		Ekofisk 2	Eko 2	2922	2936,5	3117	2616	2329,5	2482,5	2939,5	3108	3072,5	3059
		Ekofisk 1	Eko 1	2935,5	2954,5	3135		2355	2482,5	2969,5	3126	3088	3088
Maastrichtian	Latest	Top Tor	Top Tor	2954	2960	3167	2616	2389,5	2488,5	2993	3163	3102,5	3100
		Upper Tor 2	UT2		2967	3185	2642	2421	2488,5		3185,5	3130	3125
		Upper Tor 1	UT1	2954	2984	3209	2655	2438	2498,5	2993	3210,5	3164	3149
	Late	Middle Tor 2	MT2	2980	3011	3256,5	2663	2465,5	2507	3007	3242	3184	3161
		Middle Tor 1	MT1	2989	3044	3338,5	2678,5		2555,5		3333	3228	3188
	Early	Lower Tor 3	LT3	3020	3065,5	3406	2719		2583		3400	3244	
		Lower Tor 2	LT2										
		Lower Tor 1	LT1										
Campanian	Late	Top Hod	Top Hod	3020	3065,5	3406	2719	2465,5	2583	3007	3400	3244	3188
		Upper Hod 4	UH4			3415			2583		3474	3250	3261
		Upper Hod 3	UH3			3481			2604	3007	3544,6	3314	3318
	Early	Upper Hod 2	UH2	3020		3532,5	2719		2620,5	3042,5	3600	3364	3360
		Upper Hod 1	UH1	3040		3567,5	2740		2660	3073,5	3628,5	3412,5	3392
Santonian		Middle Hod 4	MH4	3062		3626,5	2753,5				3661	3448,5	3457
		Middle Hod 3	MH3	3079		3689	2772	2465,5			3725,5	3495,5	3498
Coniacian		Middle Hod 2	MH2	3089	3065,5	3734,5	2779	2478	2660	3073,5	3757	3561	3533
		Middle Hod 1	MH1	3103,5	3083,2	3780,5	2787	2505,5	2682,5	3094,5	3790	3596	3576
Turonian		Lower Hod 4	LH4	3115	3137,8	3919	2807,5	2542,5	2722,5	3120	3830	3652	3614
		Lower Hod 3	LH3	3133	3187,5	3845	2825			3120	3855	3687	3631,5
		Lower Hod 2	LH2	3155	3218,5	3877,5	2858			3137	3890	3716	3657,5
		Lower Hod 1	LH1	3173		3908				3155	3915	3744	3692
Cenomanian		Top Plenus Marl		3173									
		Top Hydra		3175		3925	2858	2542,5			3944,5	3778,5	3712
Albian		Base Chalk	Base Chalk	3214,5	3218,5	3942	2899	2555	2722,5	3155	3963	3786	3734

Chronostratigraphy		Correlations horizons	Short	Rigs-1	Rigs-2	SA-1	Sine-1	Skjold Flanke-1	T-1	T-3	W-1	West Lulu-1
				m MD	m MD	m MD	m MD	m MD	m MD	m MD	m MD	m MD
Danian		Top Chalk	Top Chalk	2790	2782	3316	1798	2127	2219,5	2484,5	3088	2875,5
		Ekofisk 3	Eko3	2795	2782	3329	1798	2138	2235	2484,5	3102	2903
		Ekofisk 2	Eko 2	2804,5	2798	3334	1812	2145,5	2235	2494,5	3123,5	2928
		Ekofisk 1	Eko 1	2820	2820	3342	1826	2145,5	2240	2510,5	3145,5	2948,5
Maastrichtian	Latest	Top Tor	Top Tor	2837	2832,5	3360	1857	2174	2260,5	2532	3173,5	2984,5
		Upper Tor 2	UT2	2846	2838	3377	1879	2208	2271	2550	3185,5	3006,5
		Upper Tor 1	UT1	2855	2849	3413	1907,5	2232,5	2283	2576,5	3219	3023,5
	Late	Middle Tor 2	MT2		2865	3433	1954	2275		2590,5	3263,5	3064
		Middle Tor 1	MT1			3470	2046,5	2351		2630	3302	3151
	Early	Lower Tor 3	LT3			3480	2133	2391,5		2662		3190
		Lower Tor 2	LT2				2204,5	2447				
Lower Tor 1		LT1				2321	2494,5					
Campanian	Late	Top Hod	Top Hod				2403	2519	2283	2262	3302	3190
		Upper Hod 4	UH4				2403	2519			3343,5	
		Upper Hod 3	UH3				2431	2547			3423	
	Early	Upper Hod 2	UH2				2448	2575	2283	2662	3500	
		Upper Hod 1	UH1				2465	2597	2325	2686	3544	
Santonian		Middle Hod 4	MH4				2482	2620			3586	3190
		Middle Hod 3	MH3				2523	2620	2325			3278
Coniacian		Middle Hod 2	MH2				2553,5	2640,5	2342	2686	3586	3309,5
		Middle Hod 1	MH1				2587	2662		2695	3611	3345,5
Turonian		Lower Hod 4	LH4				2655,5	2685		2735	3658	3400
		Lower Hod 3	LH3				2672,5	2685				
		Lower Hod 2	LH2				2694	2691,5			3658	3400
		Lower Hod 1	LH1				2741	2720			3698,5	3455
Cenomanian		Top Plenus Marl						2743				
		Top Hidra		2855	2865	3480	2776	2749,5	2342	2735	3726	3477,5
Albian		Base Chalk	Base Chalk	2855	2865	3480	2802	2772	2342	2735	3759,5	3500

Appendix 2: Cross plots of log data

Log displays and cross plots of V_p - ϕ , V_p -Z and ϕ -Z for the chalk in 28 wells:

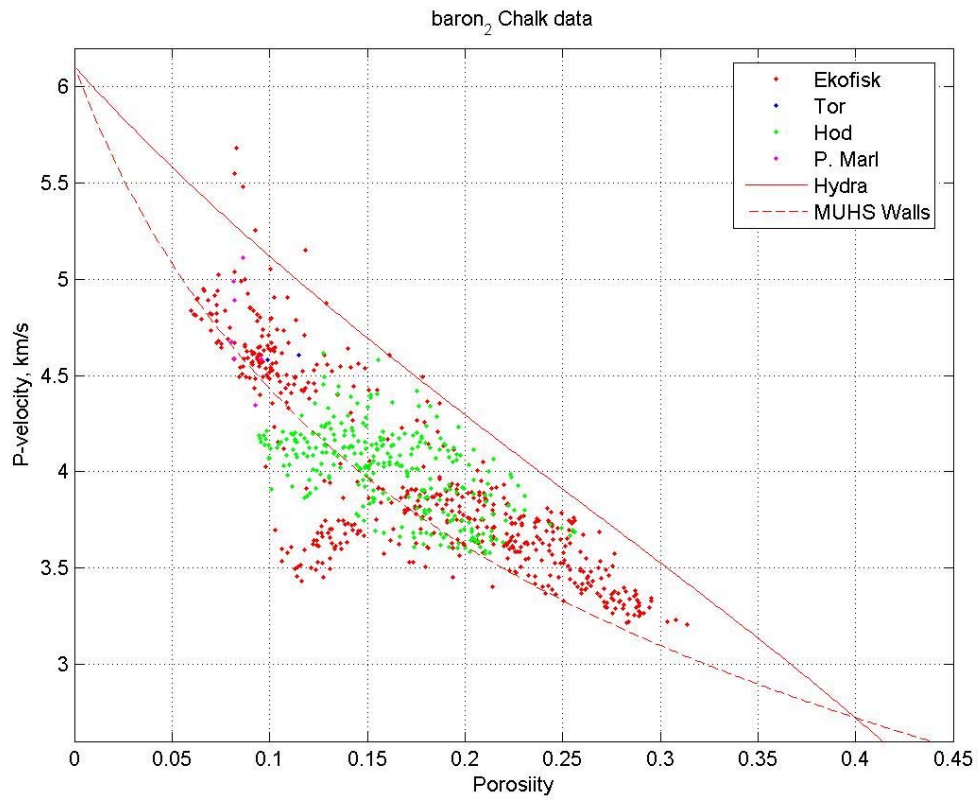
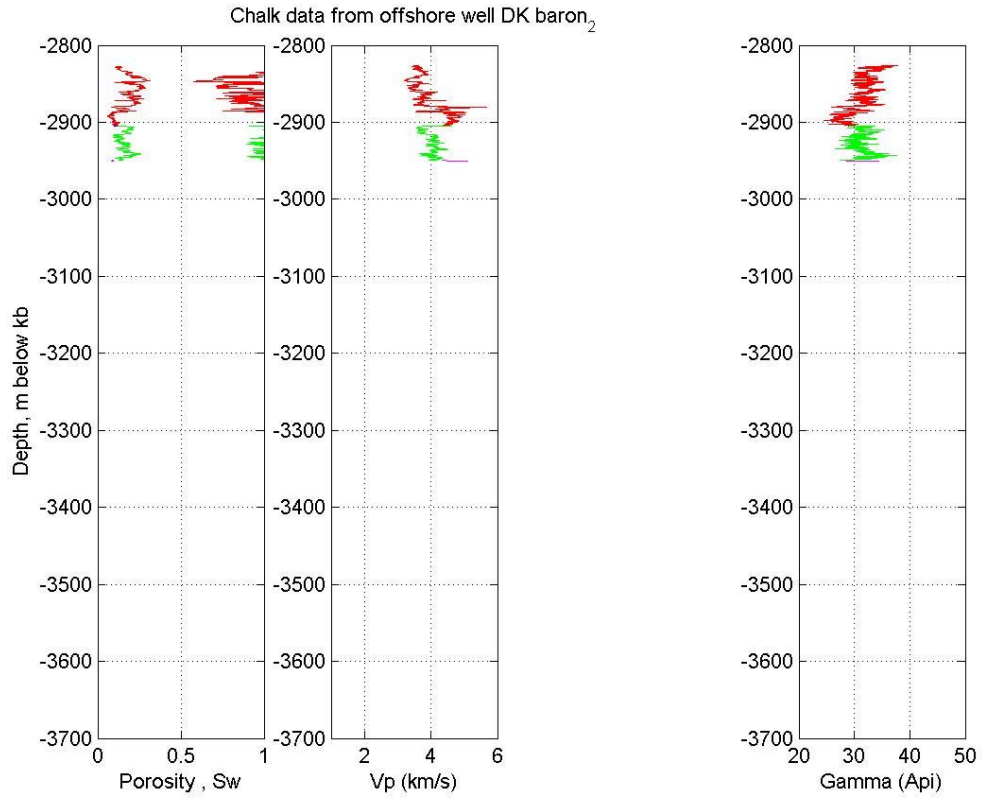
Baron-2
Bertel-1A
Diamant-1
Elin-1
Elly-1
Elly-2
Falk-1
Gert-1
Gwen-2
I-1
Iris-1
Isak-1
Jette-1
Nora-1
NW Adda-1
Otto-1
P-1
Q-1
Ravn-1
Ravn-2
Rigs-2
SA-1
Sine-1
Skjold Flank-1
T-1
T-3
W. Lulu-1
W-1

Cross plots of V_s - ϕ , V_p/V_s - ϕ and V_p - V_s for the chalk in 4 wells:

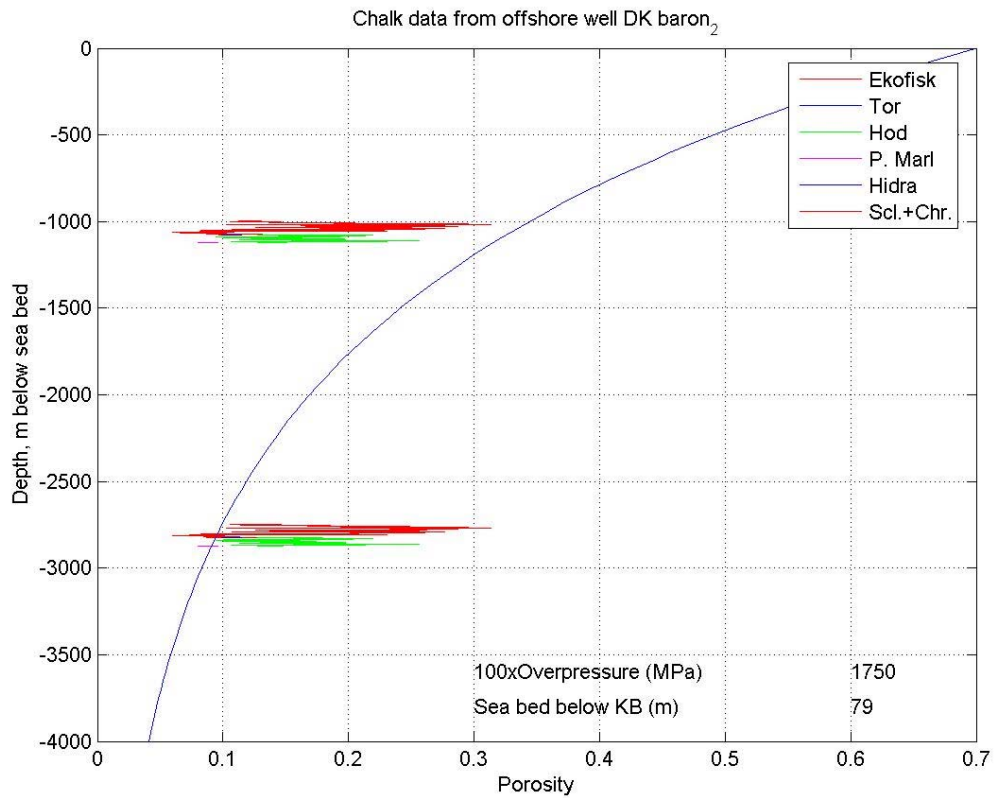
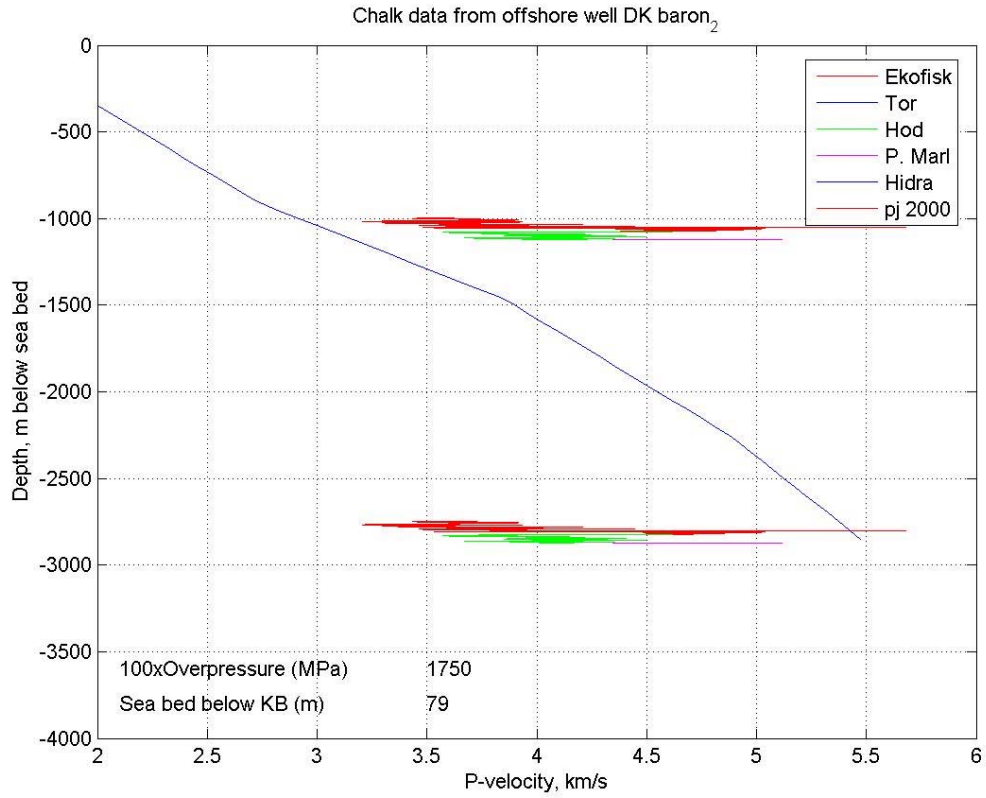
Isak-1
Jette-1
NW Adda-1
Sine-1
Skjold Flank-1

pj 2000: Japsen (2000), Scl.+Chr.: Sclater & Christie (1980), MUHS/MLHS Walls: Modified upper and Lower Hashin-Shtrikman model (Walls et al. 1998).

Vp plots

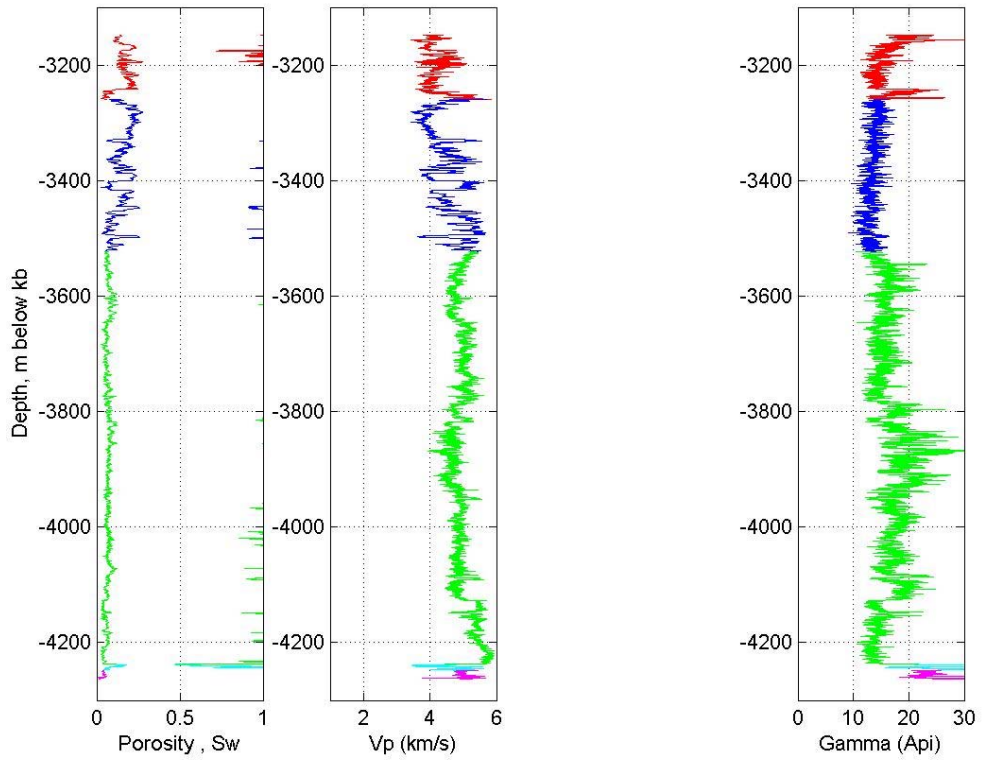


Baron-2

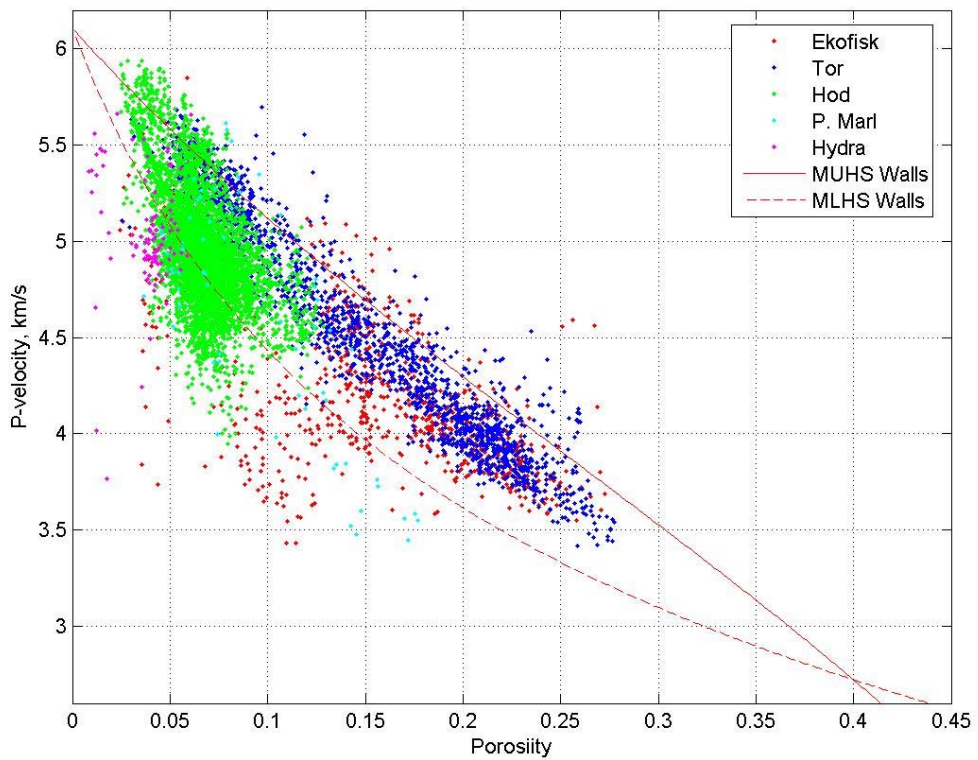


Baron-2

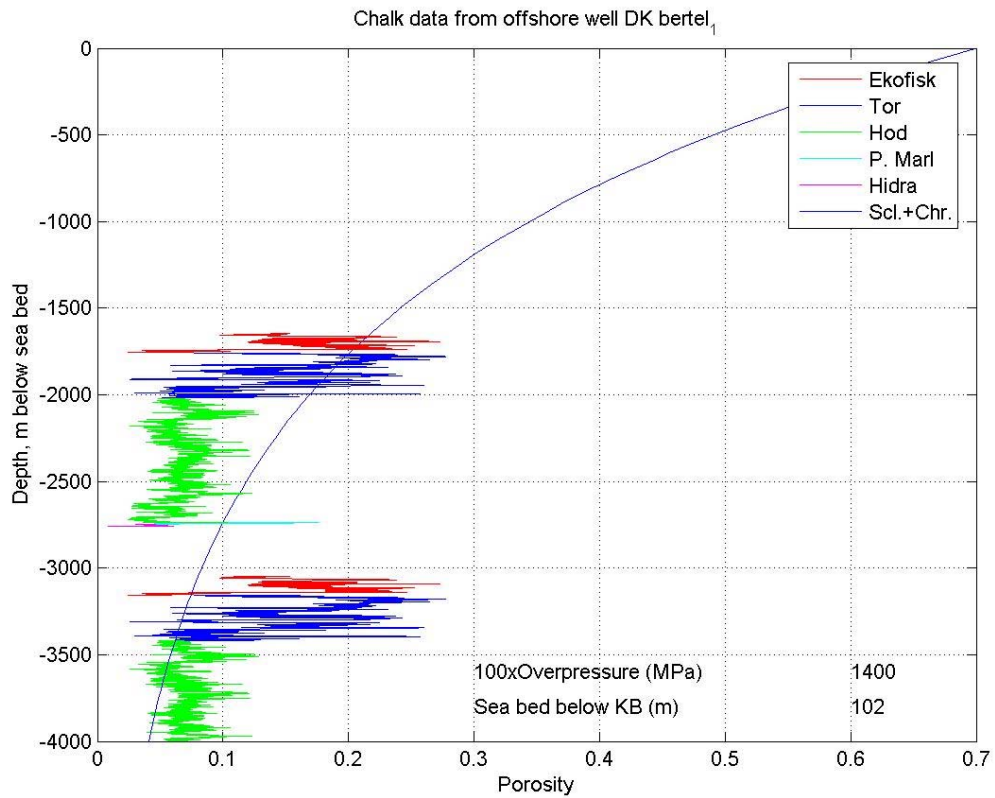
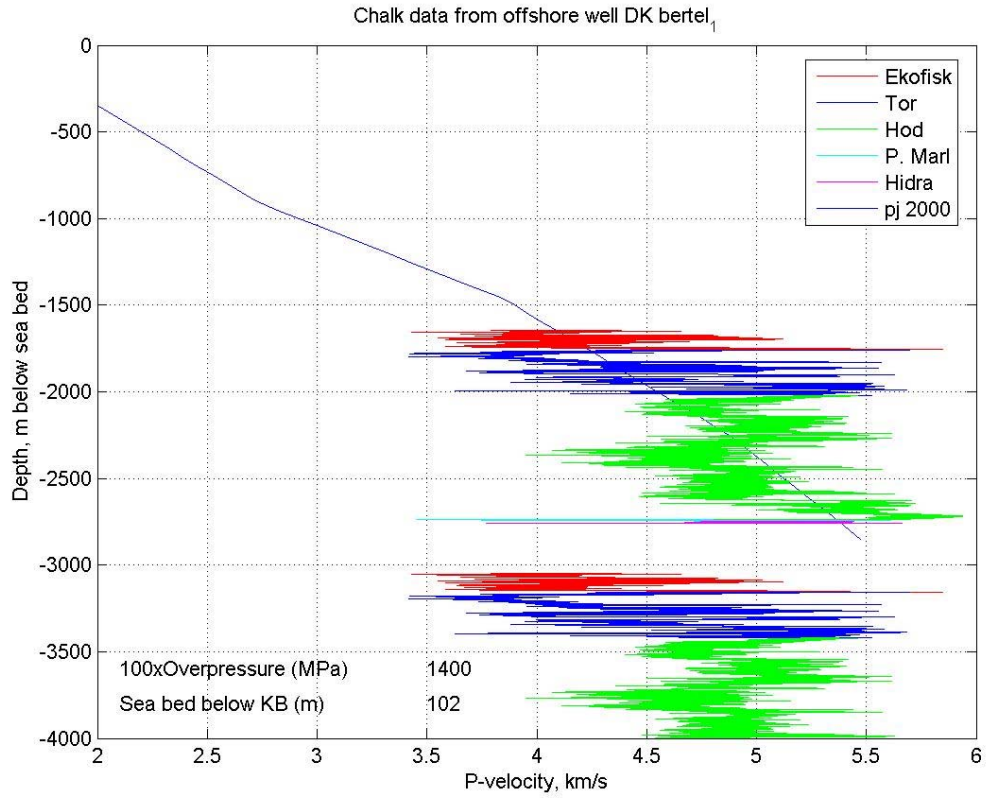
Chalk data from offshore well DK bertel₁



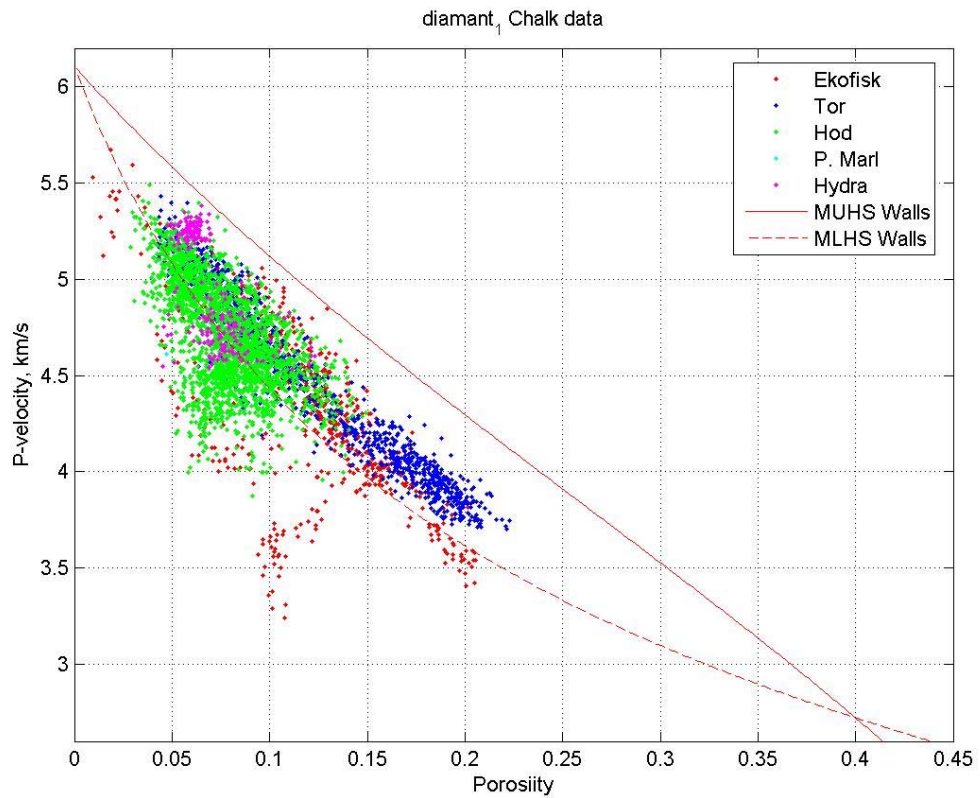
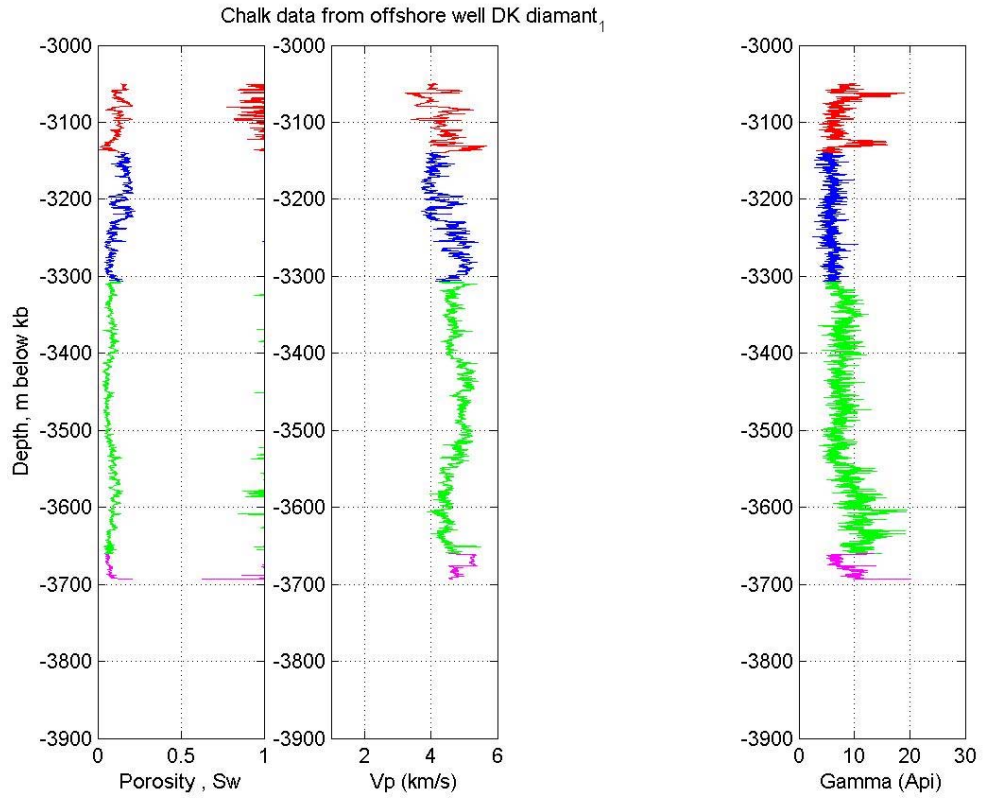
bertel₁ Chalk data



Bertel-1

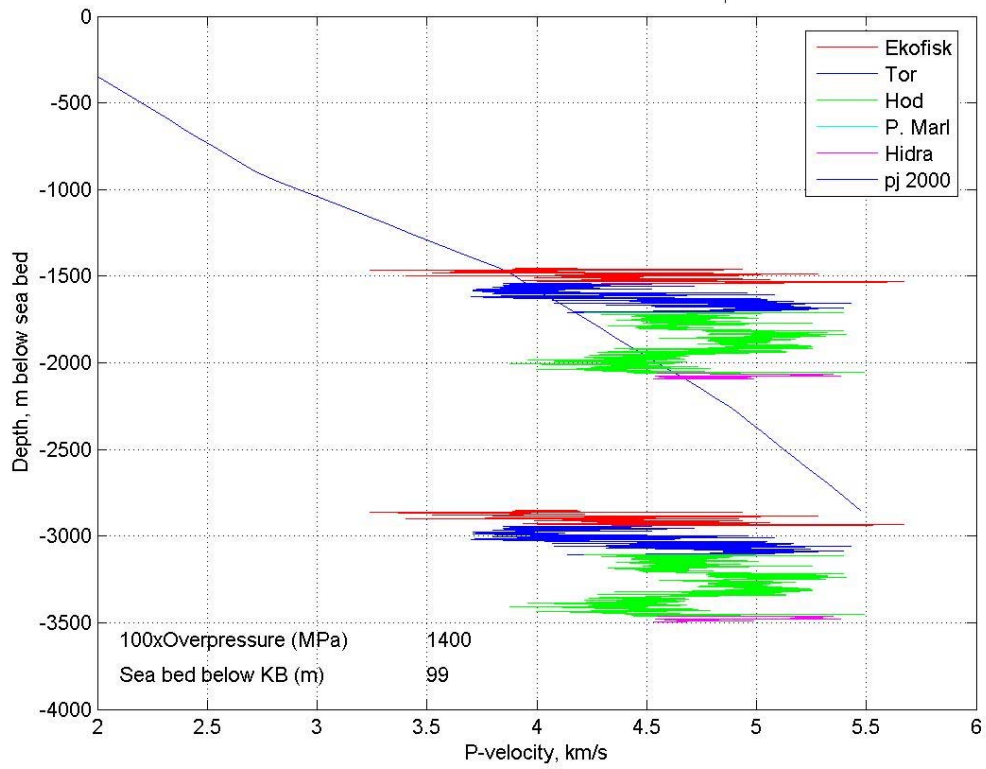


Bertel-1

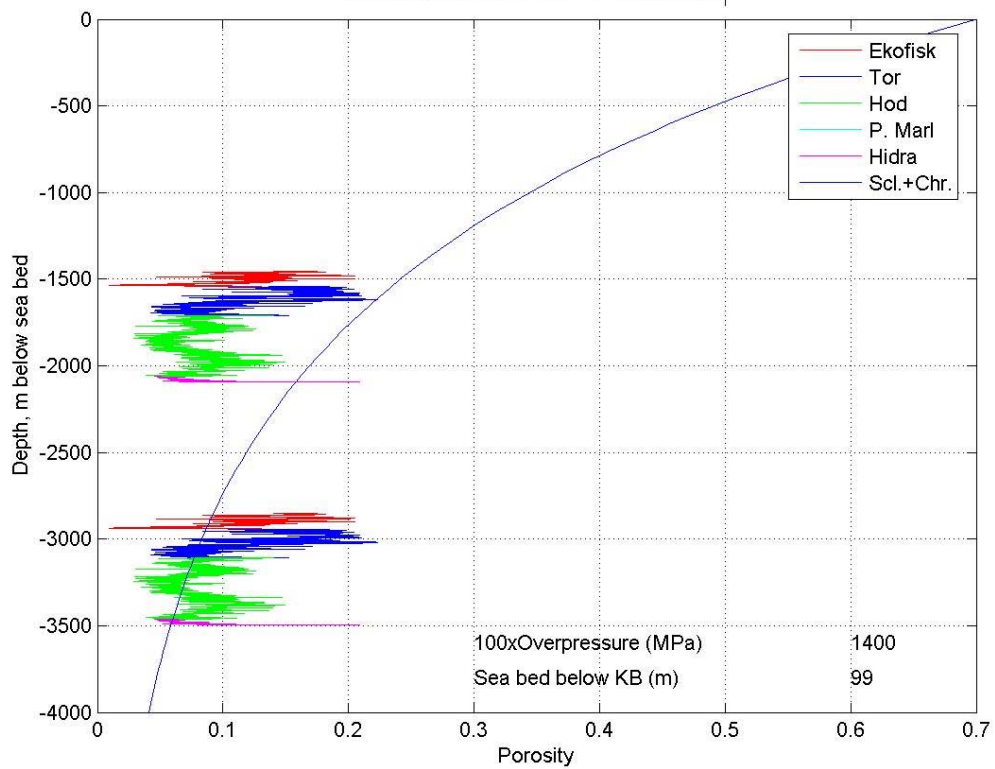


Diamant-1

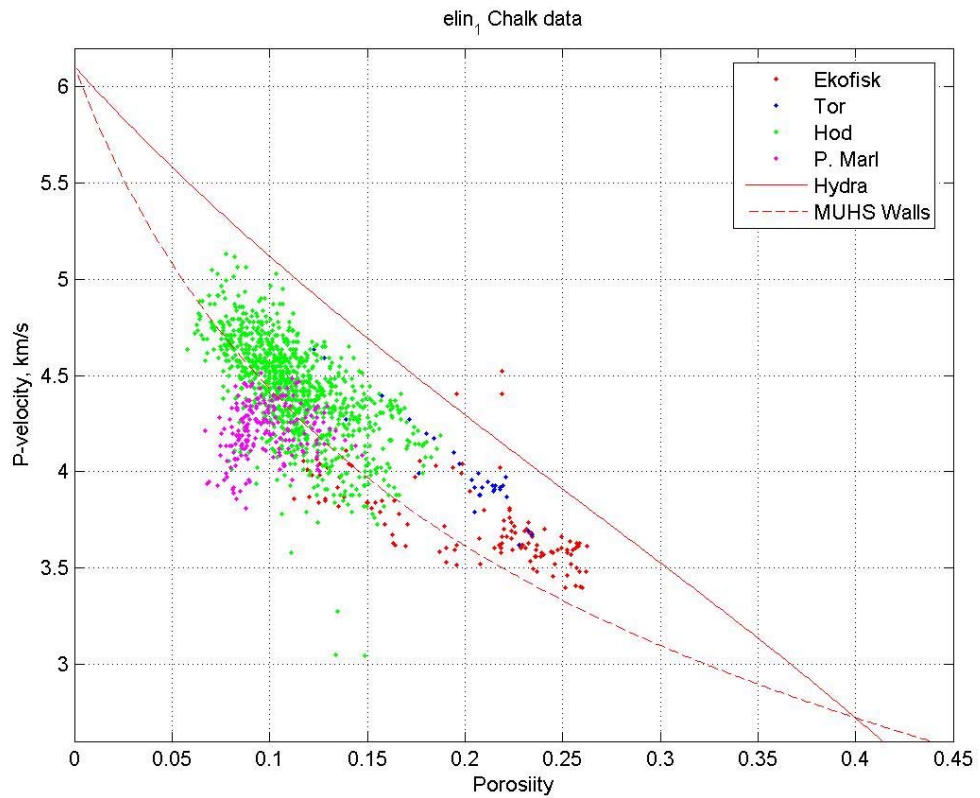
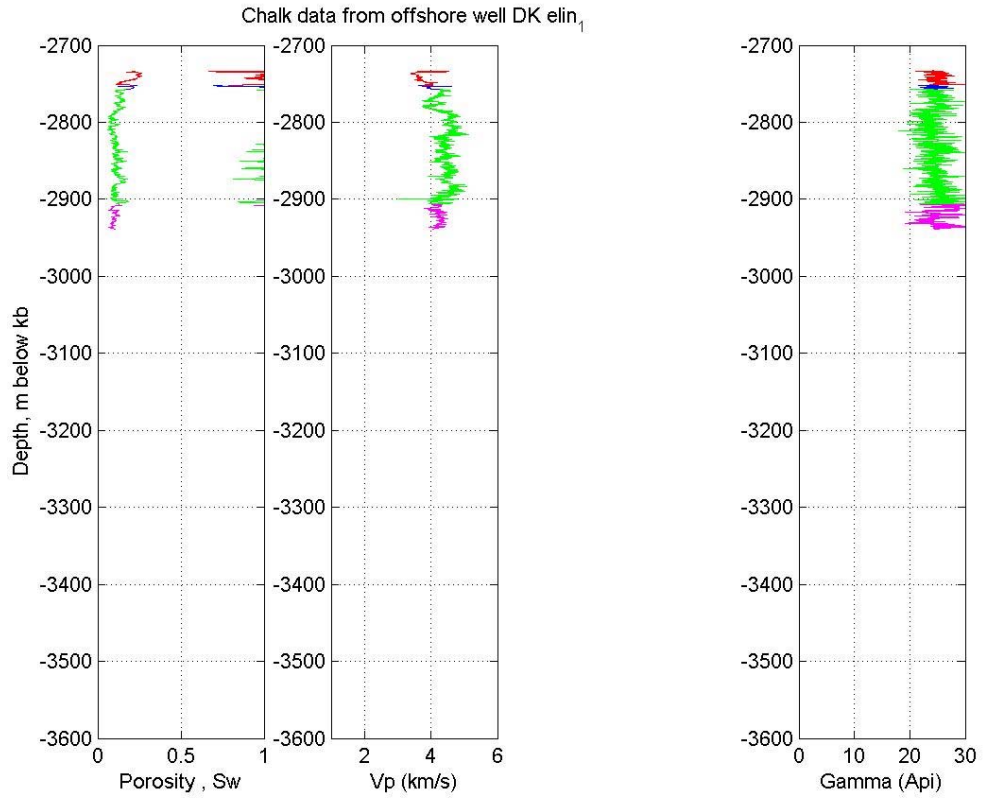
Chalk data from offshore well DK diamant₁



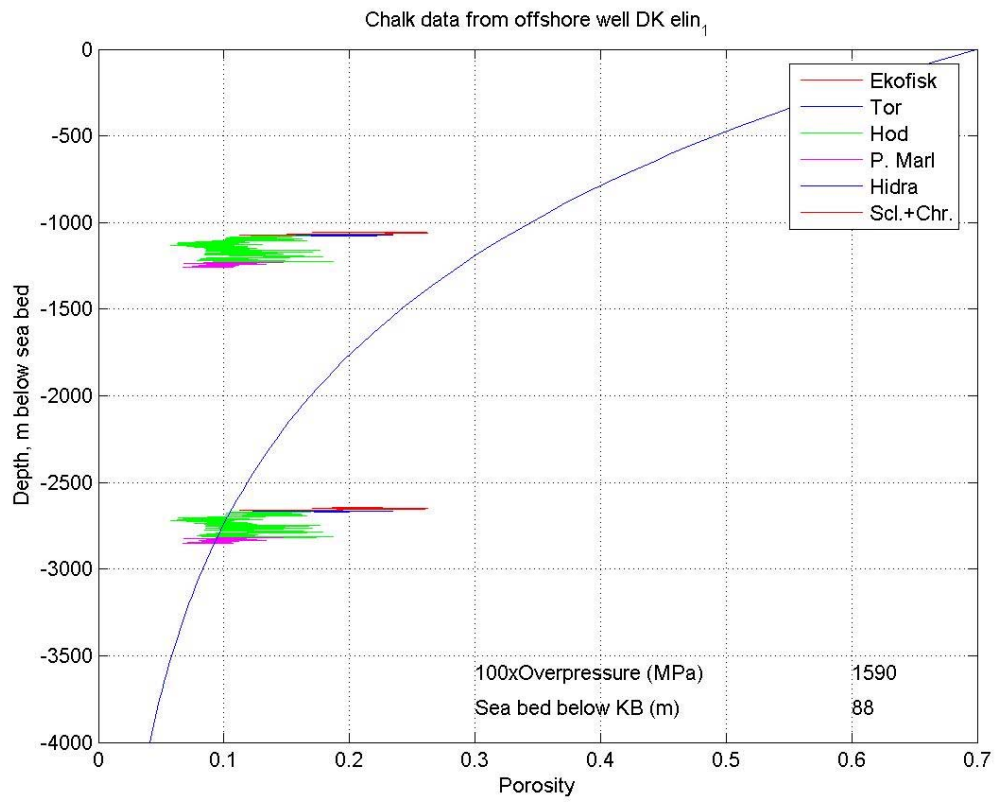
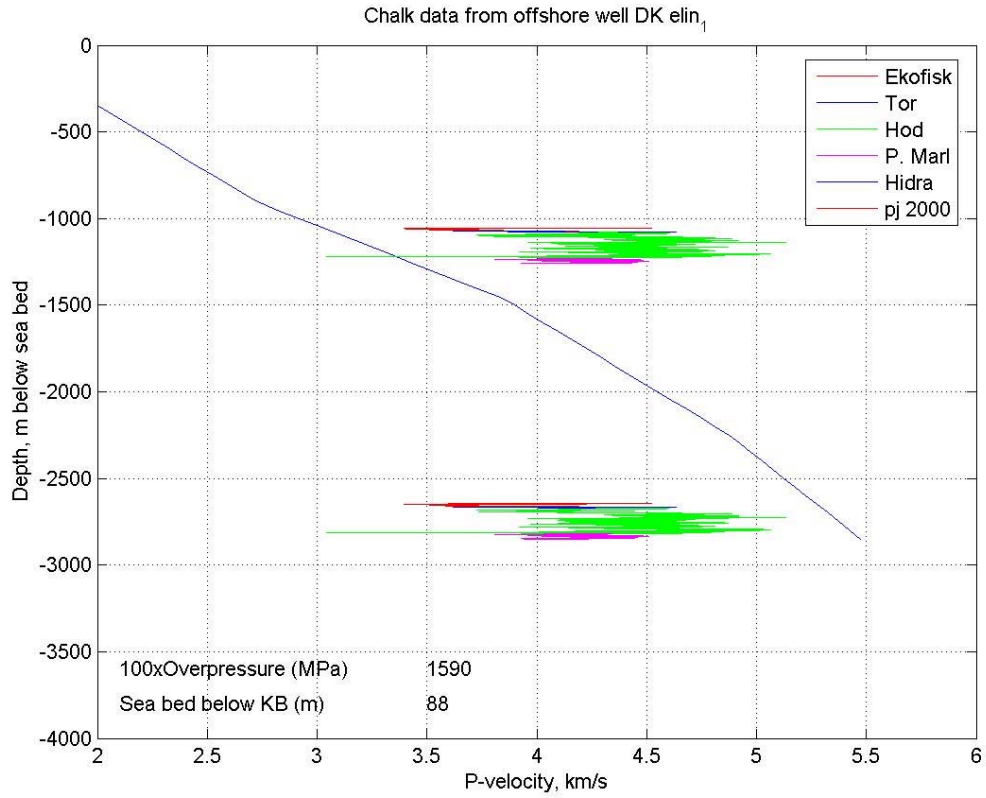
Chalk data from offshore well DK diamant₁



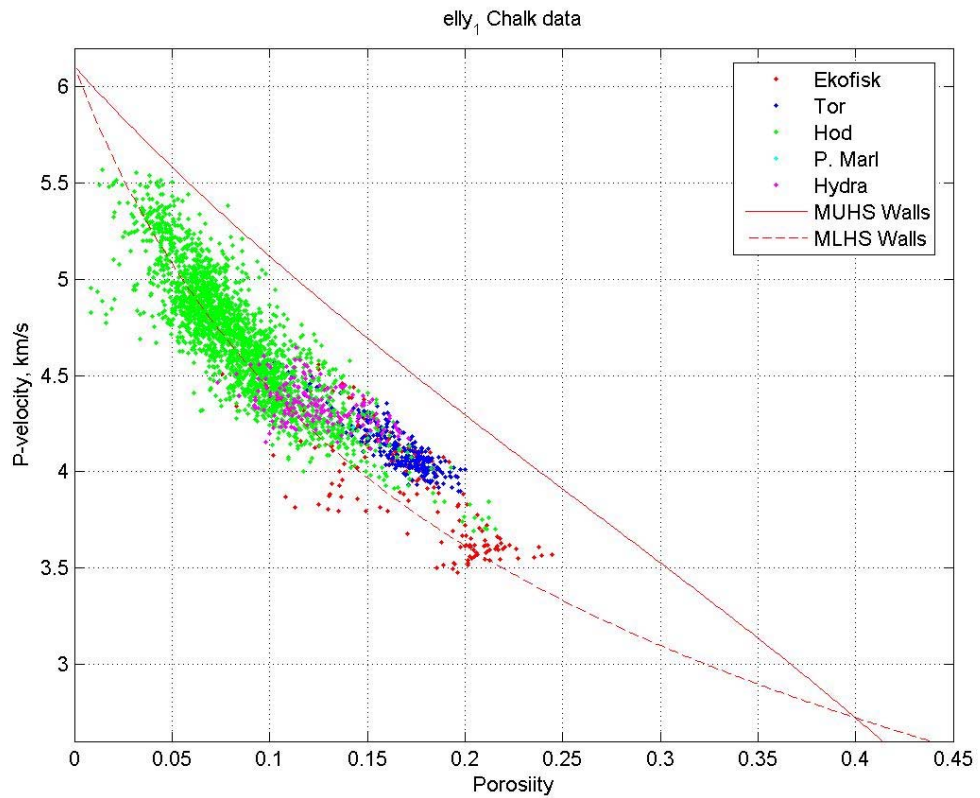
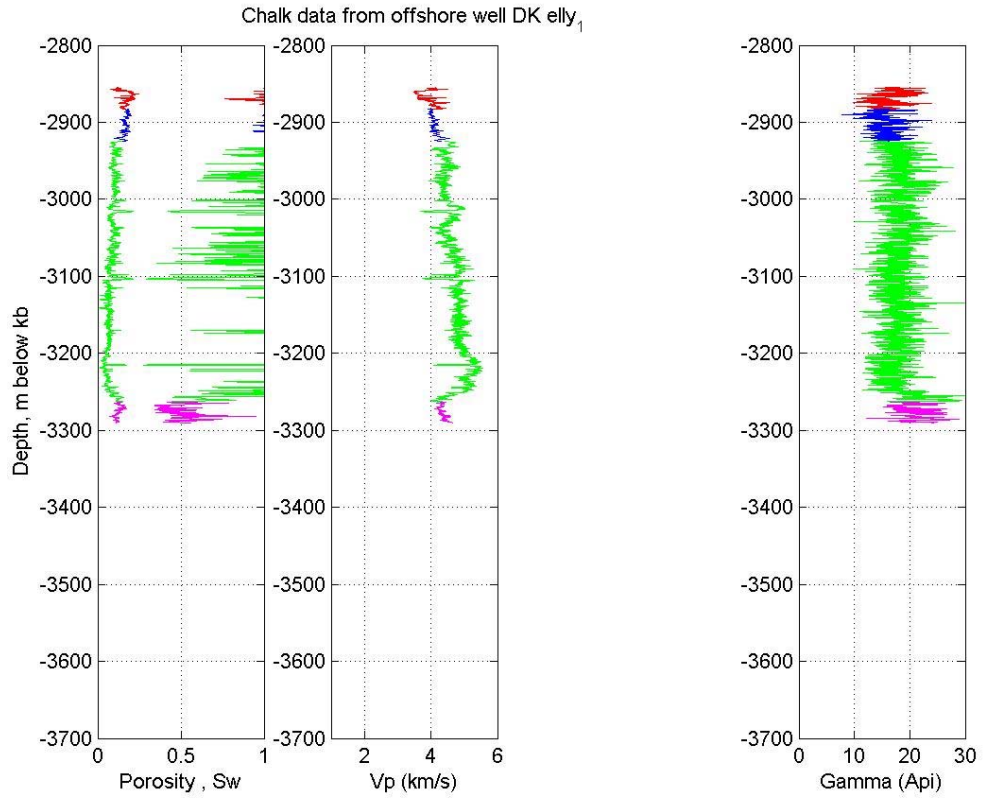
Diamant-1



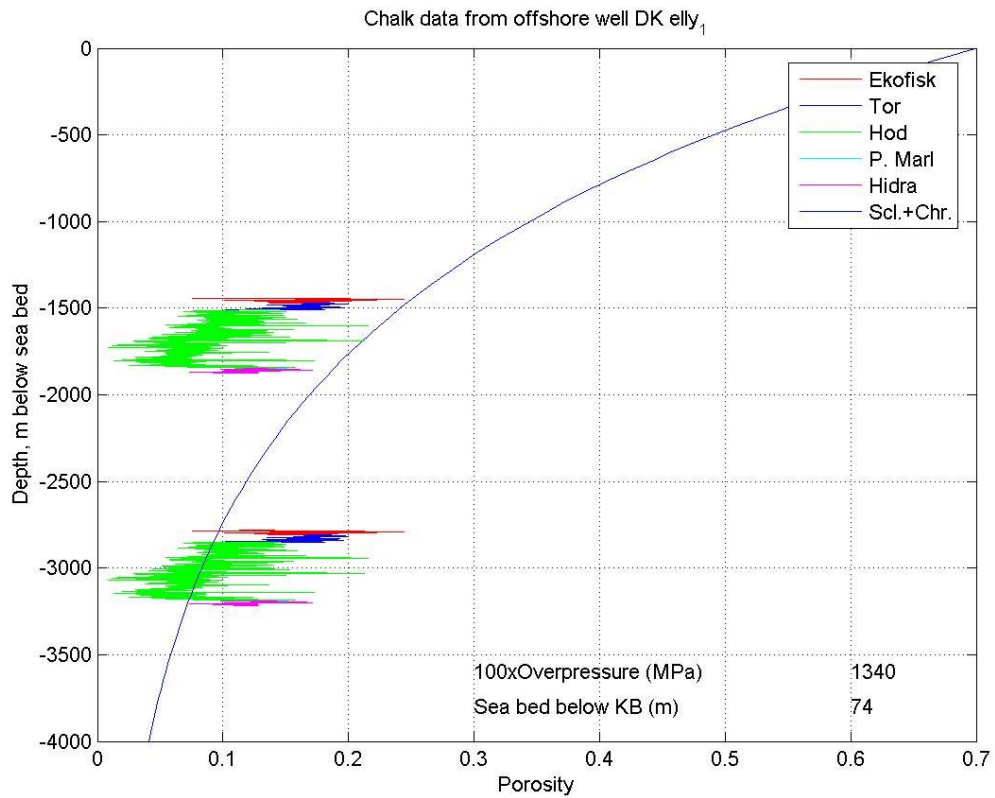
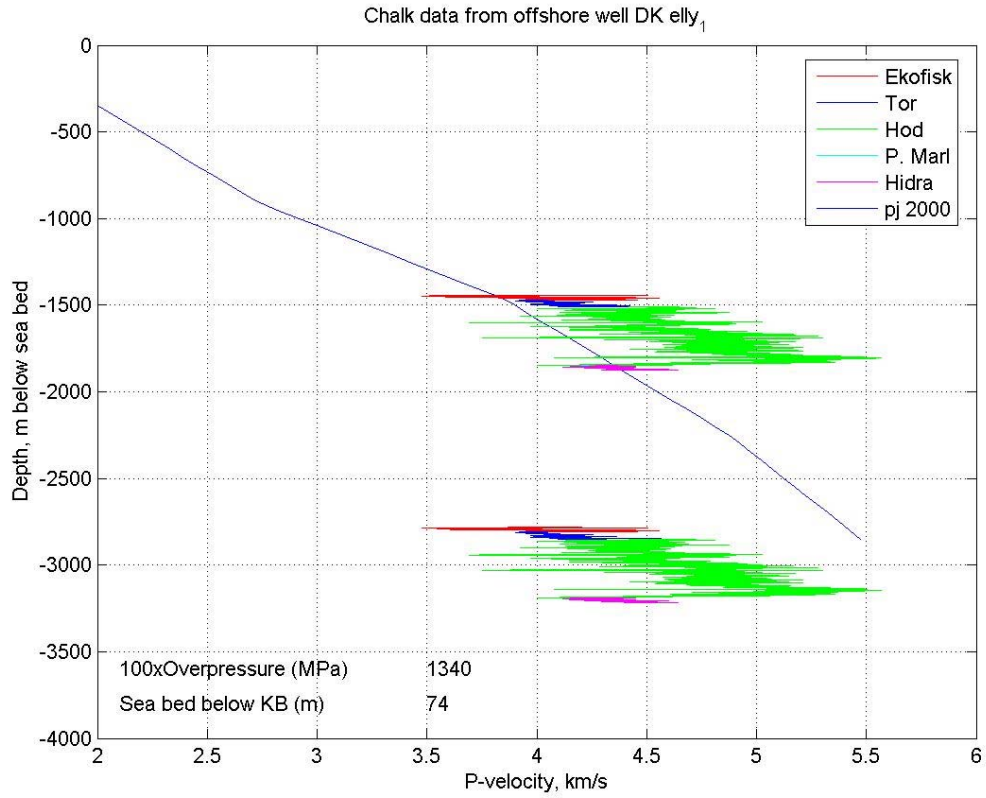
Elin-1



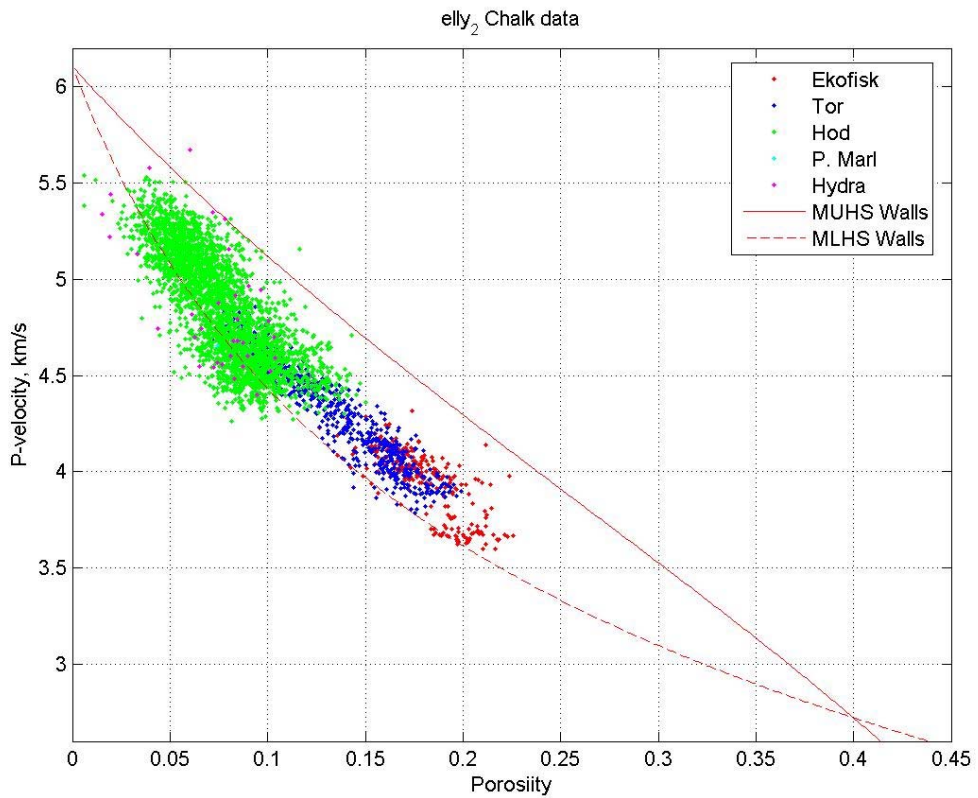
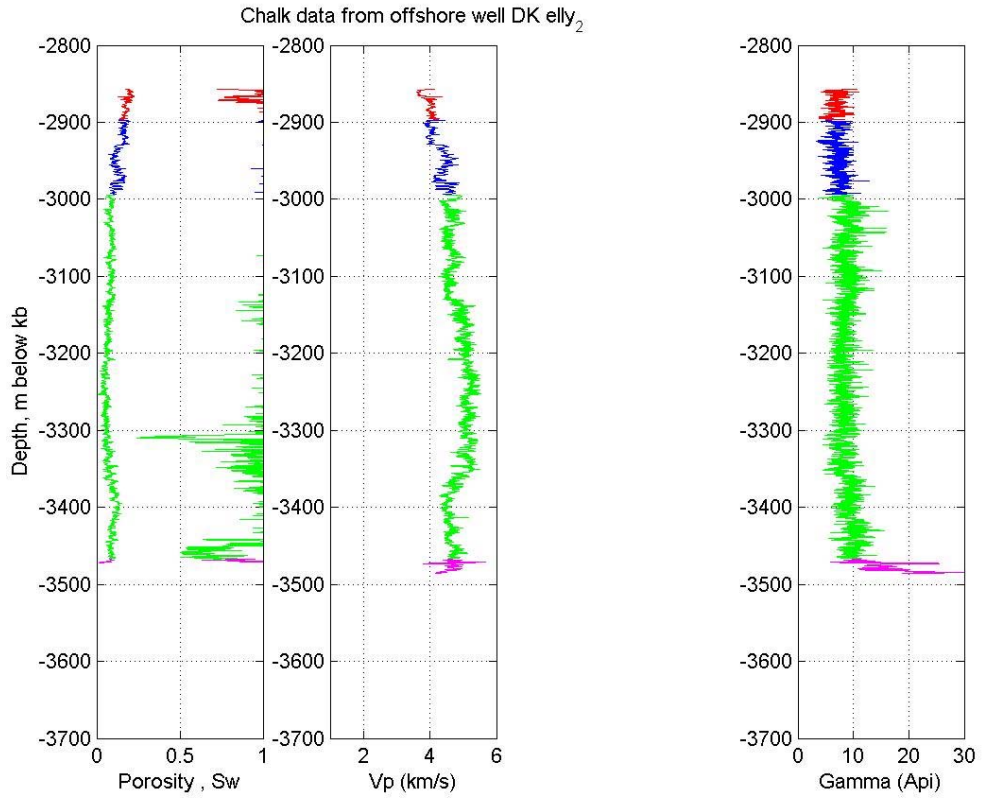
Elin-1



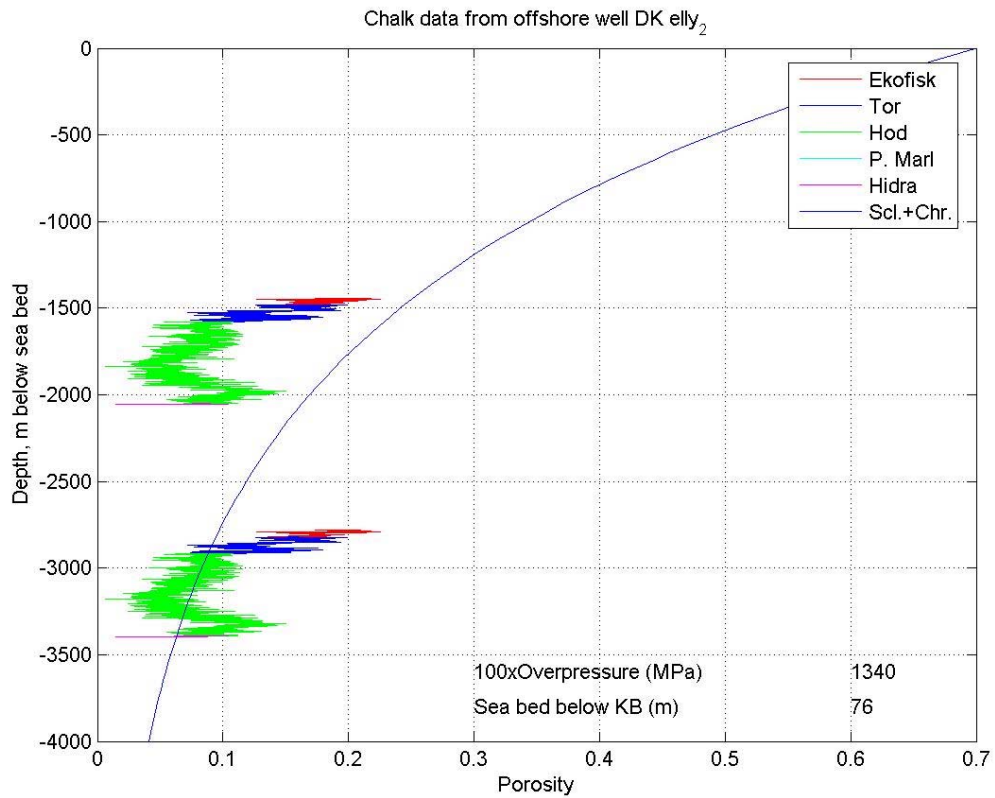
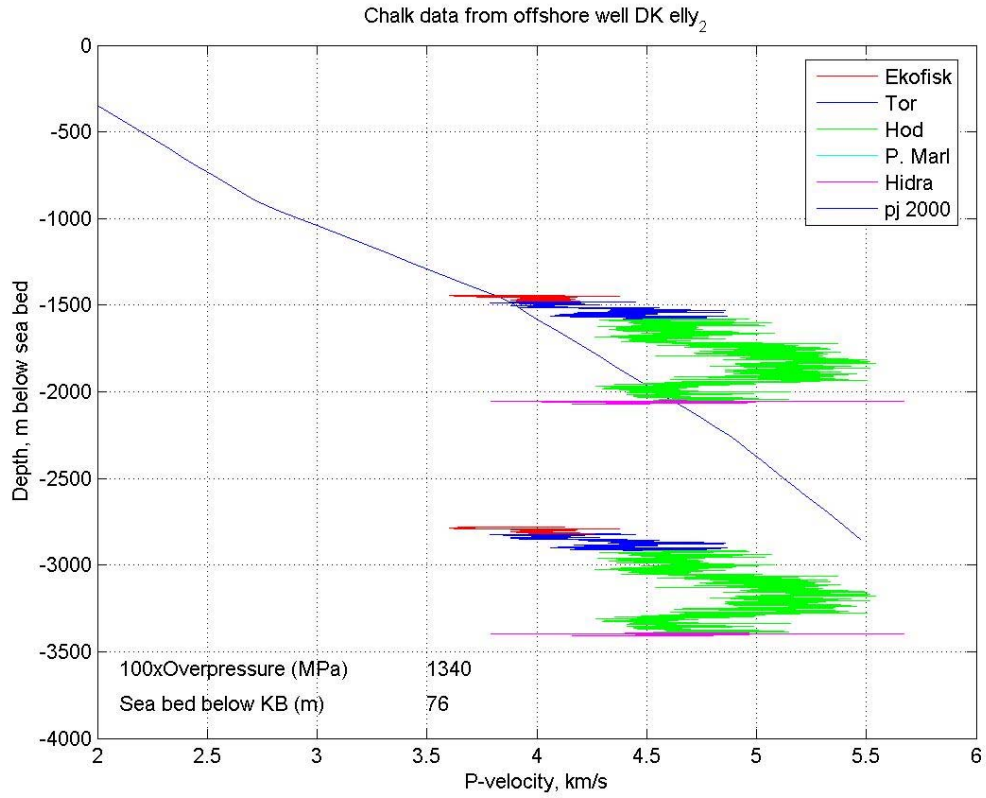
Elly-1



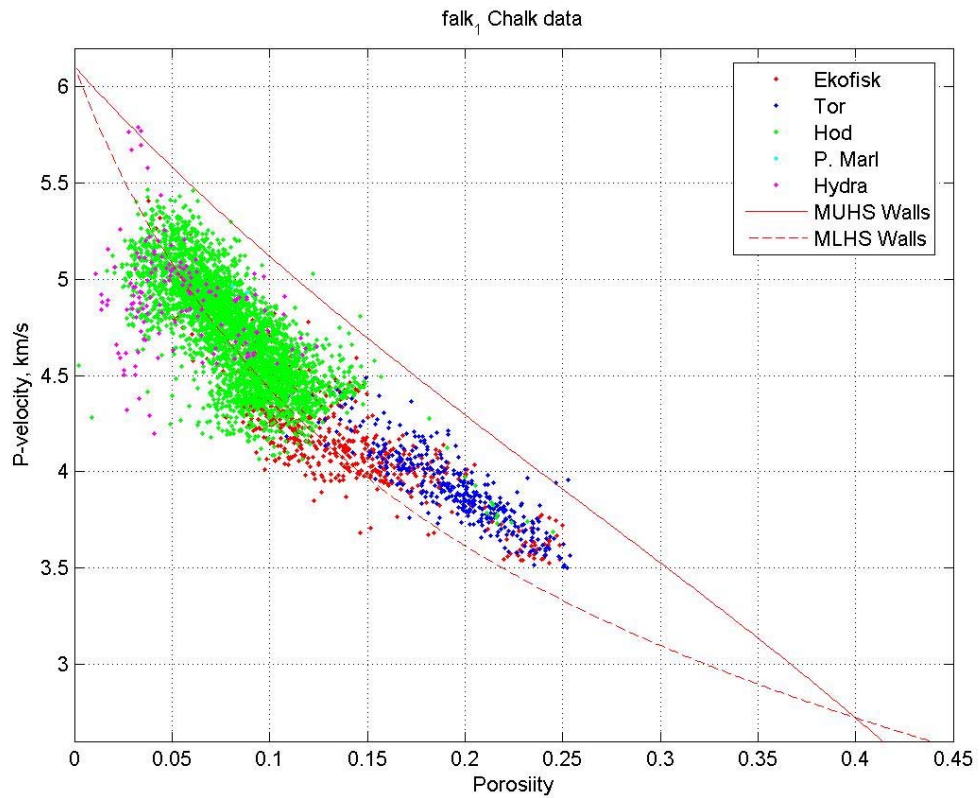
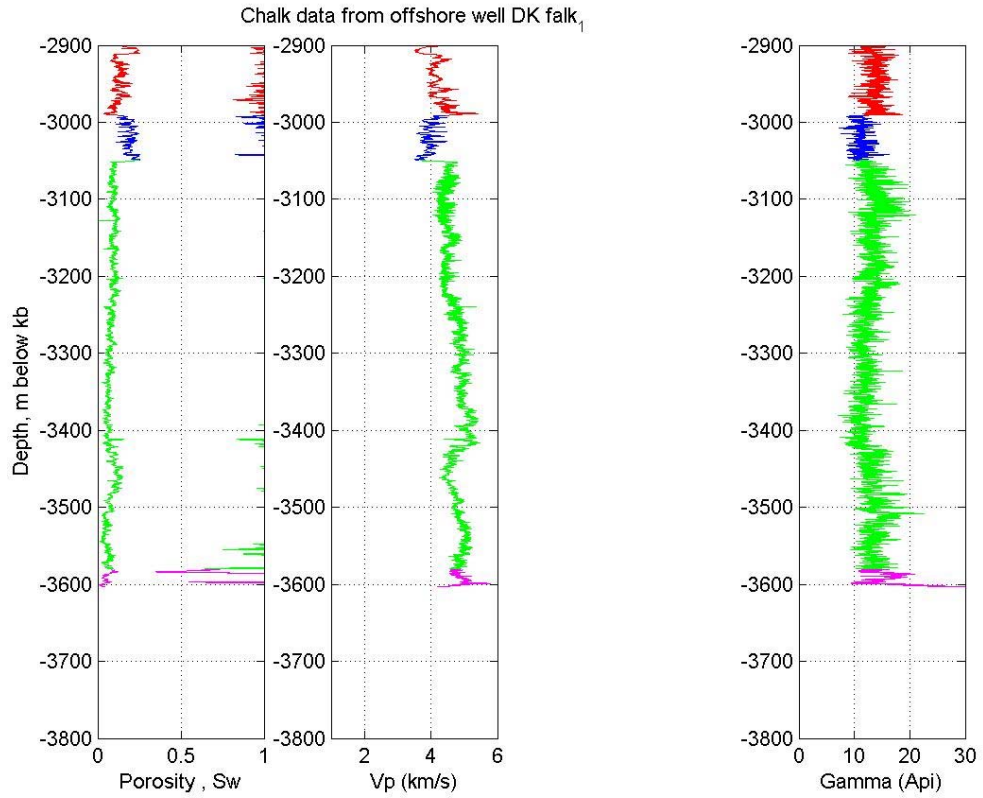
Elly-1



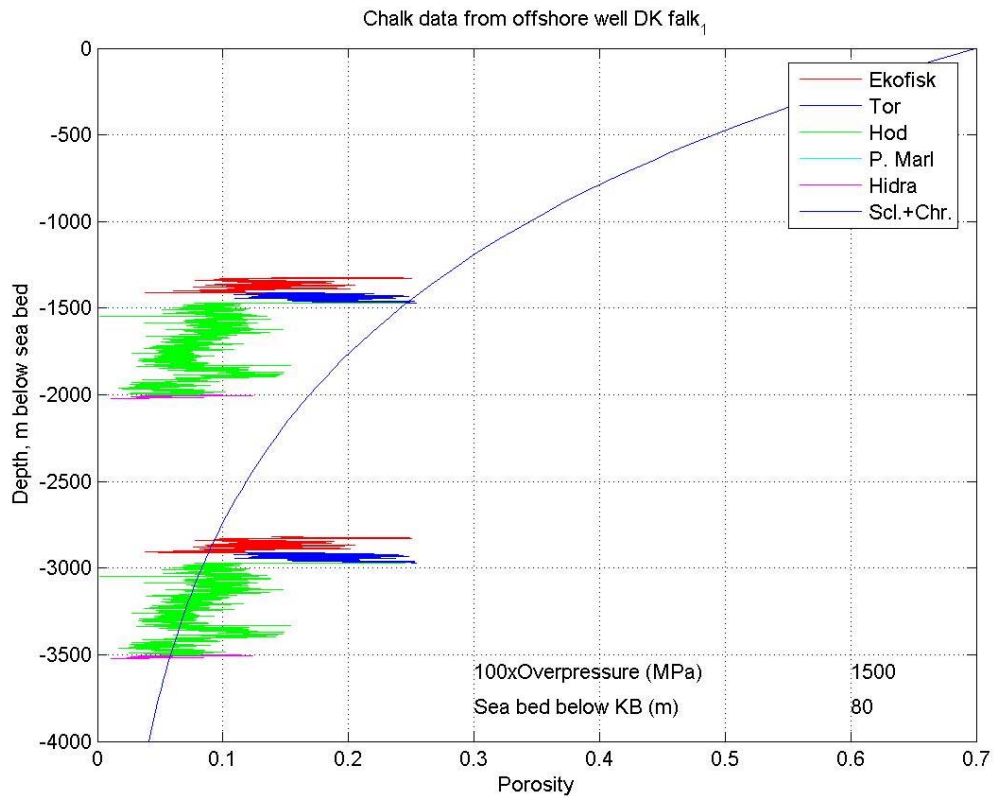
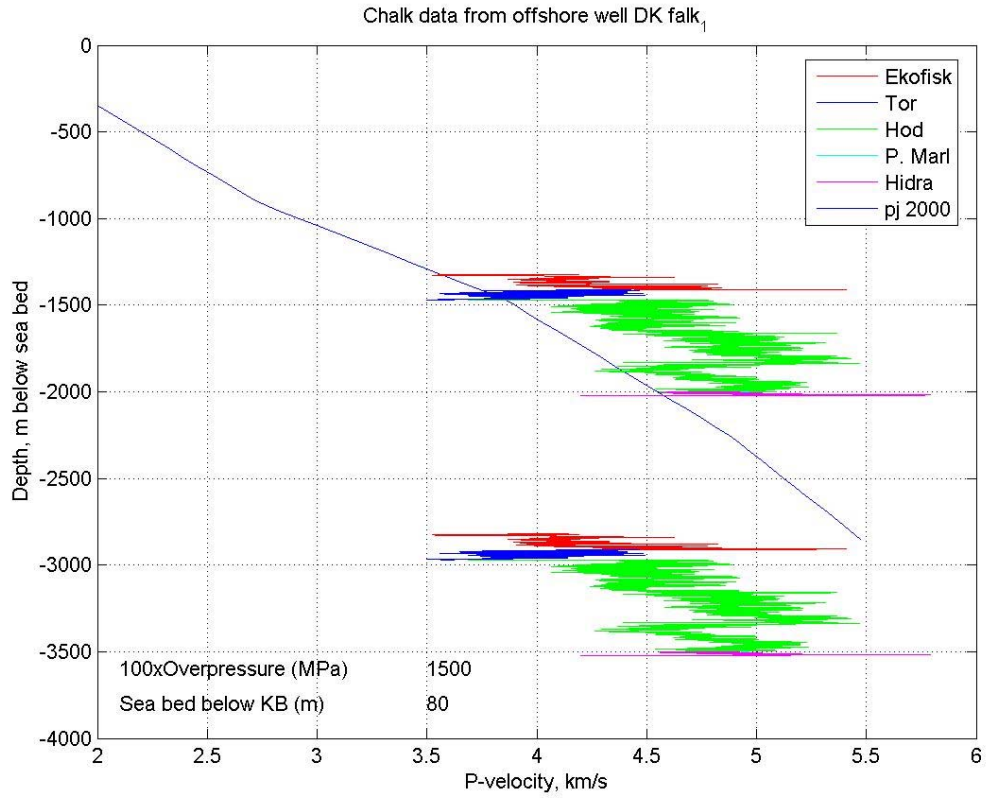
Elly-2



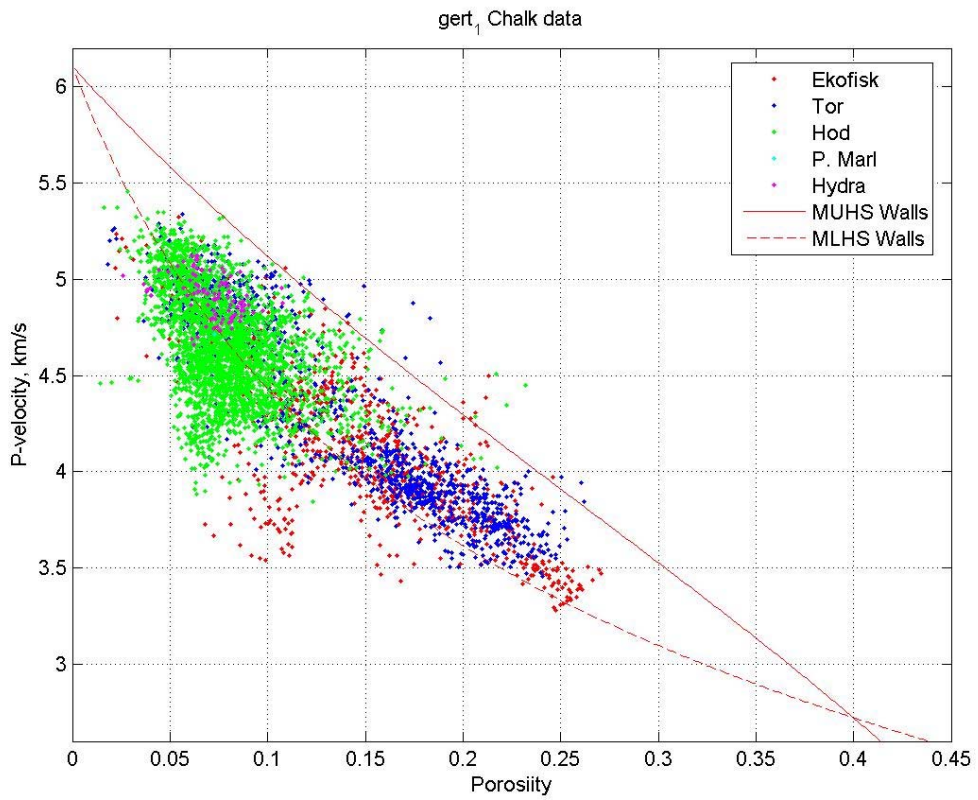
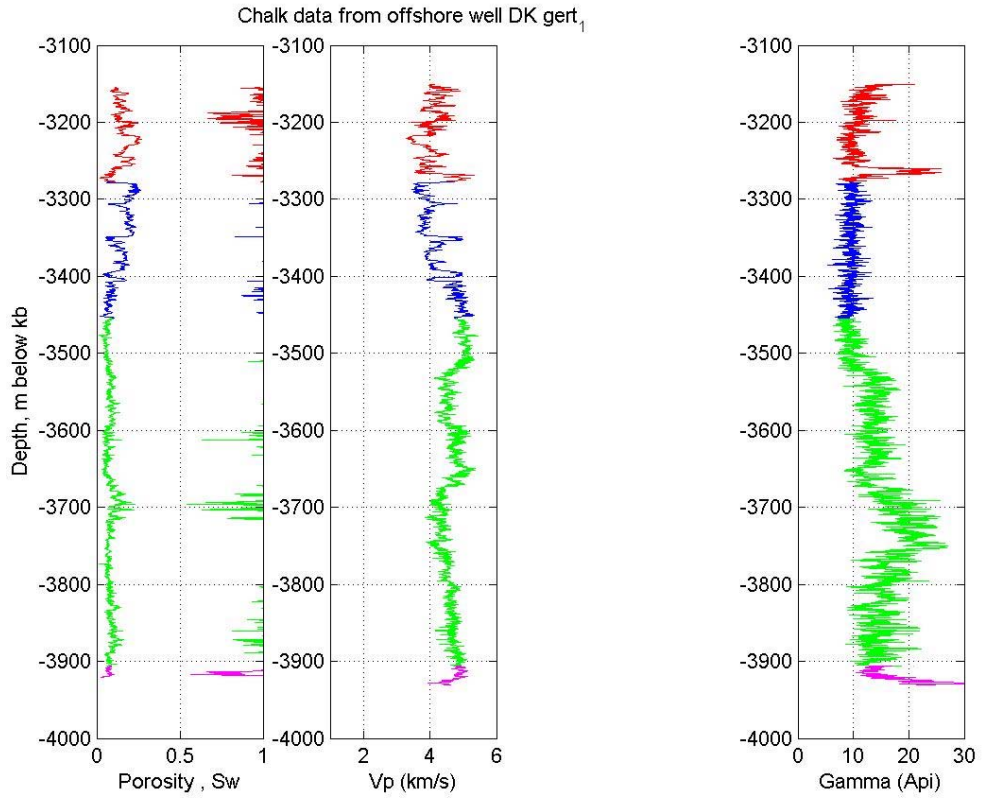
Elly-2



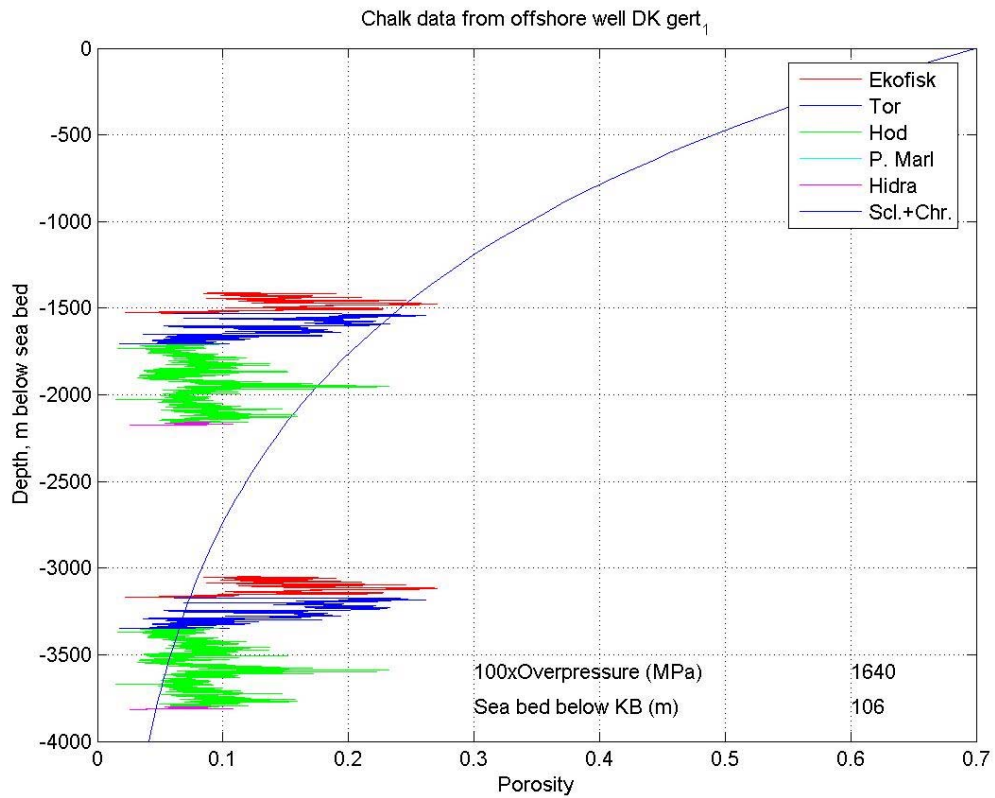
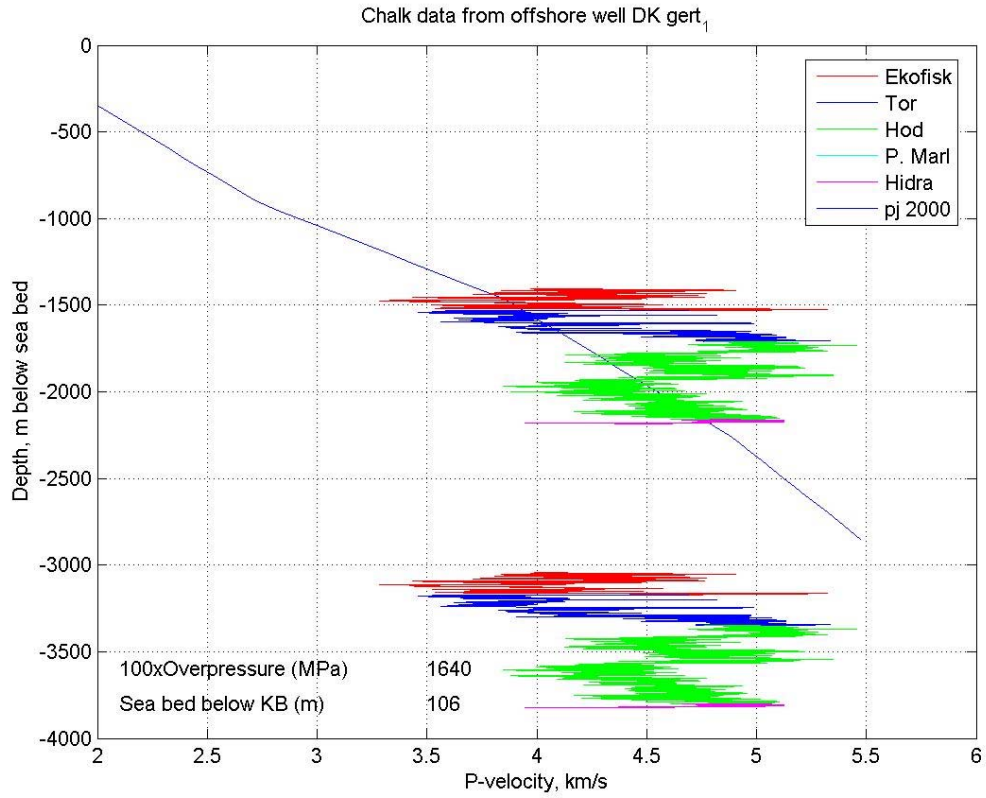
Falk-1



Falk-1

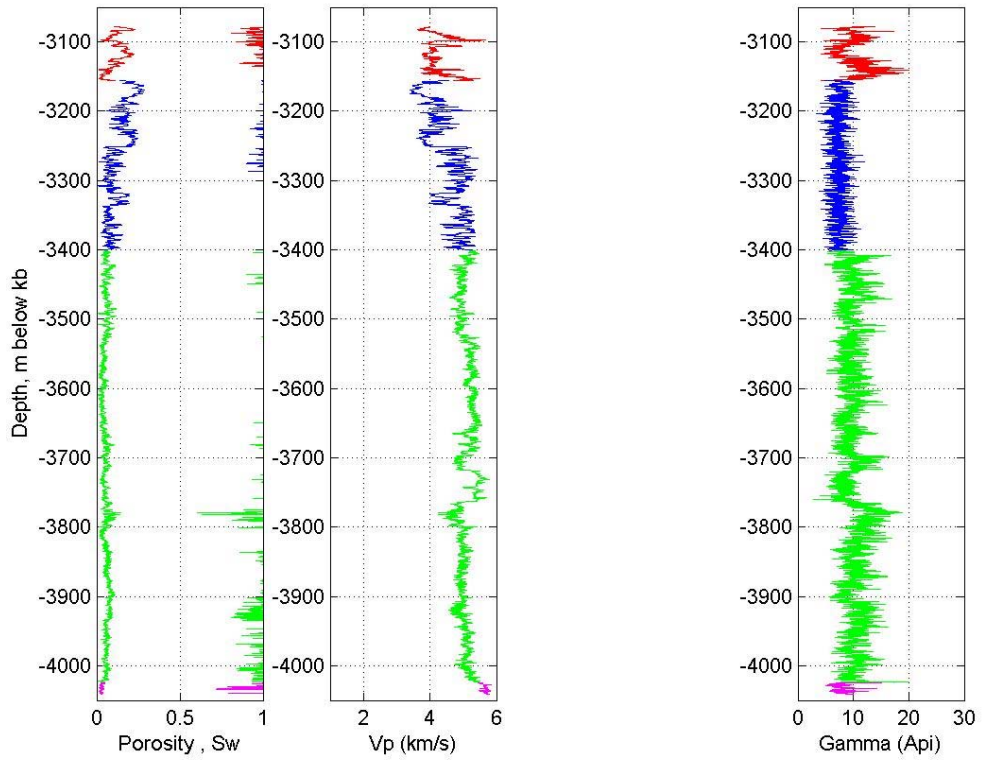


Gert-1

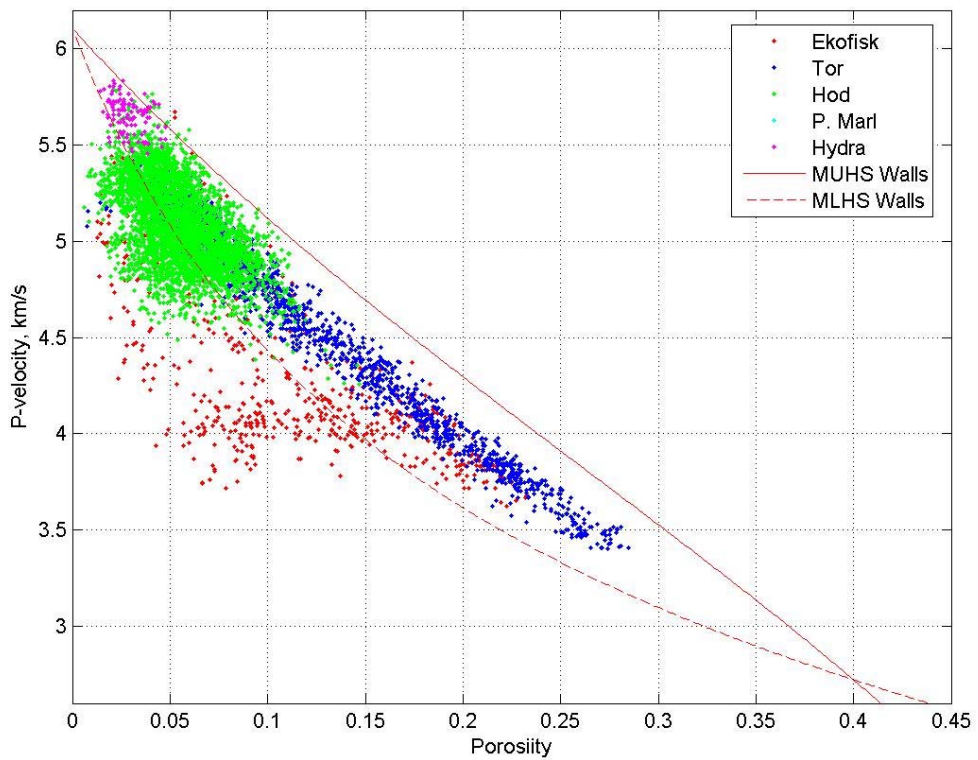


Gert-1

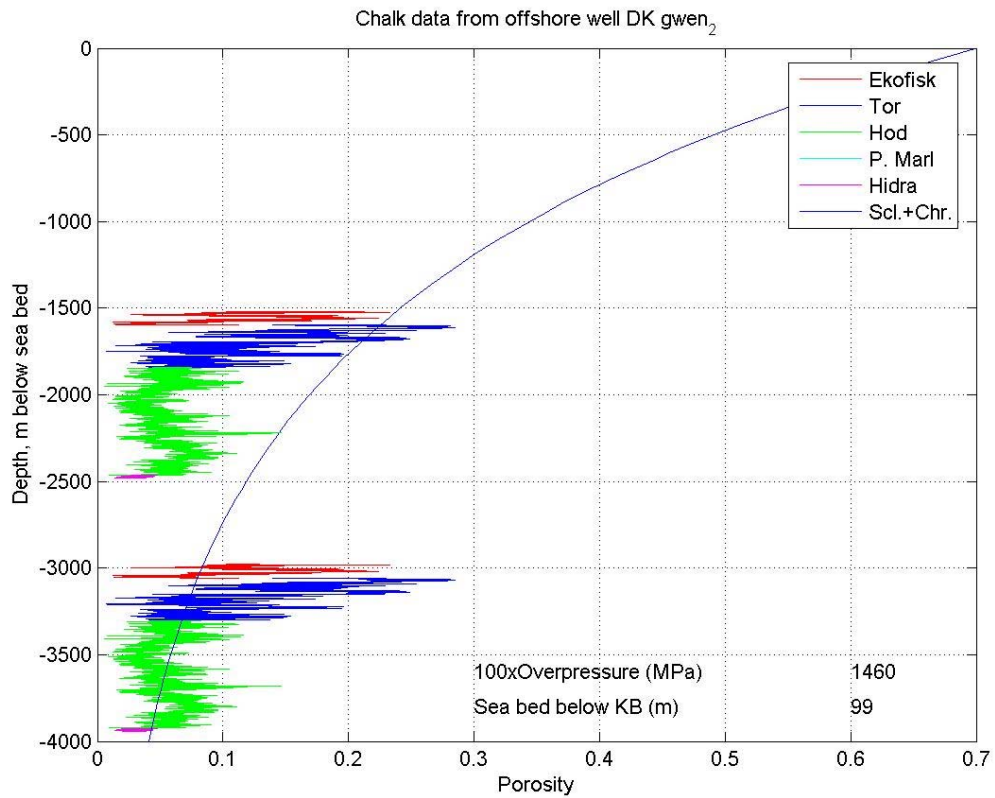
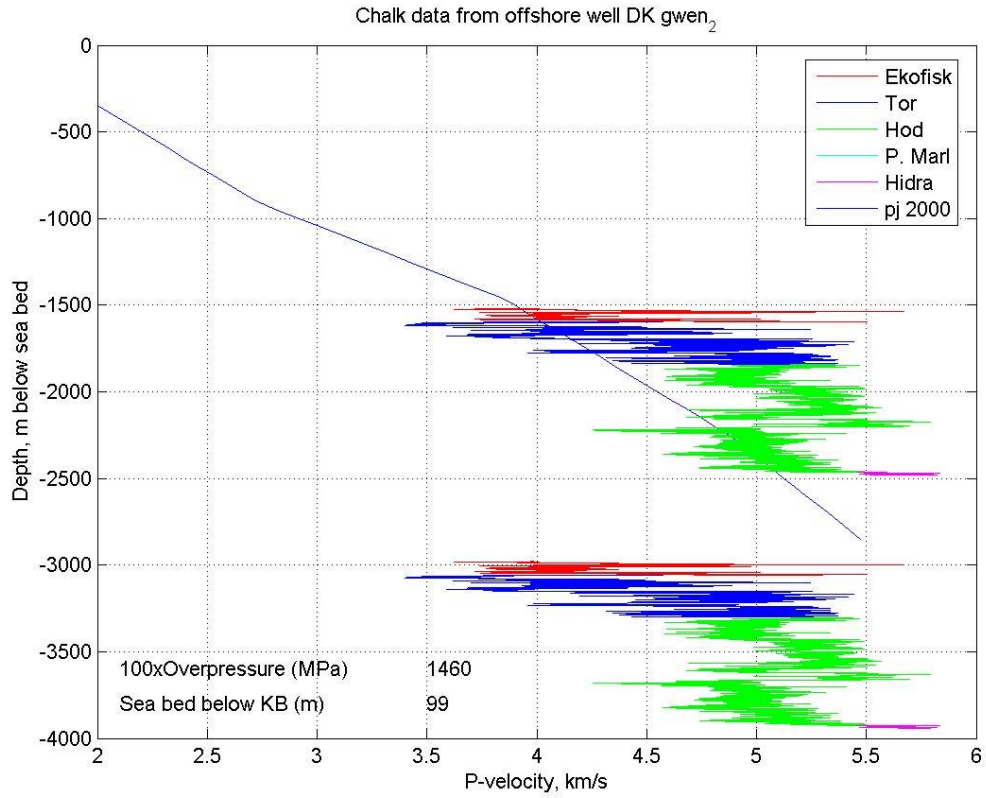
Chalk data from offshore well DK gwen₂



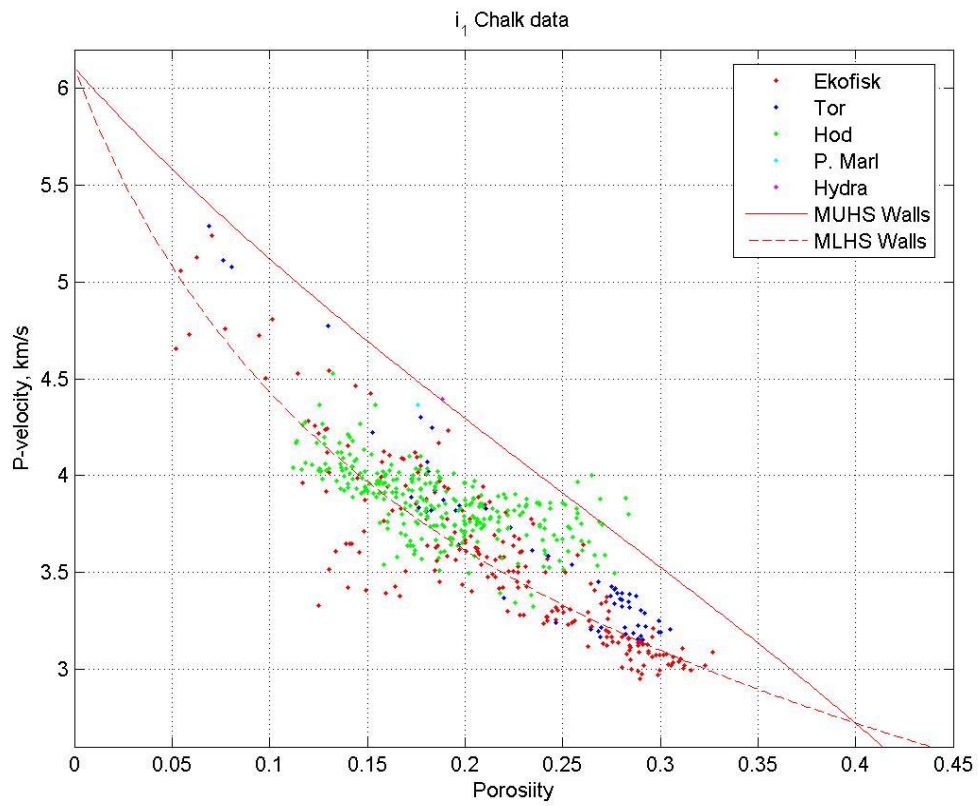
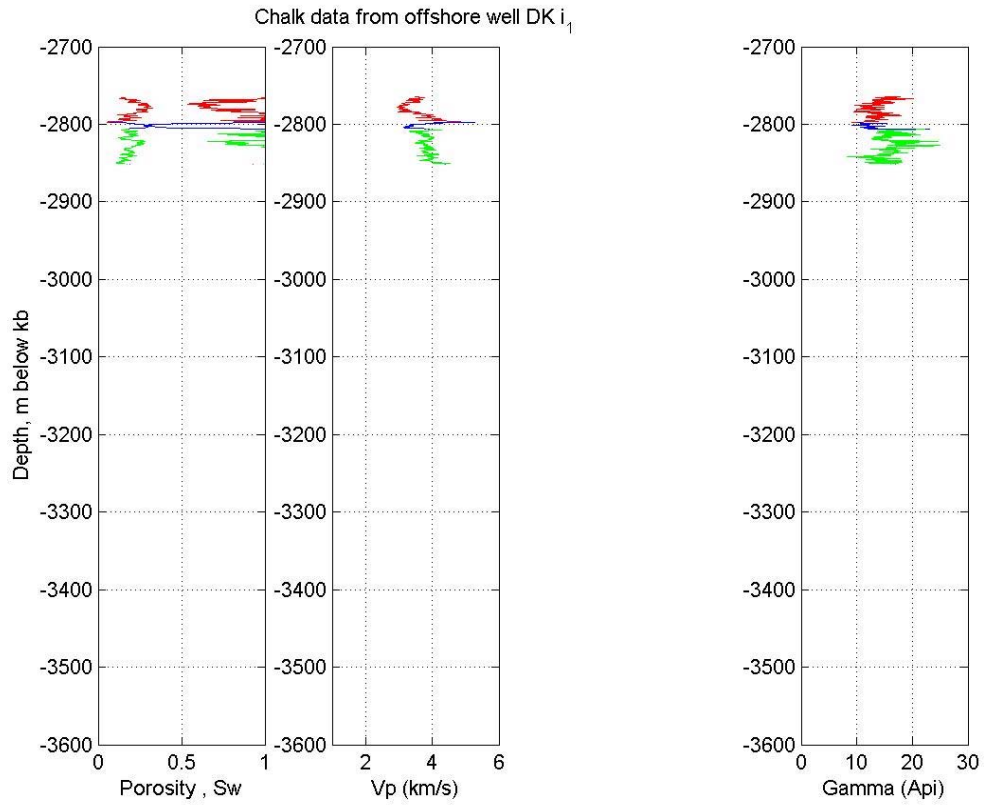
gwen₂ Chalk data



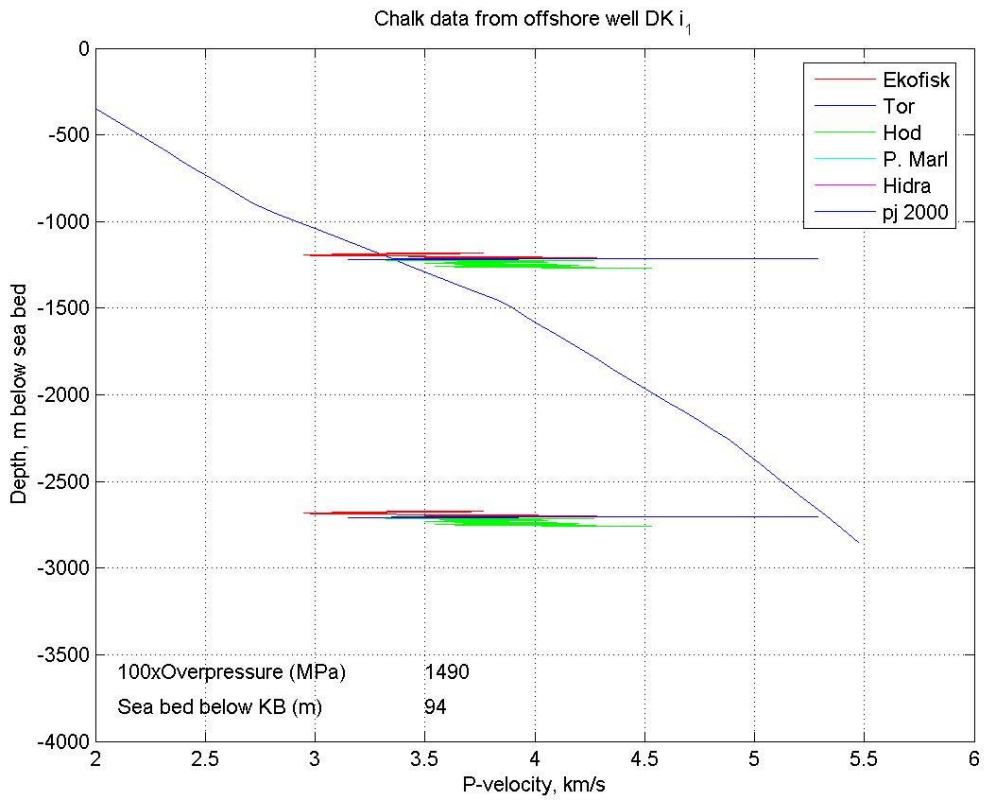
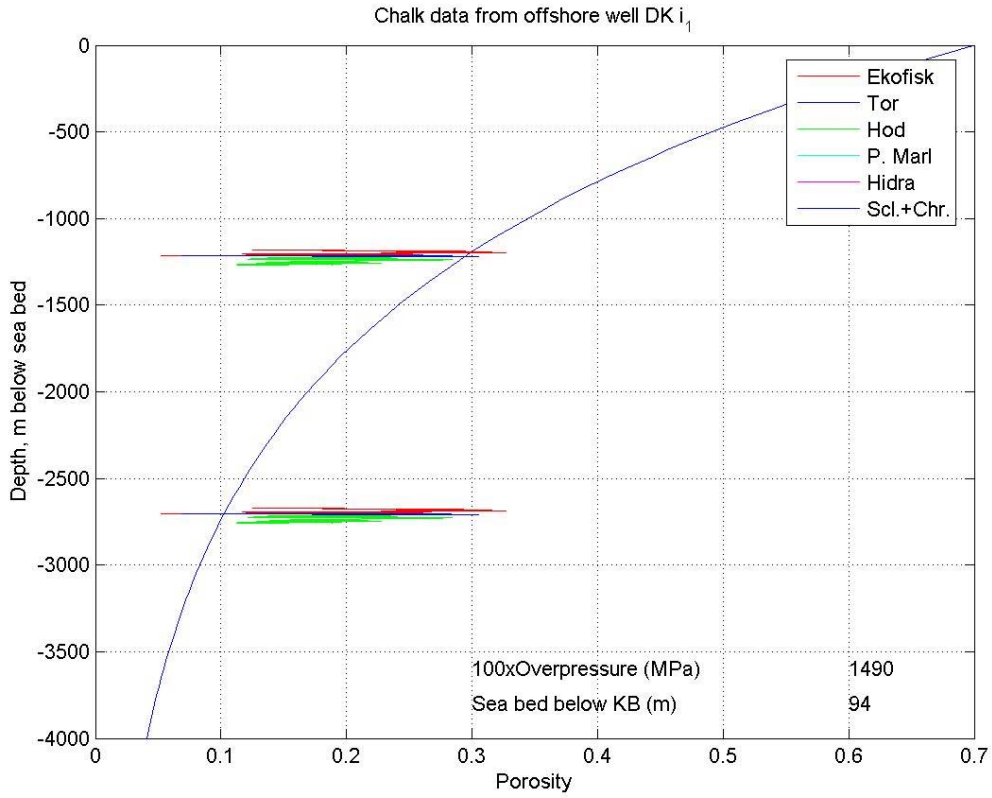
Gwen-2

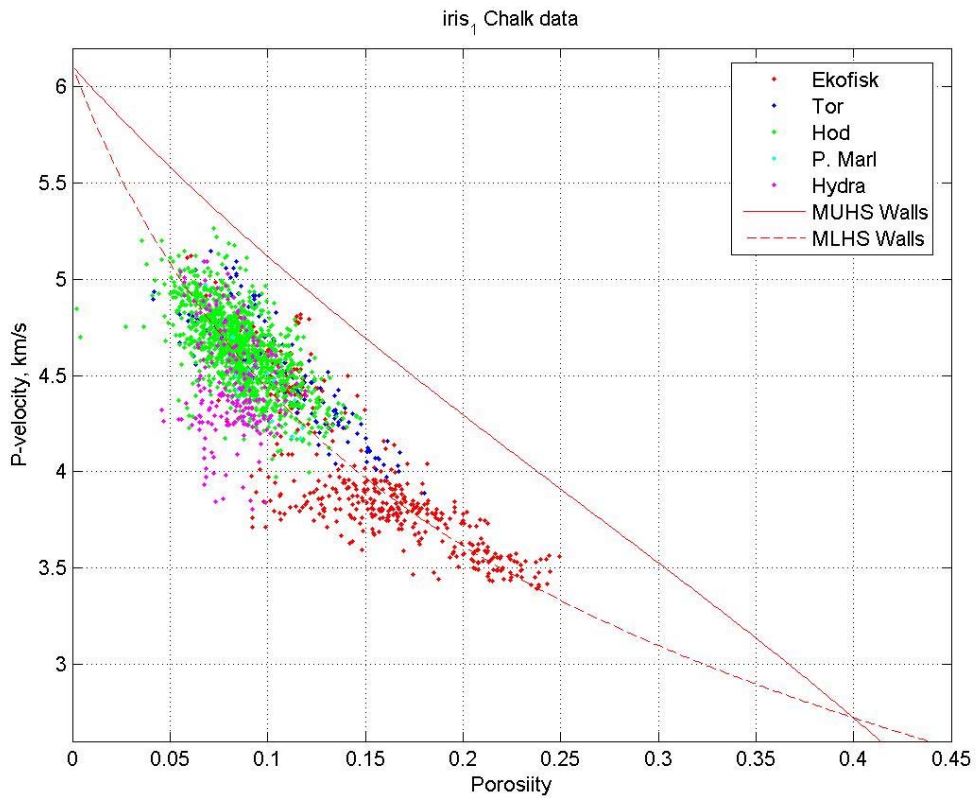
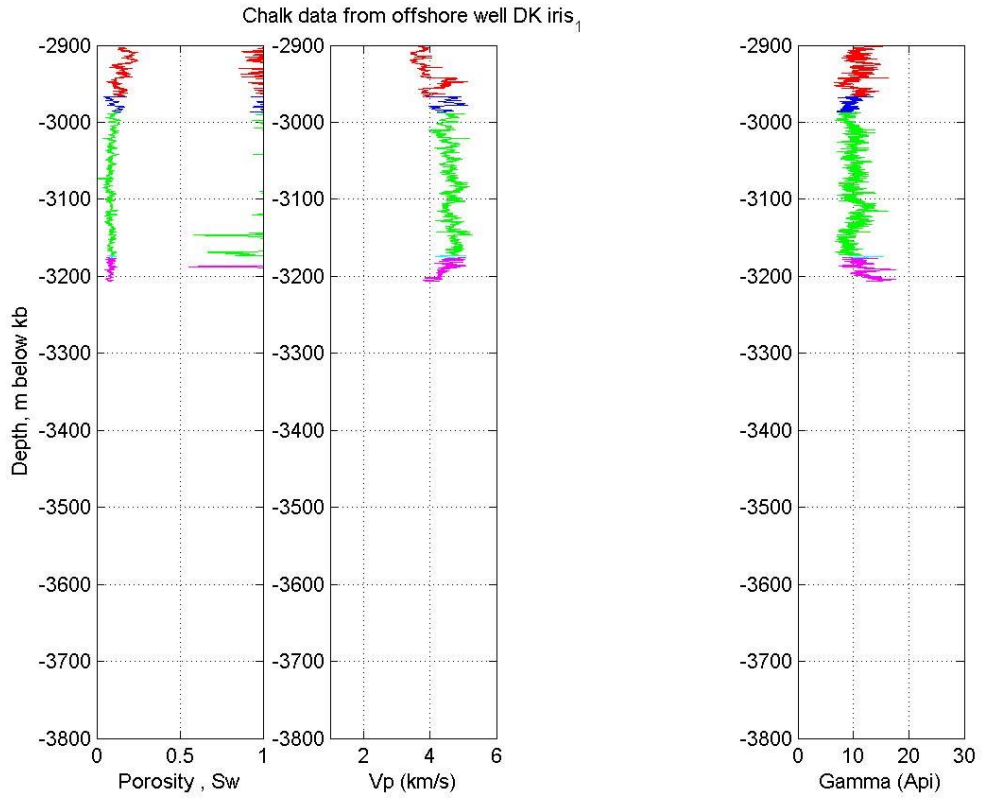


Gwen-2

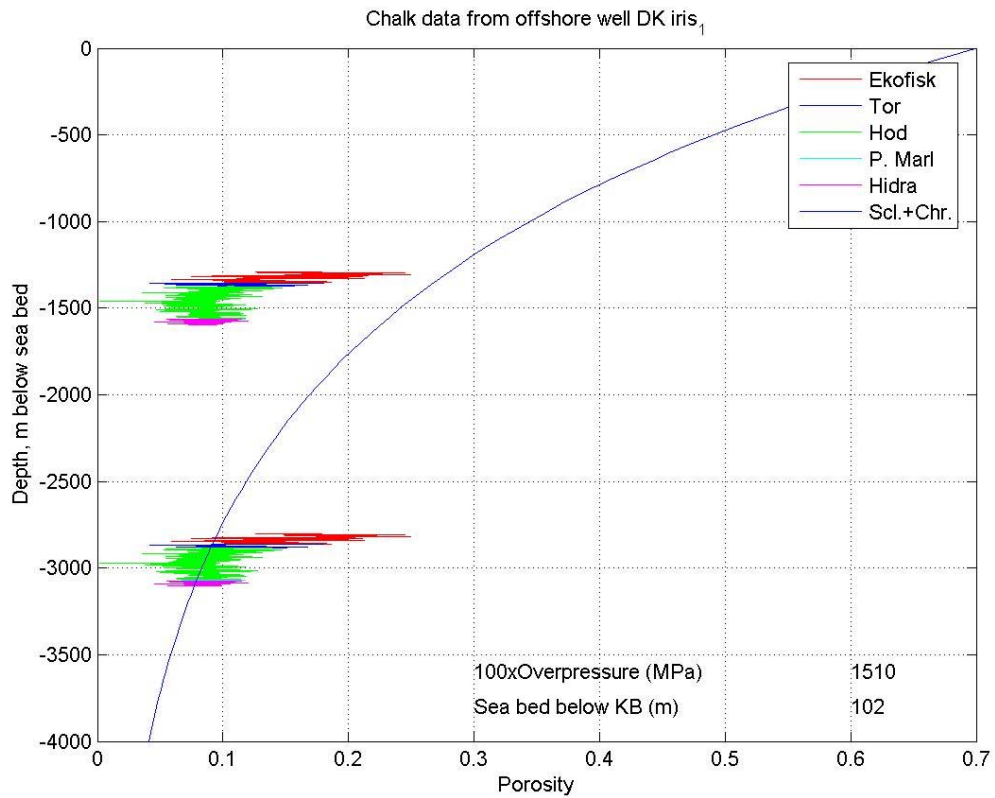
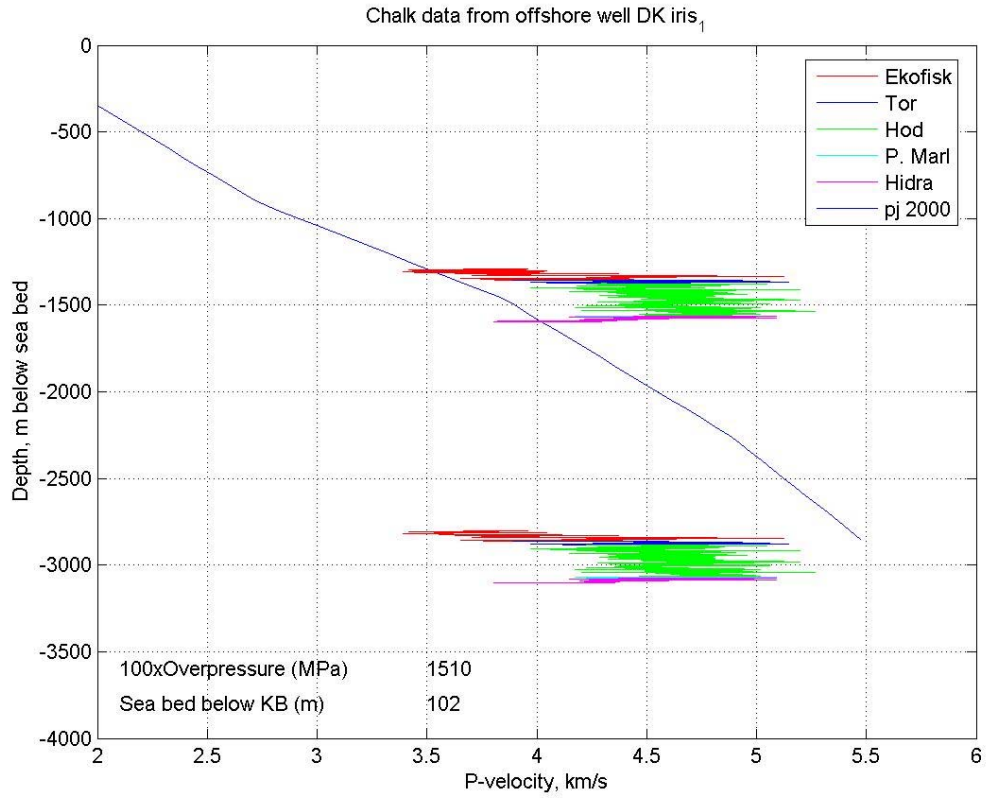


I-1

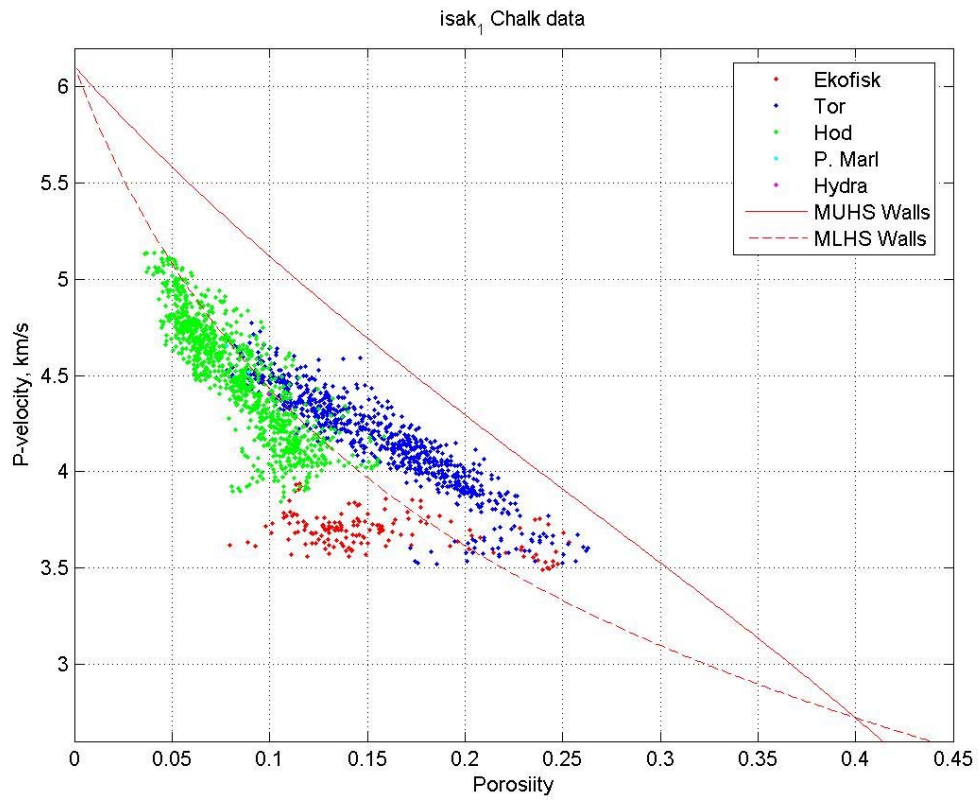
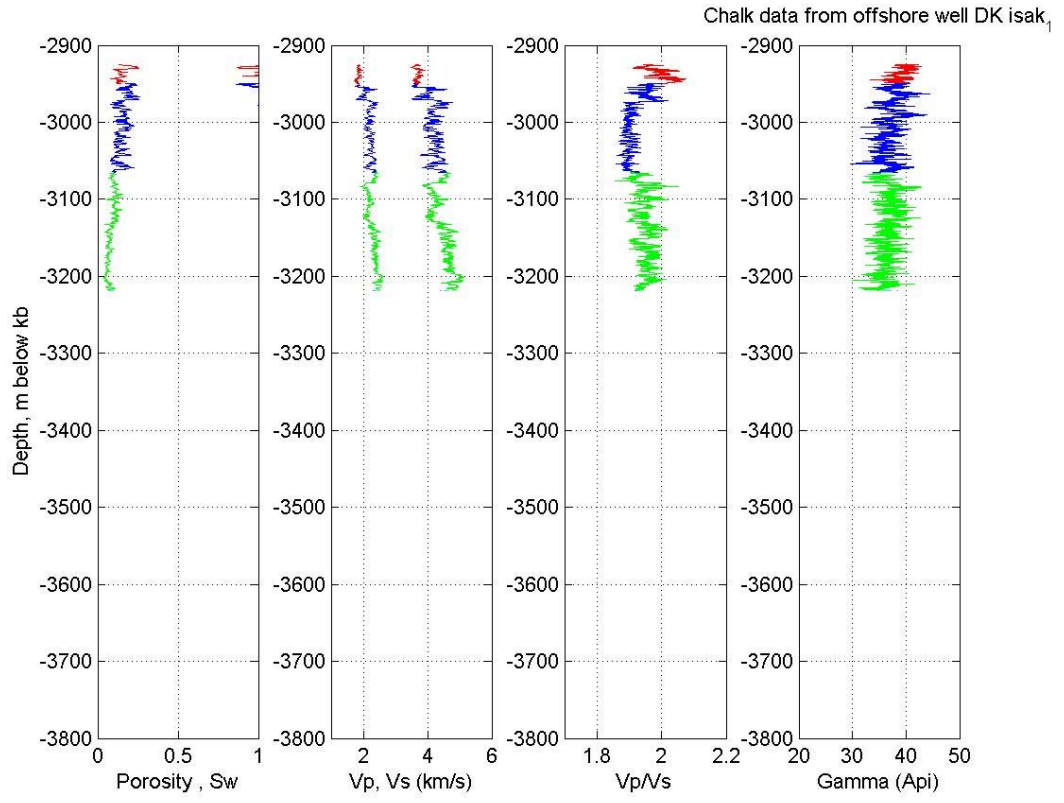




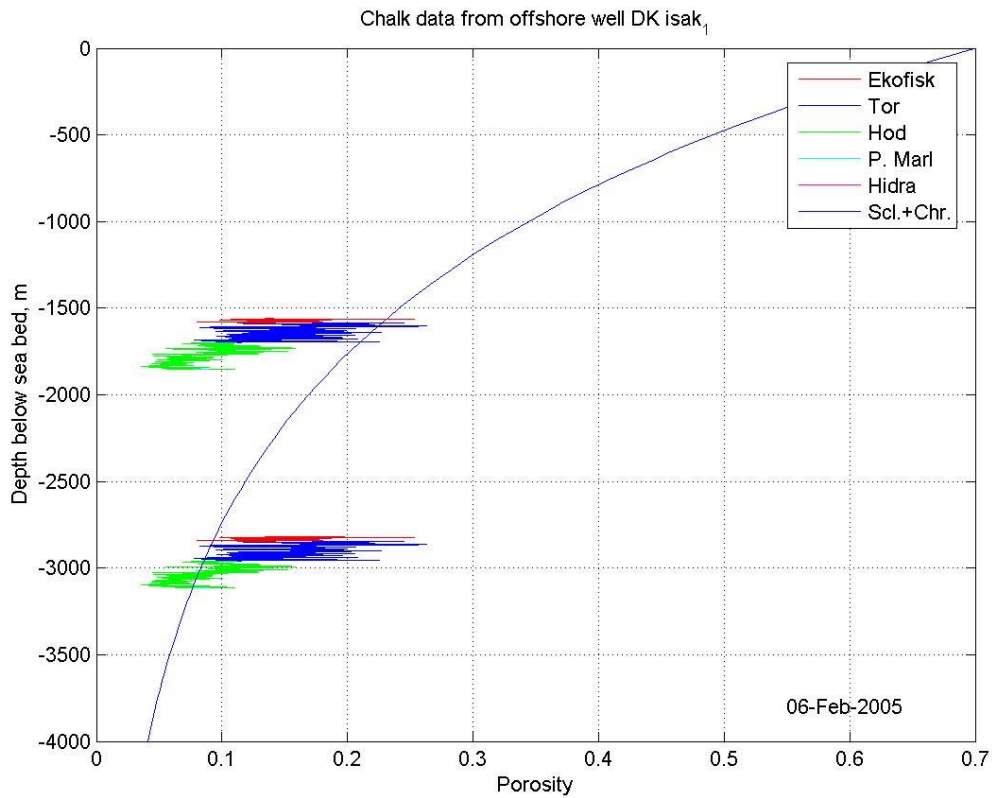
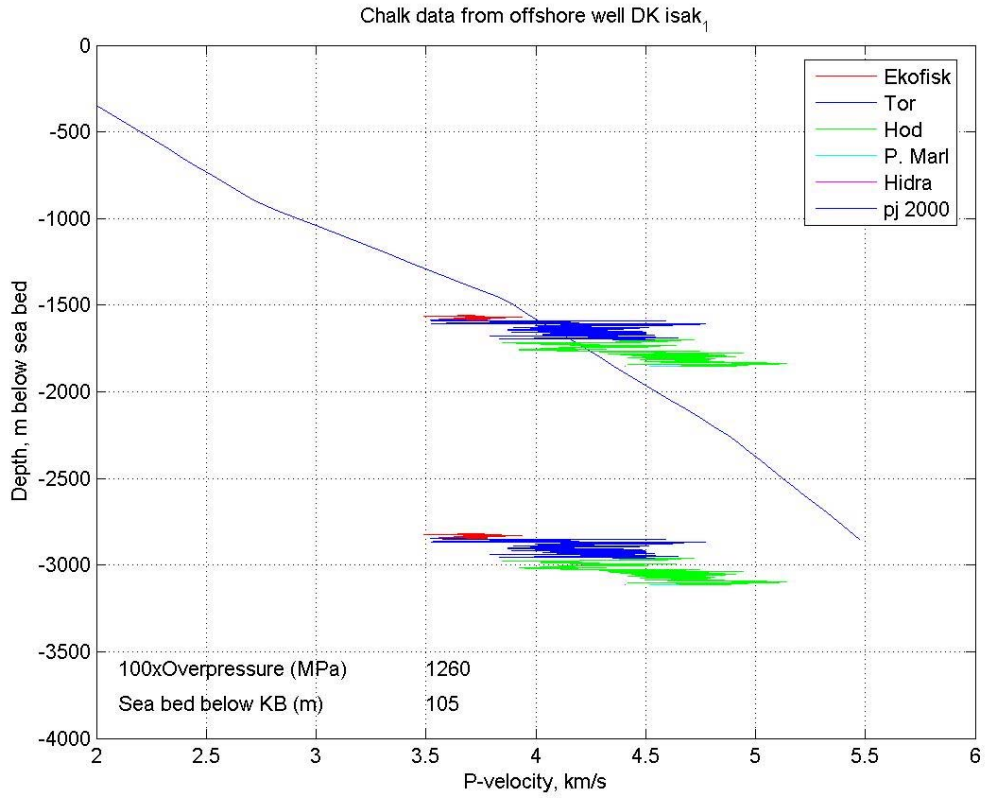
Iris-1



Iris-1

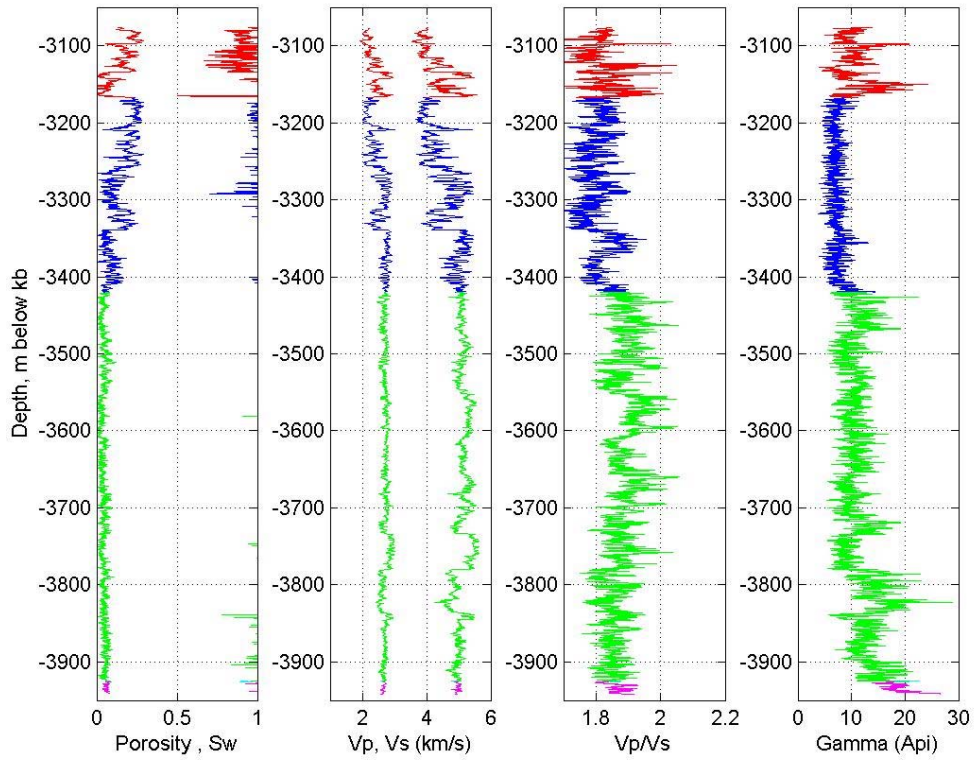


Isak-1

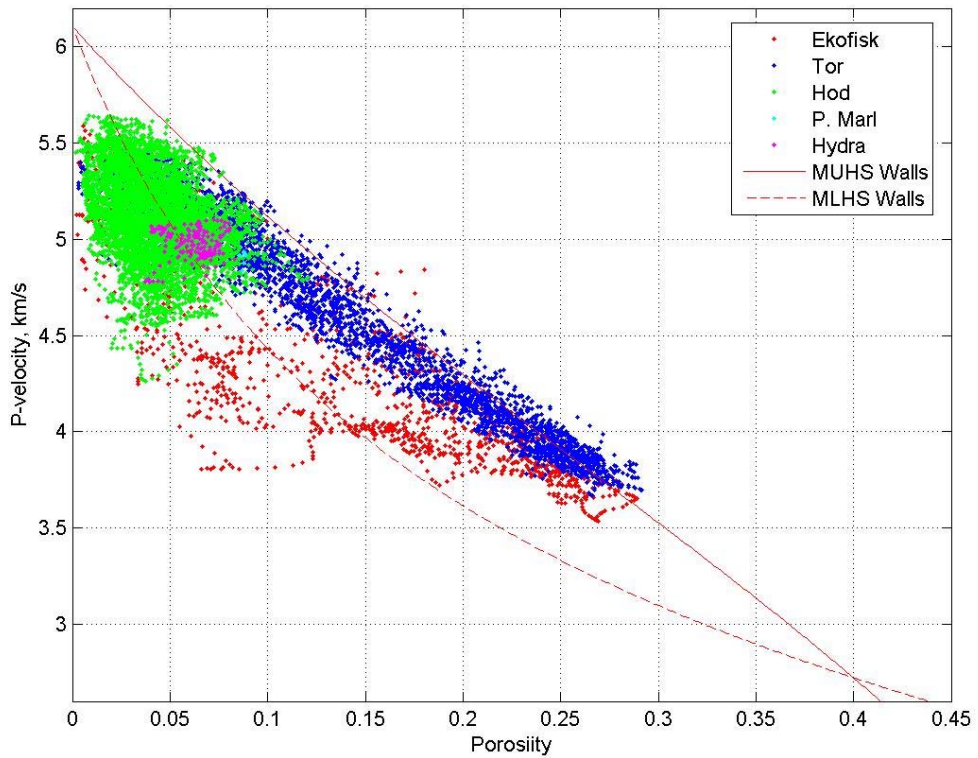


Isak-1

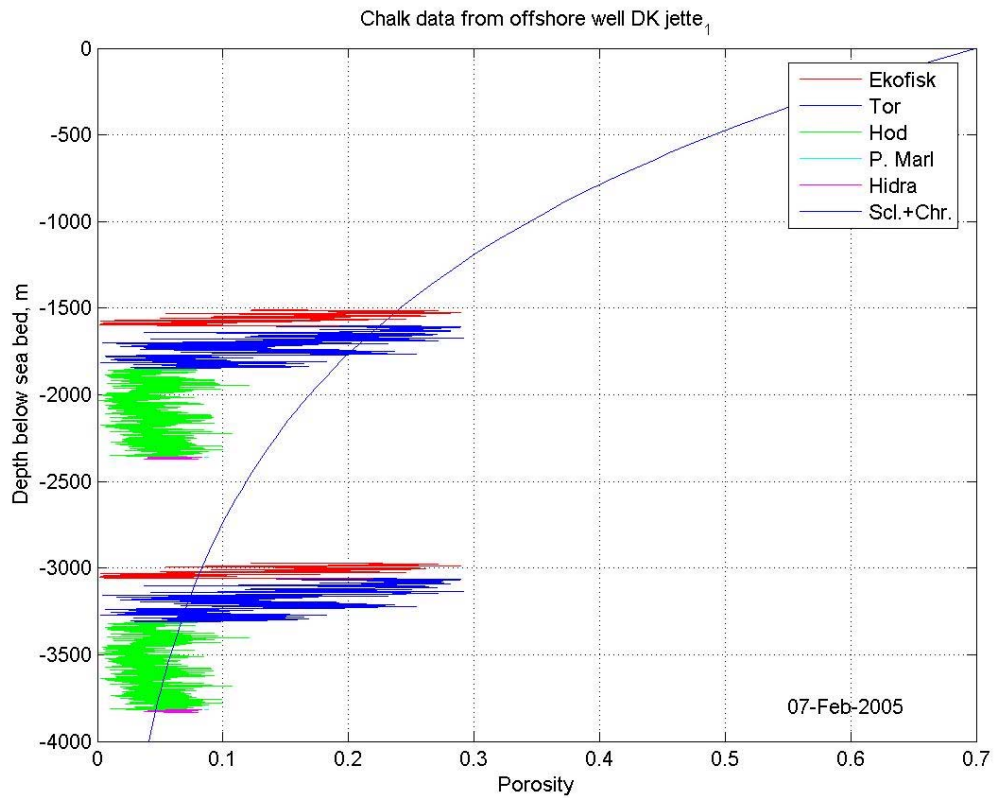
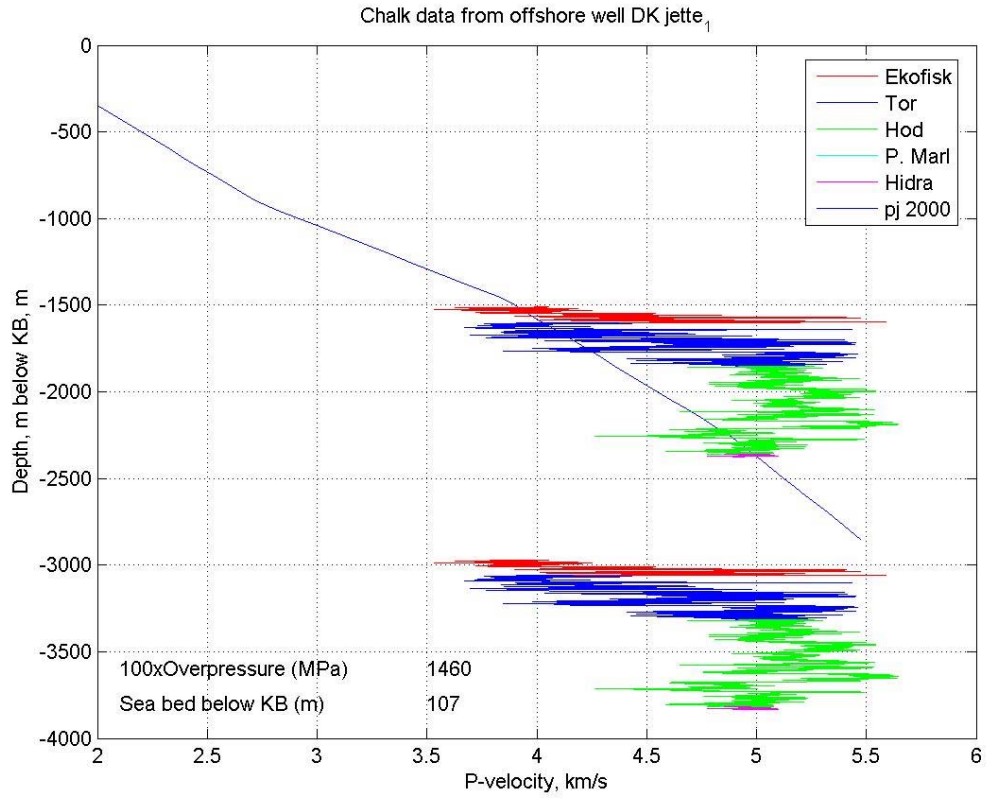
Chalk data from offshore well DK jette₁



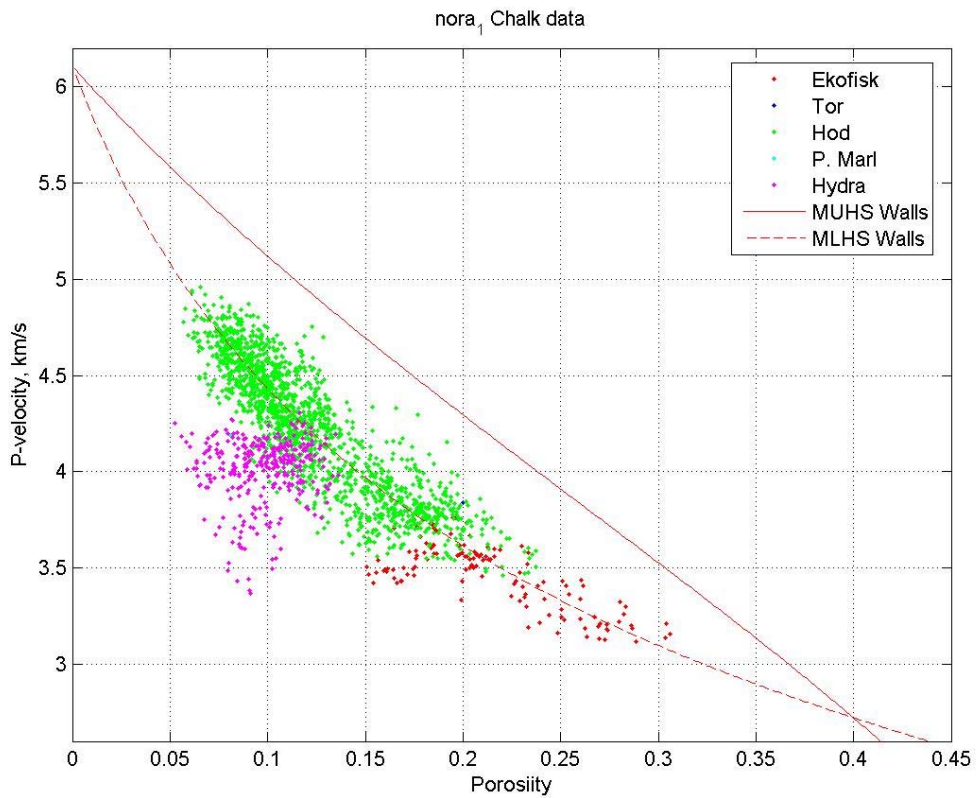
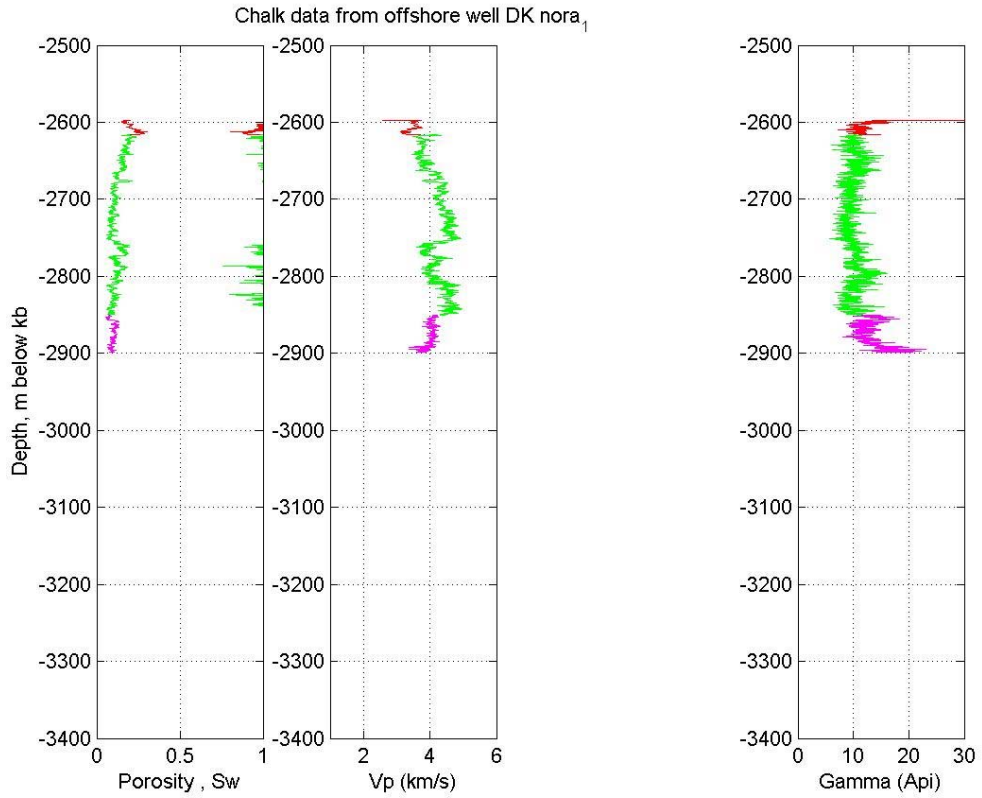
jette₁ Chalk data



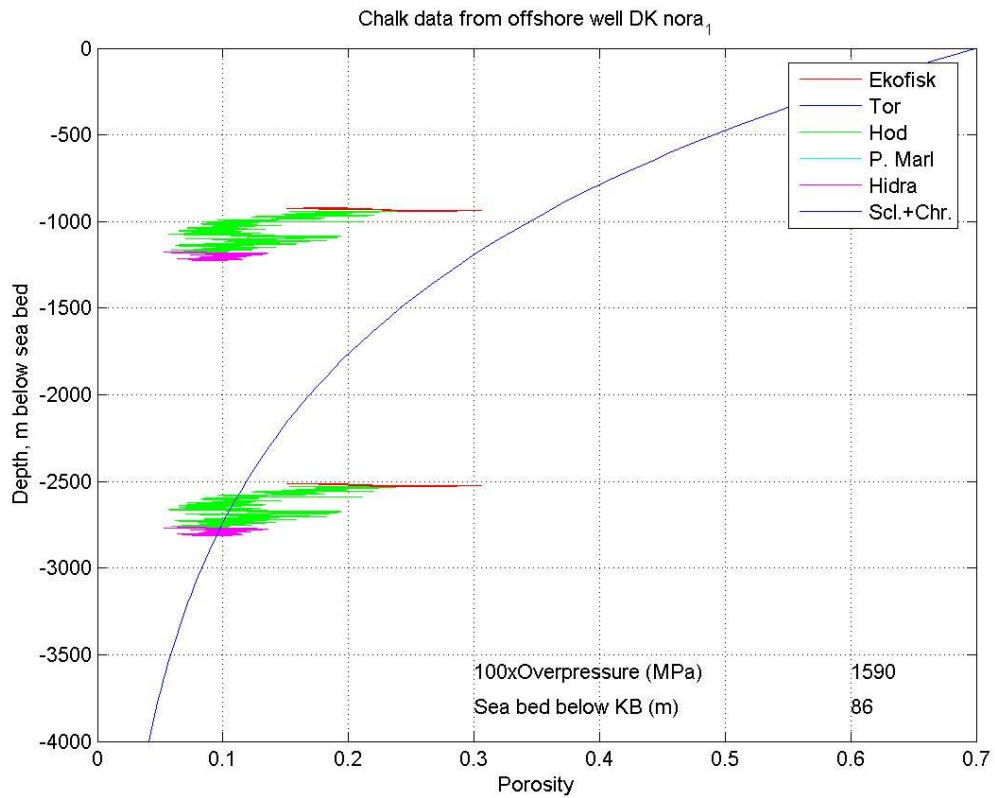
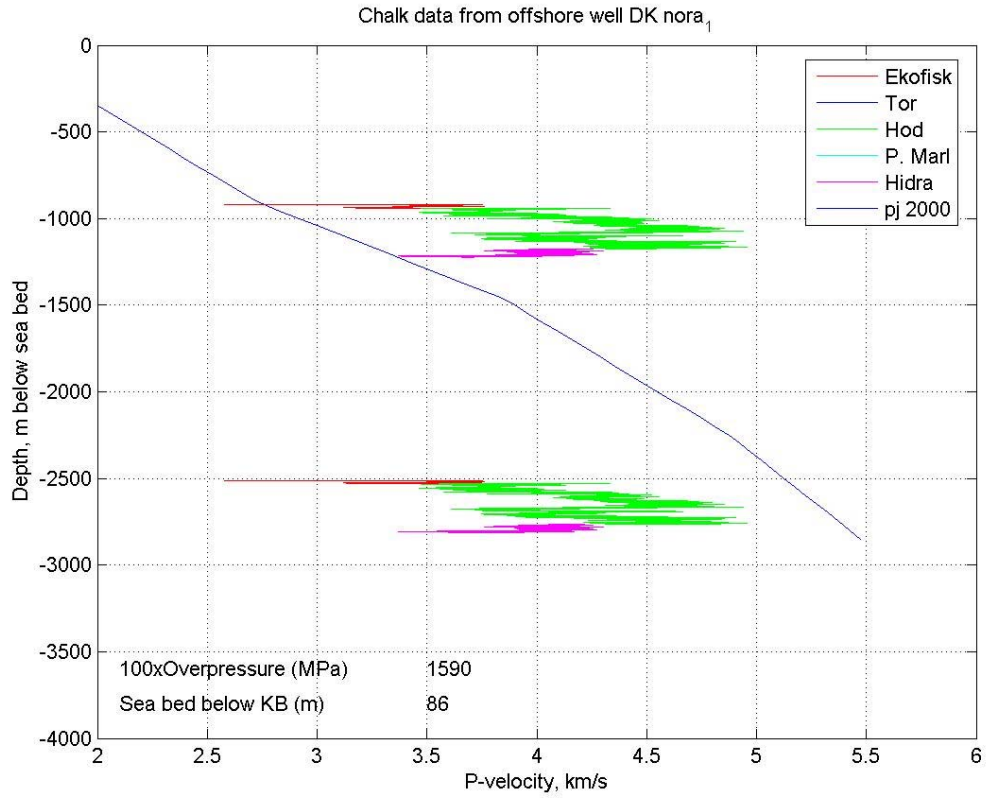
Jette-1



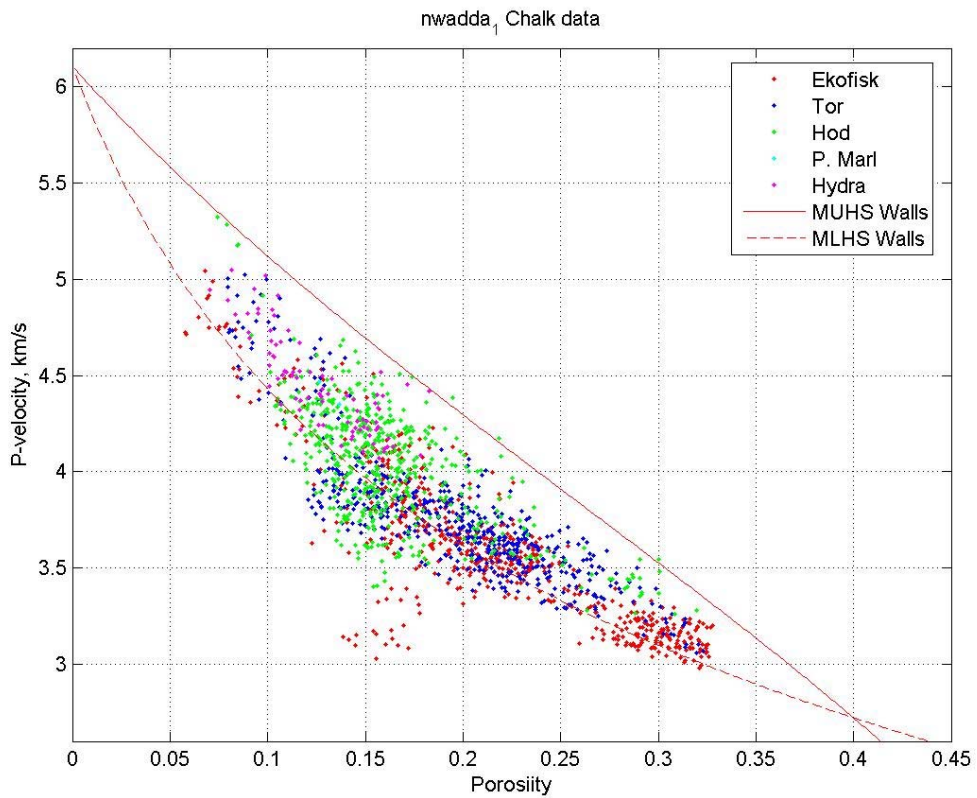
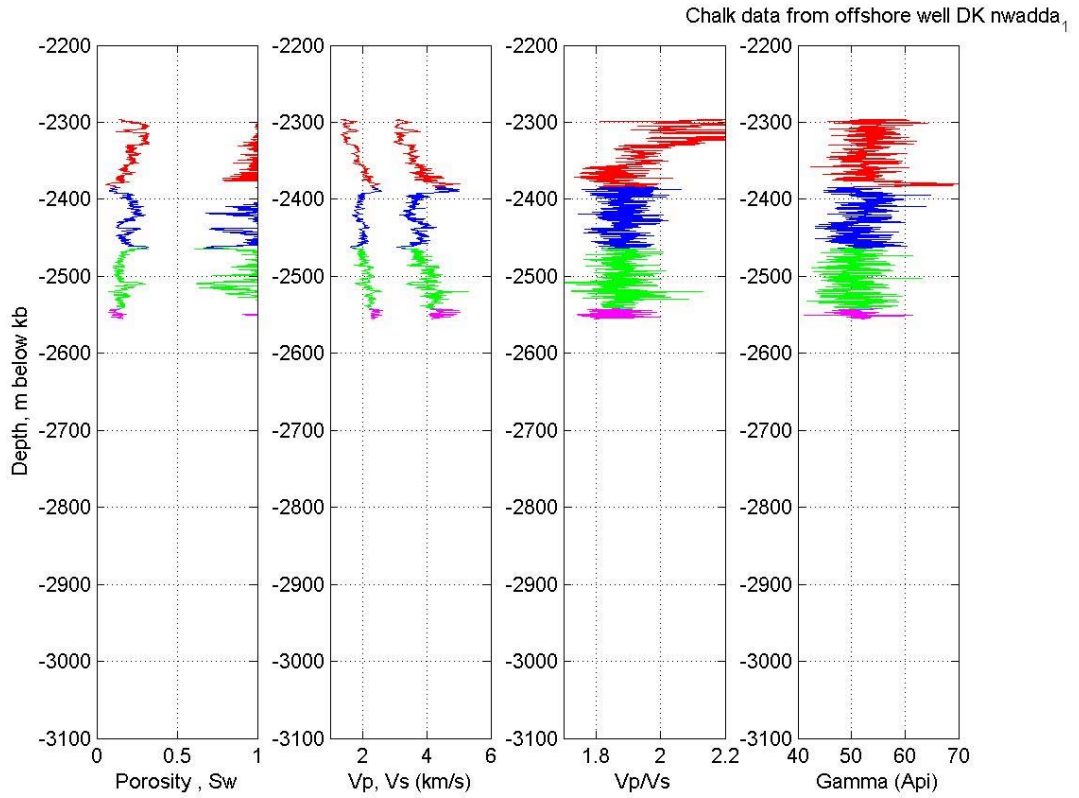
Jette-1



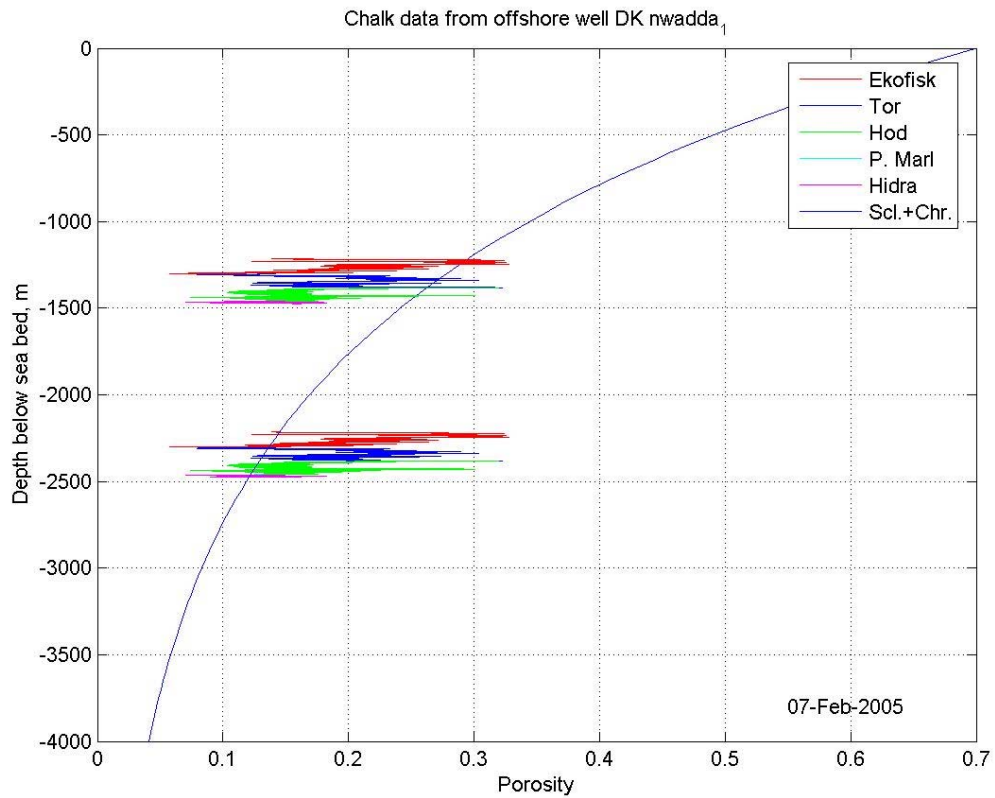
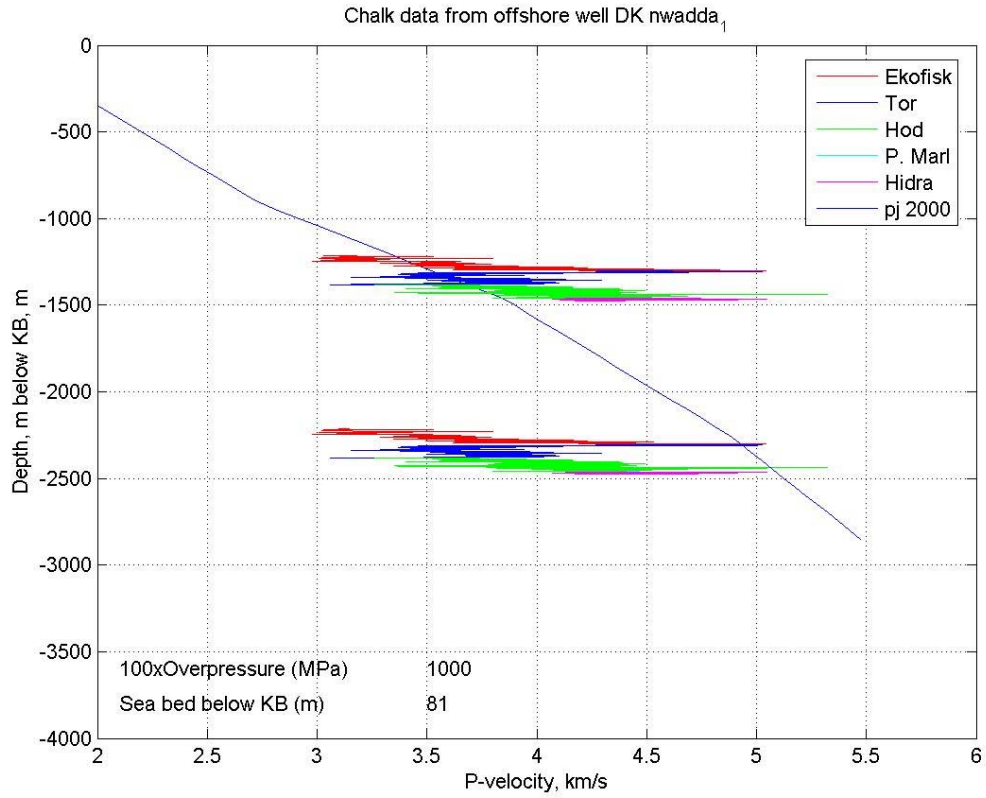
Nora-1



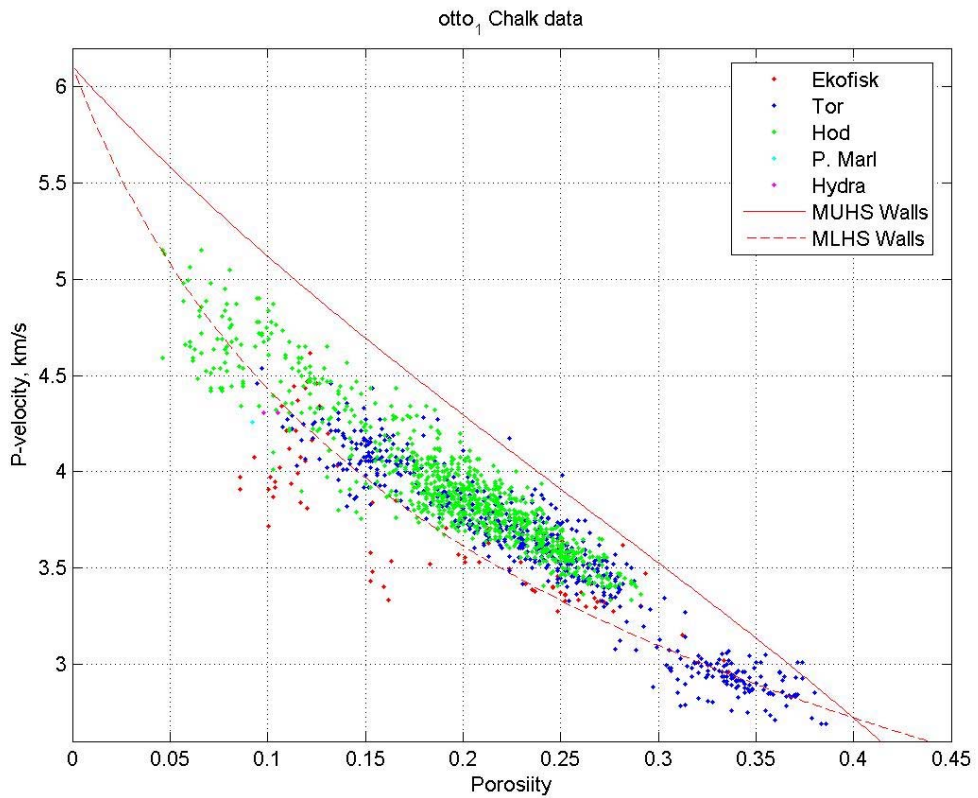
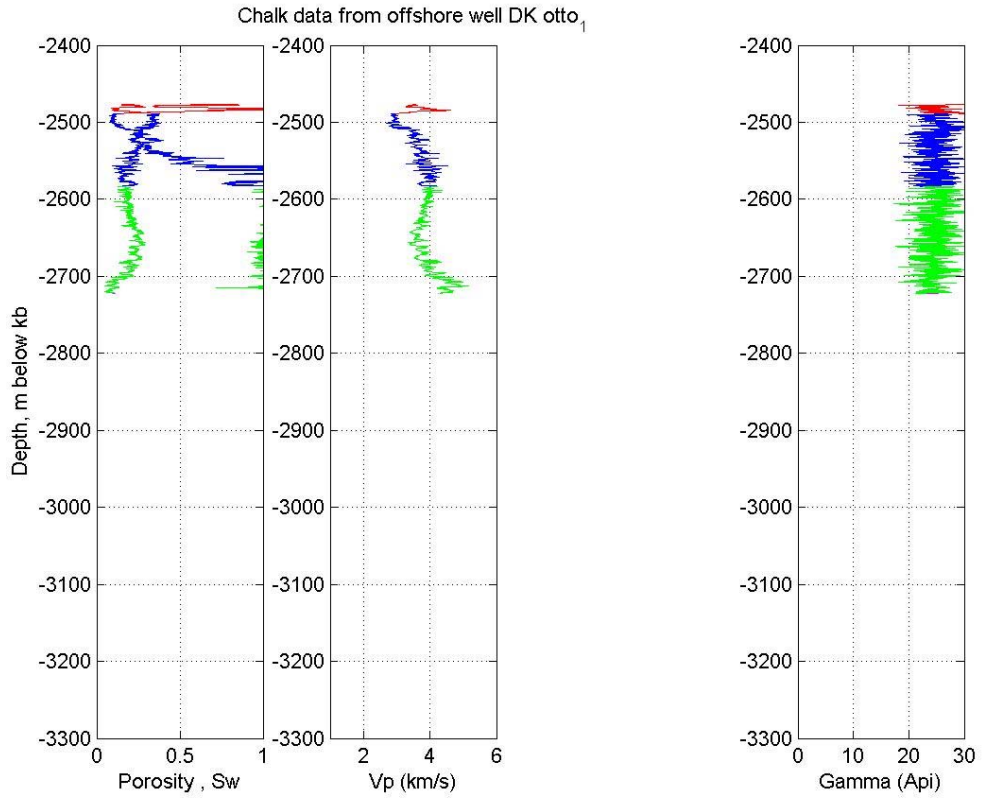
Nora-1



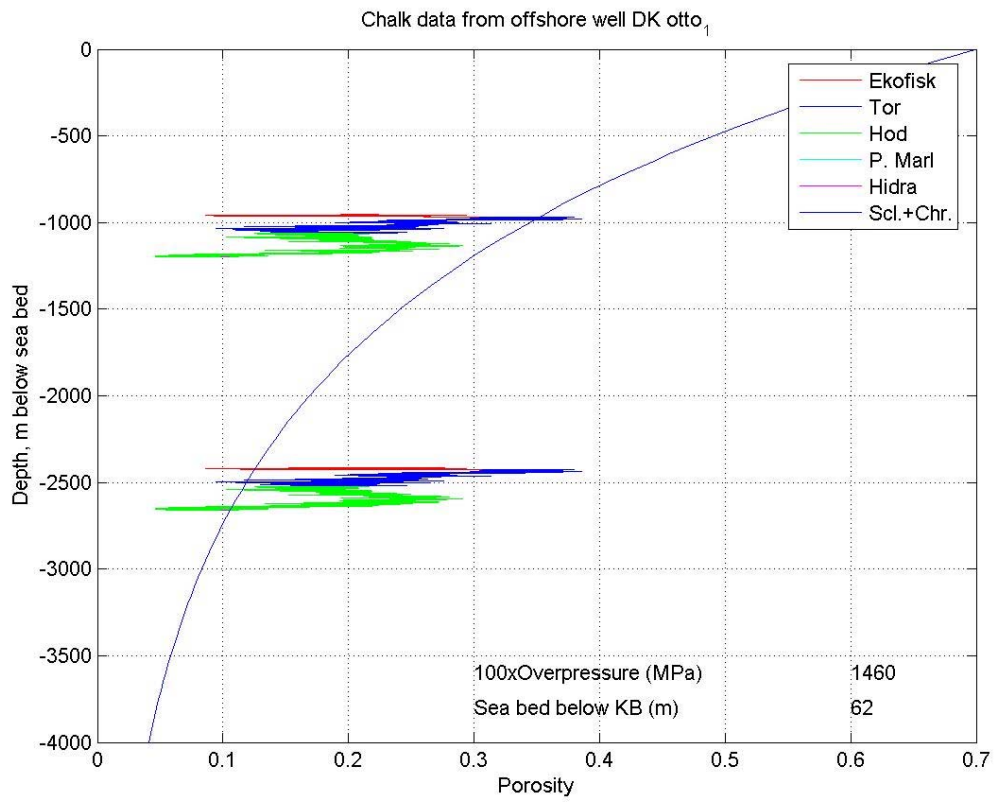
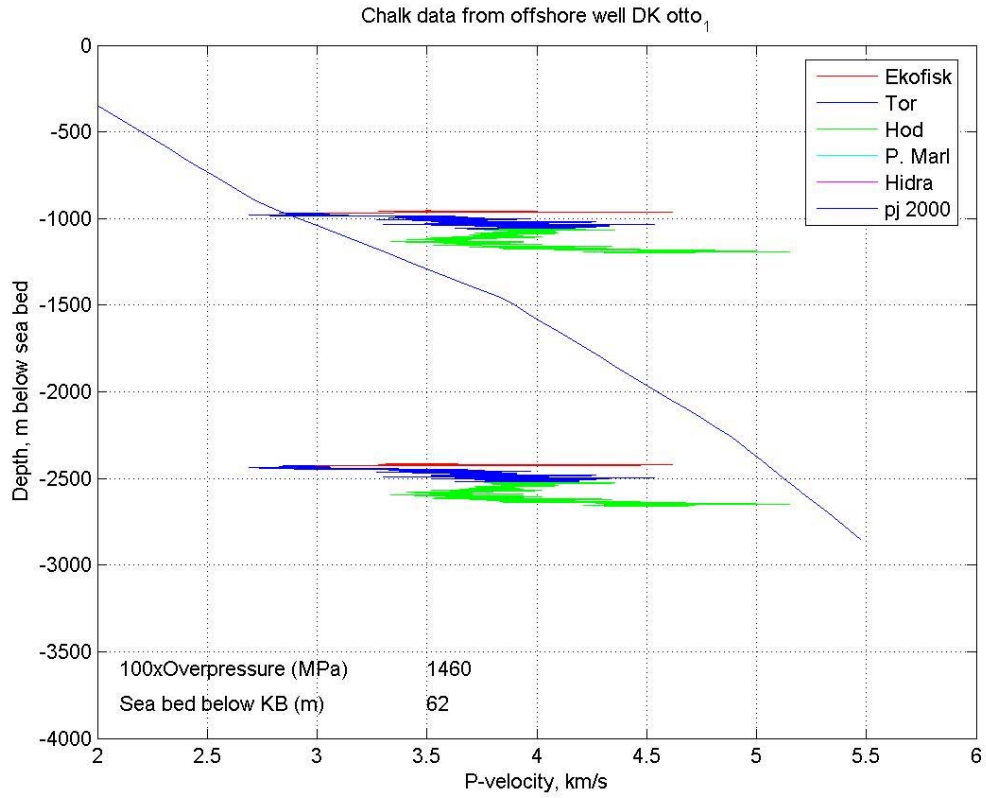
NW Adda-1



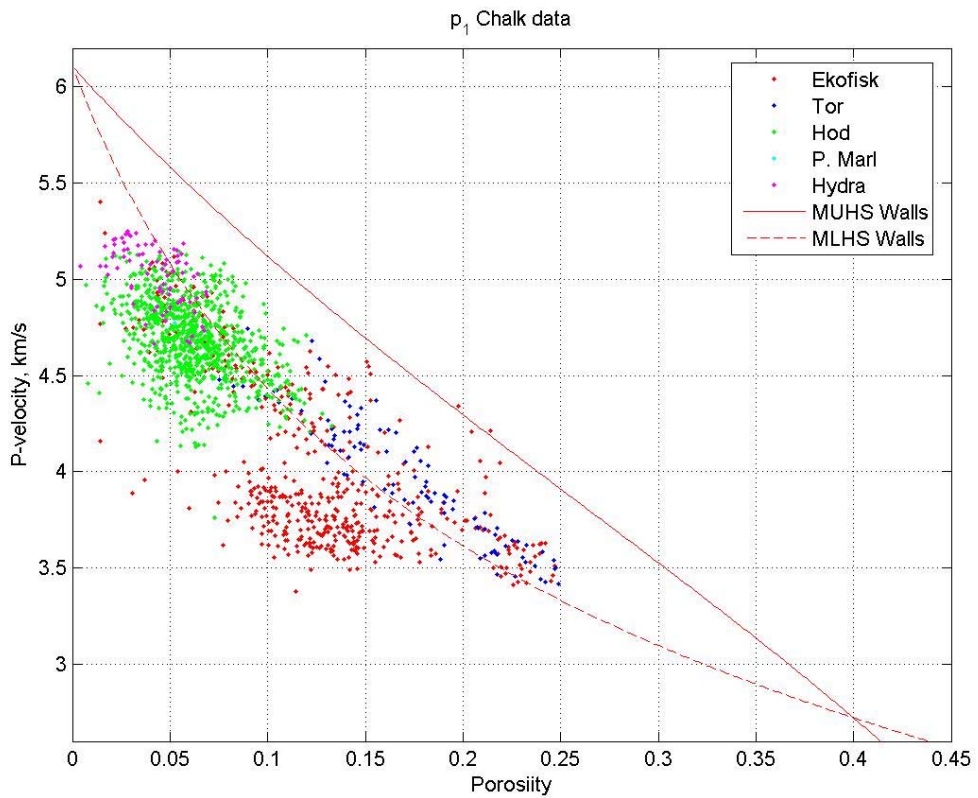
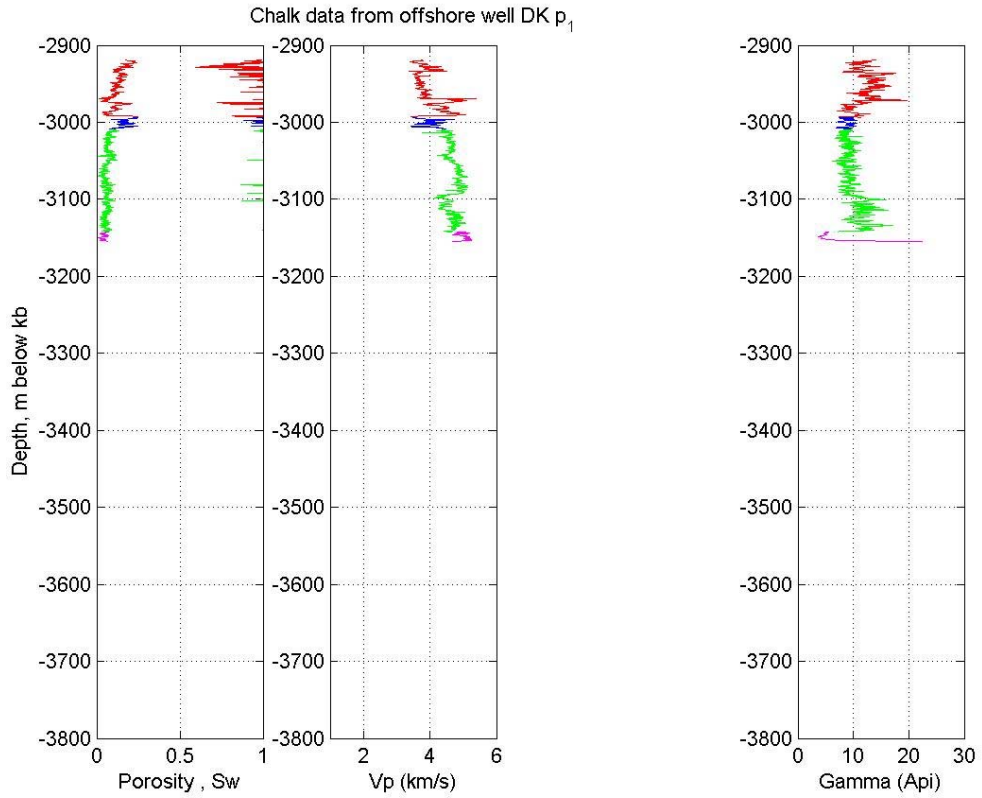
NW Adda-1



Otto-1

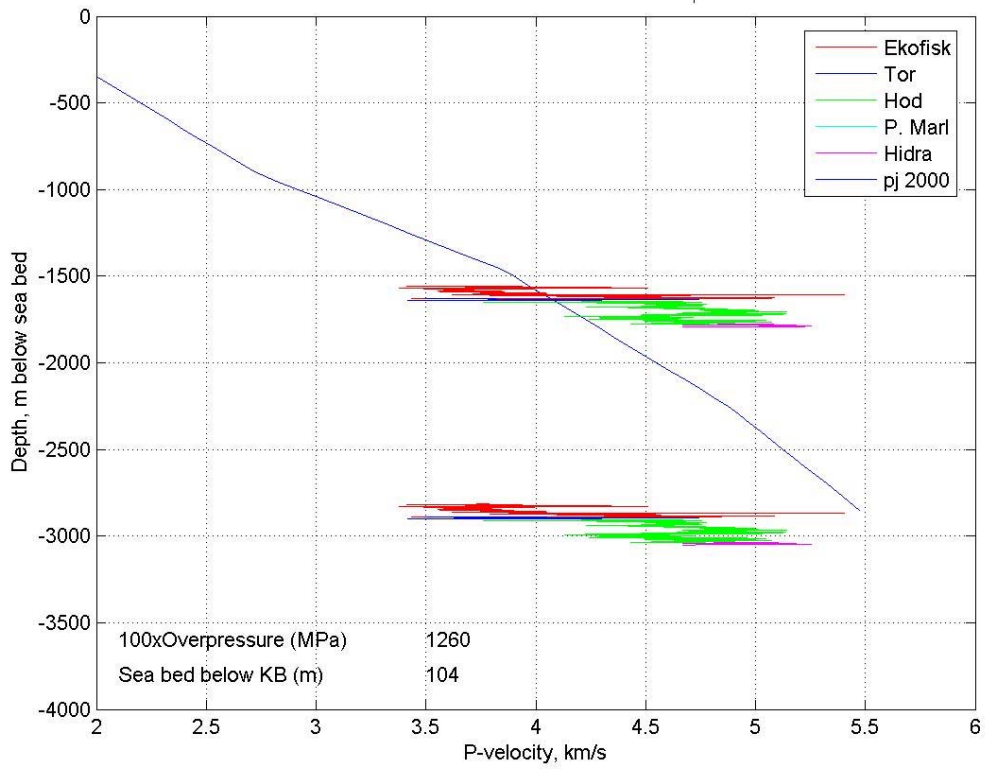


Otto-1

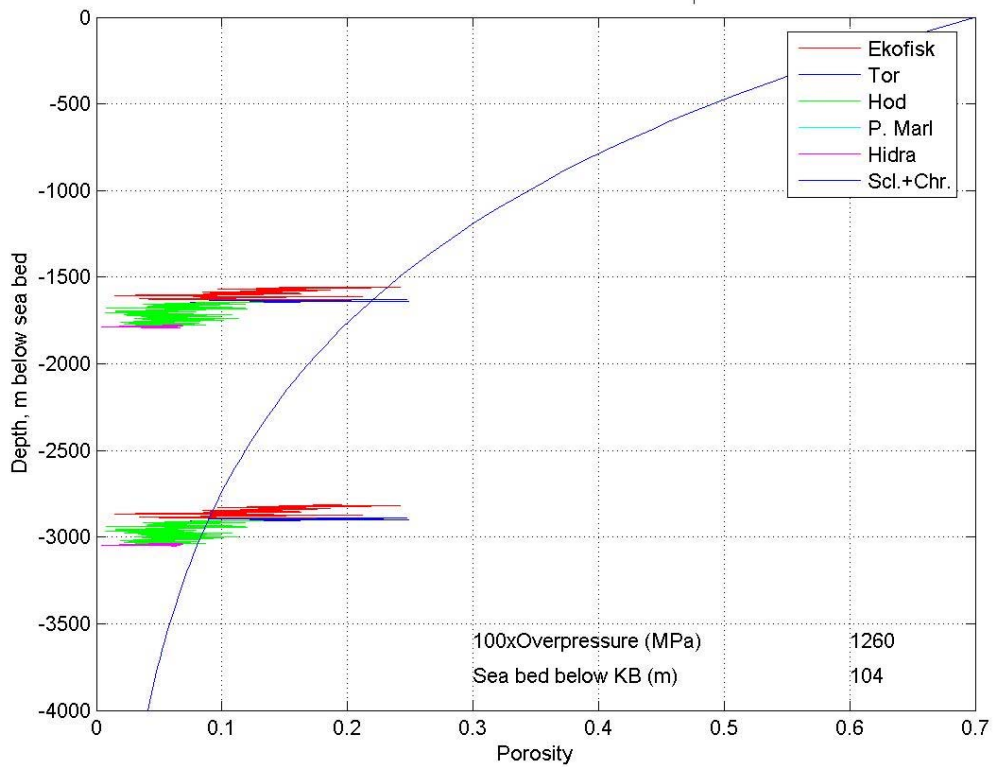


P-1

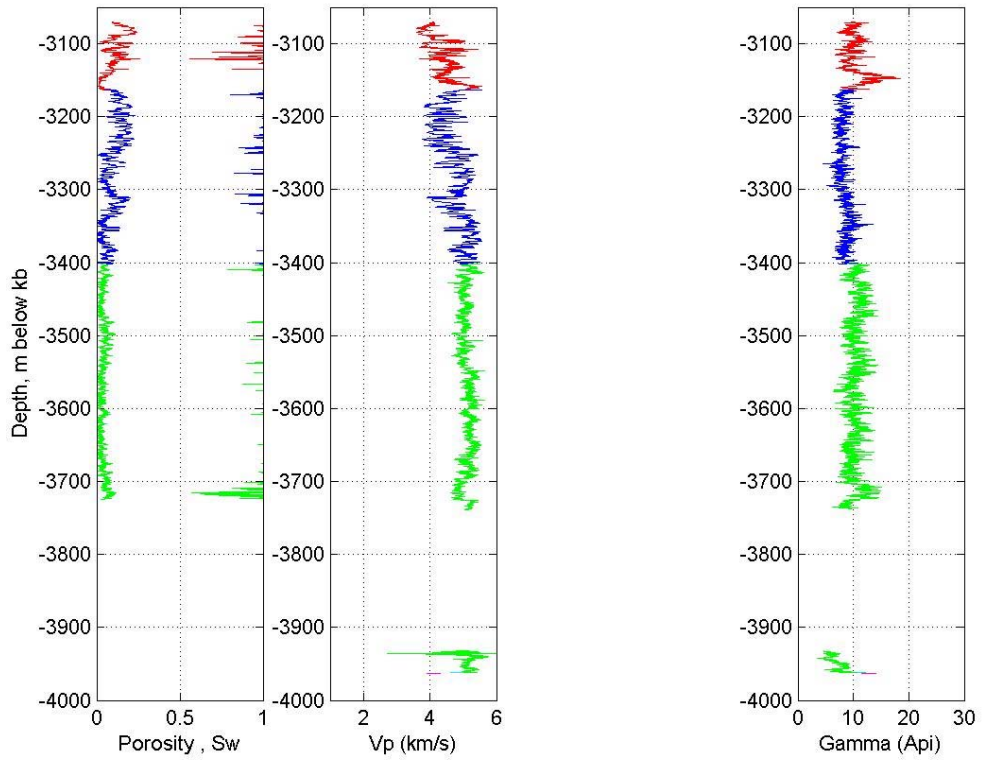
Chalk data from offshore well DK p₁



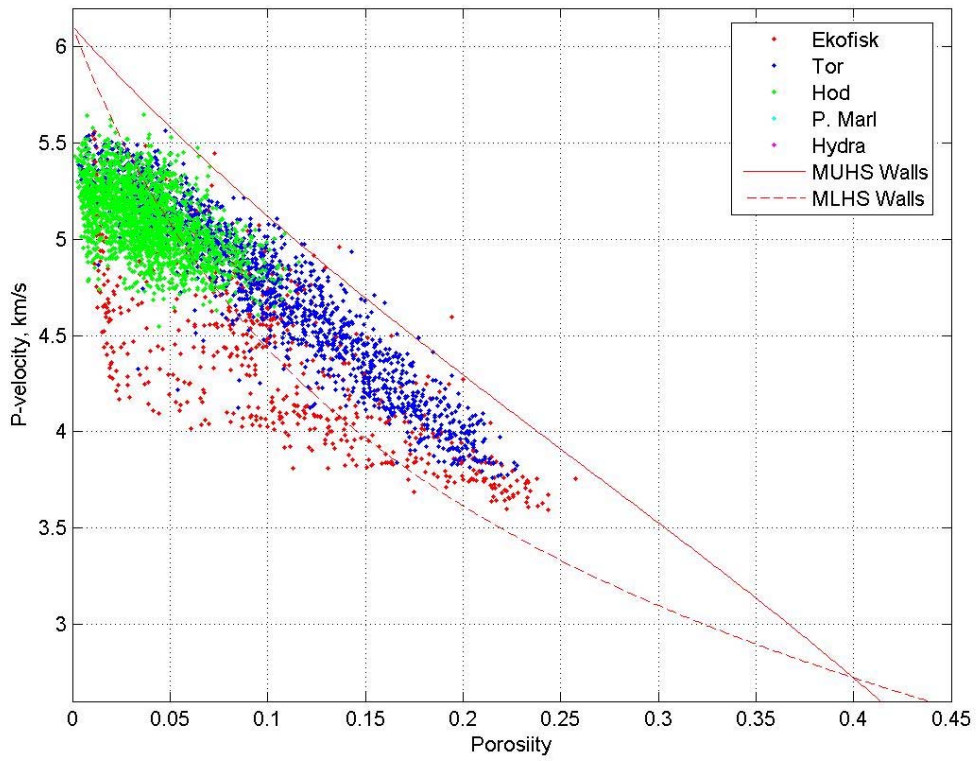
Chalk data from offshore well DK p₁



Chalk data from offshore well DK q₁

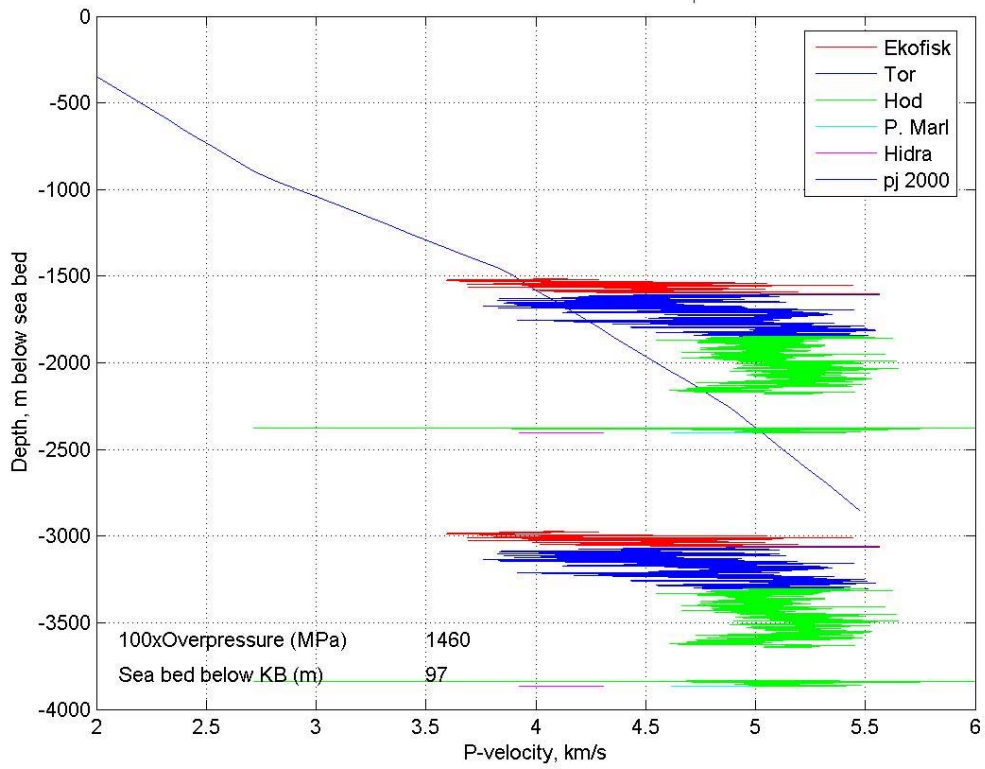


q₁ Chalk data

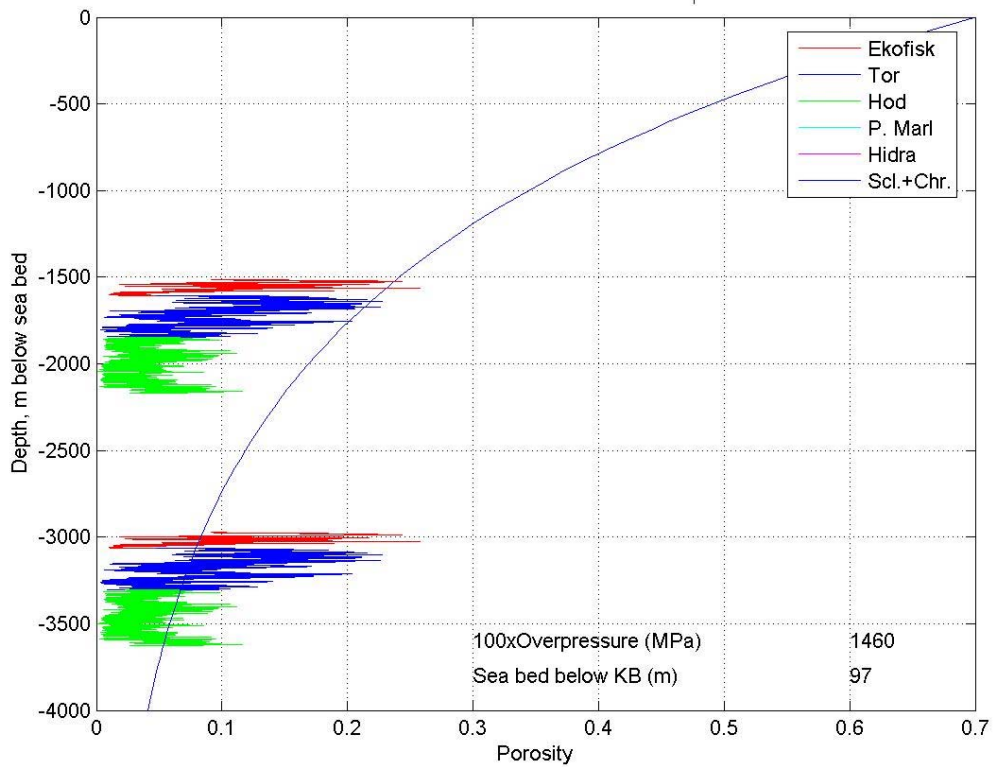


Q-1

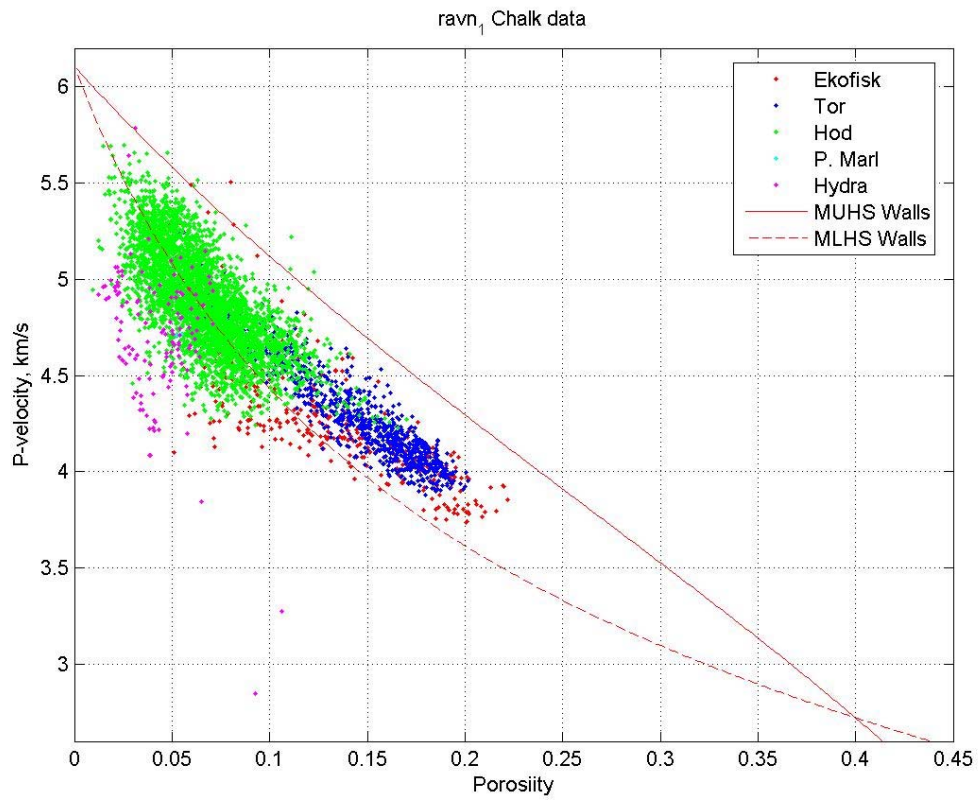
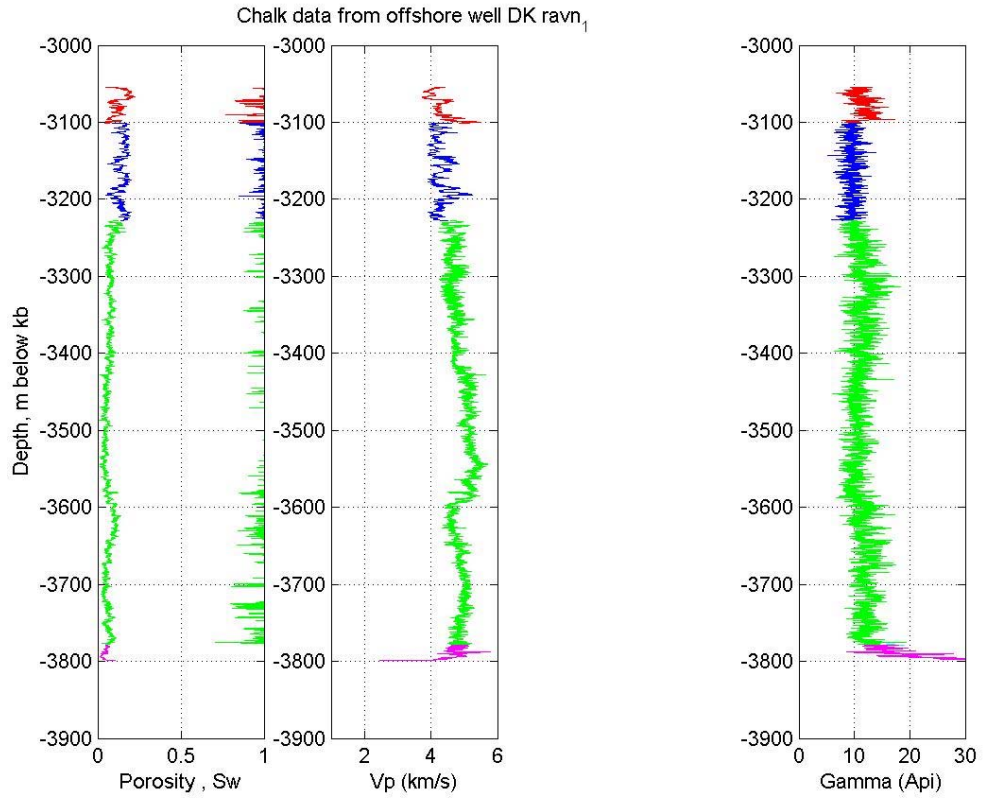
Chalk data from offshore well DK q₁



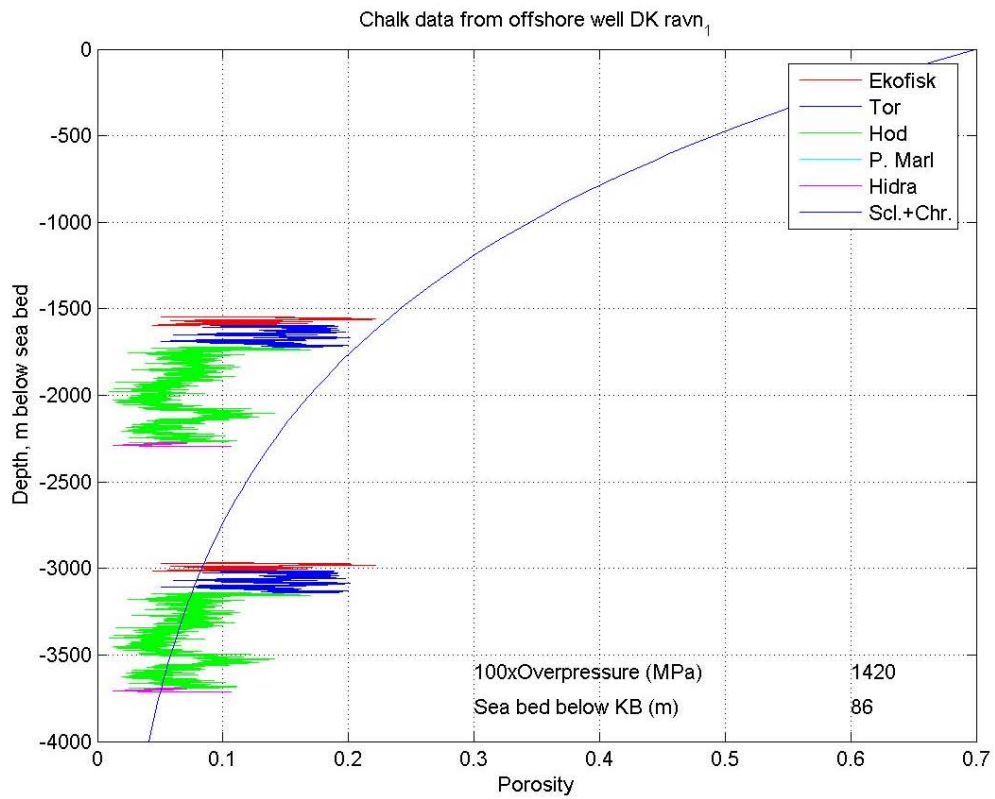
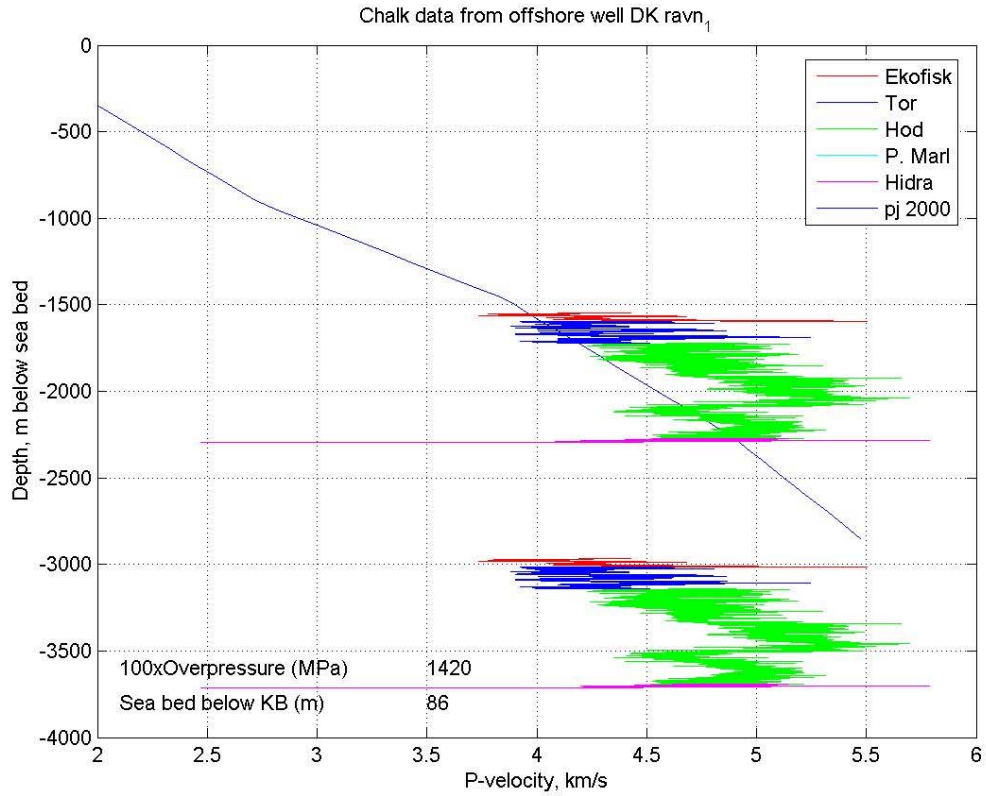
Chalk data from offshore well DK q₁



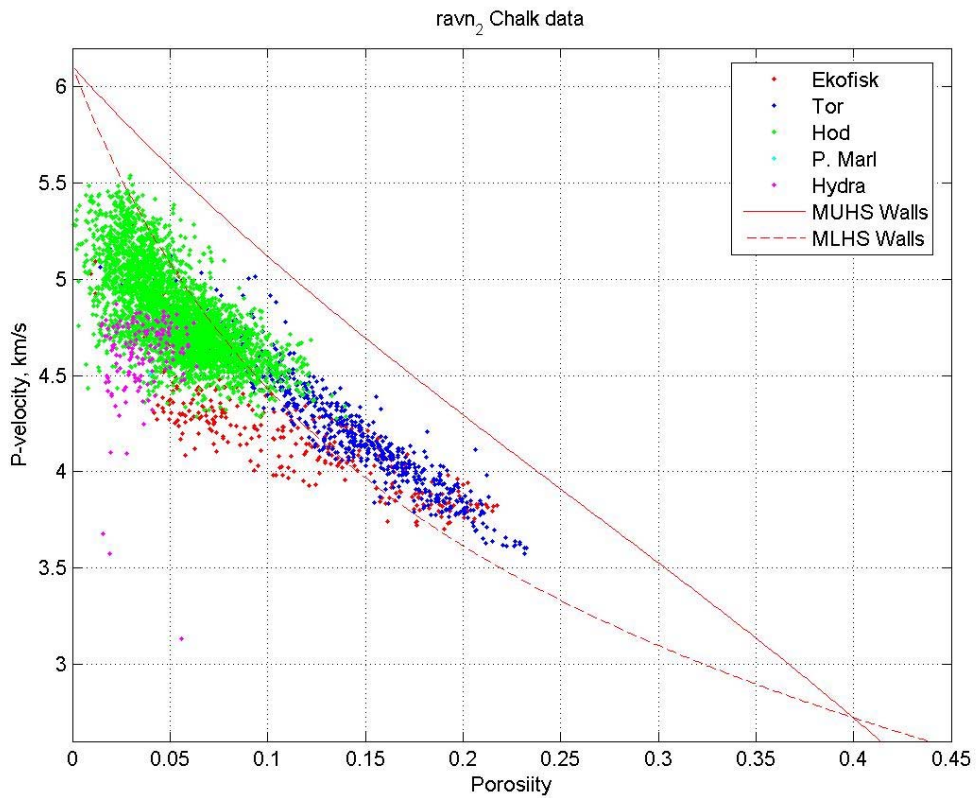
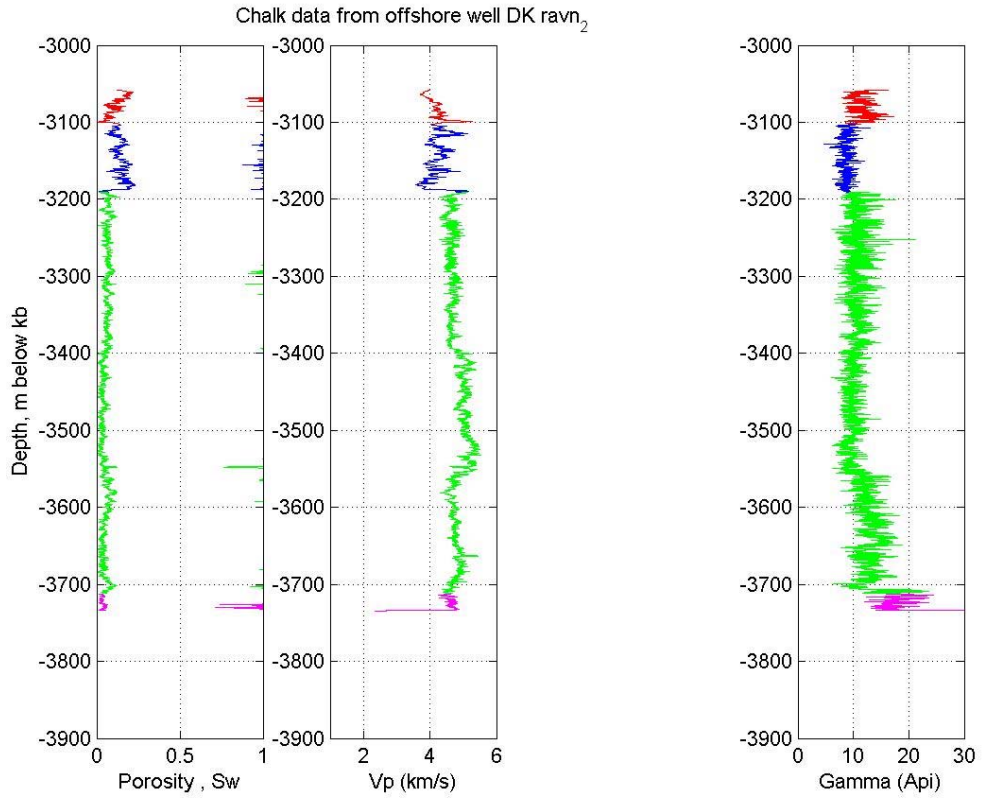
Q-1



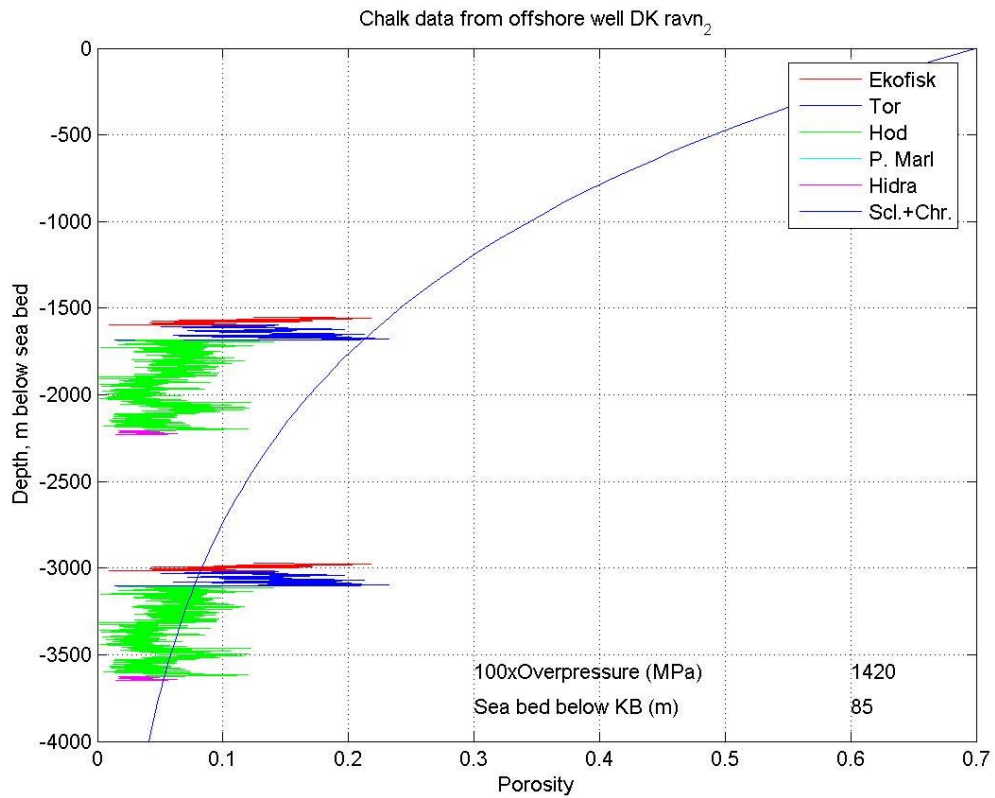
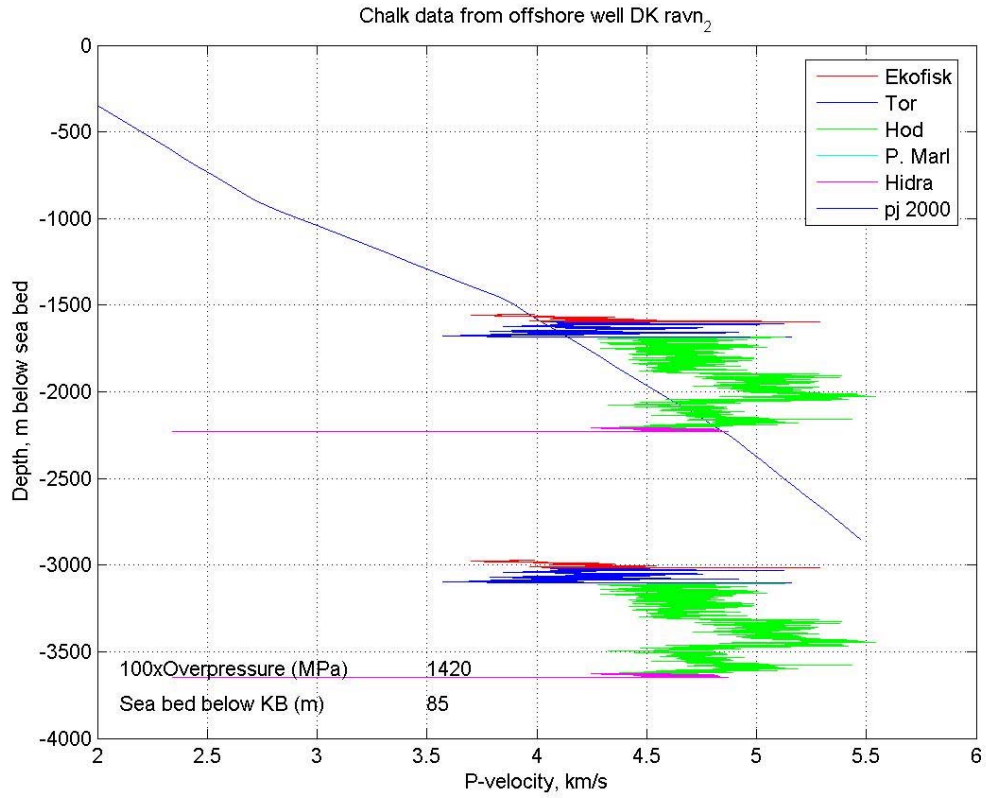
Ravn-1



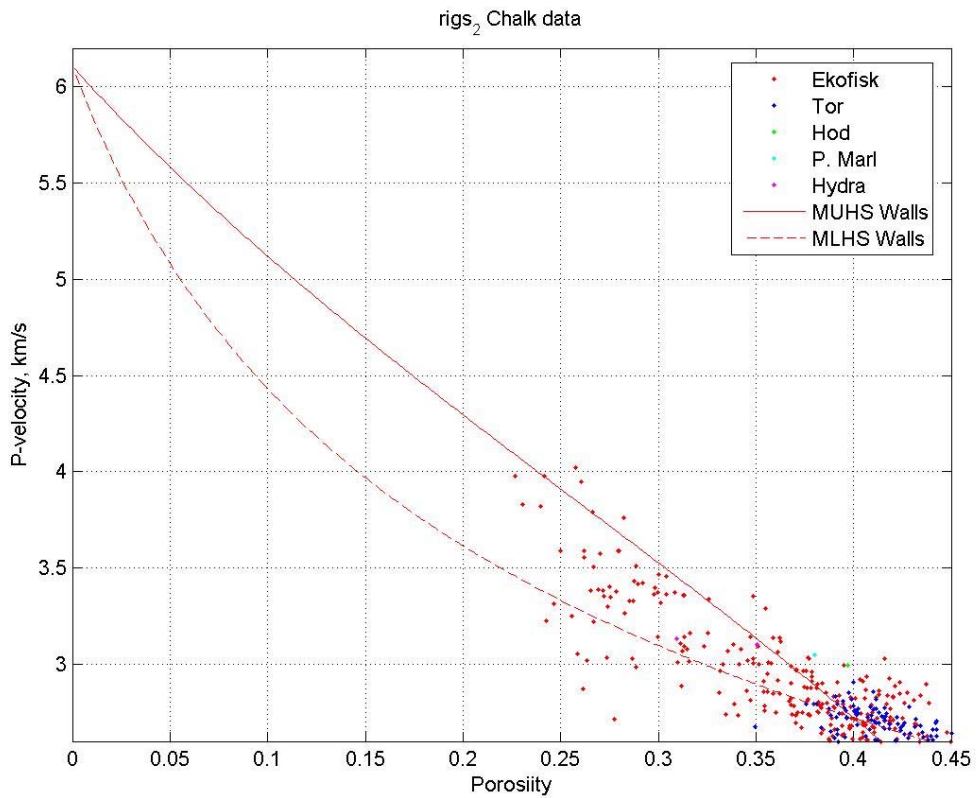
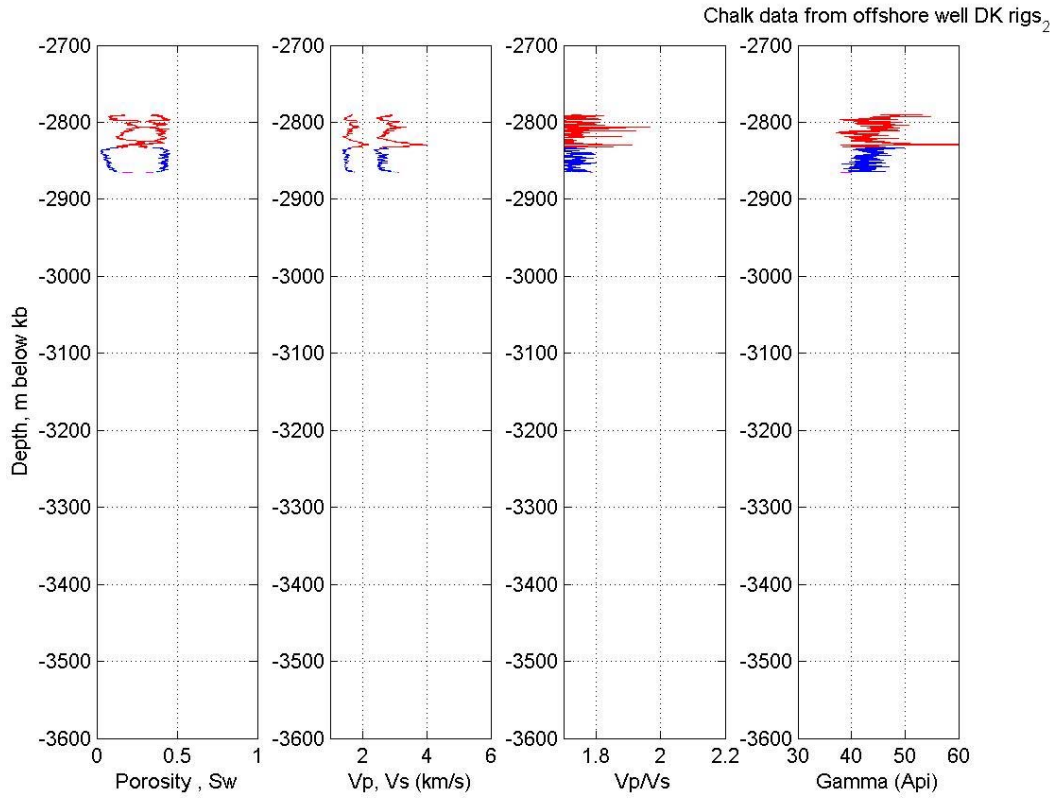
Ravn-1



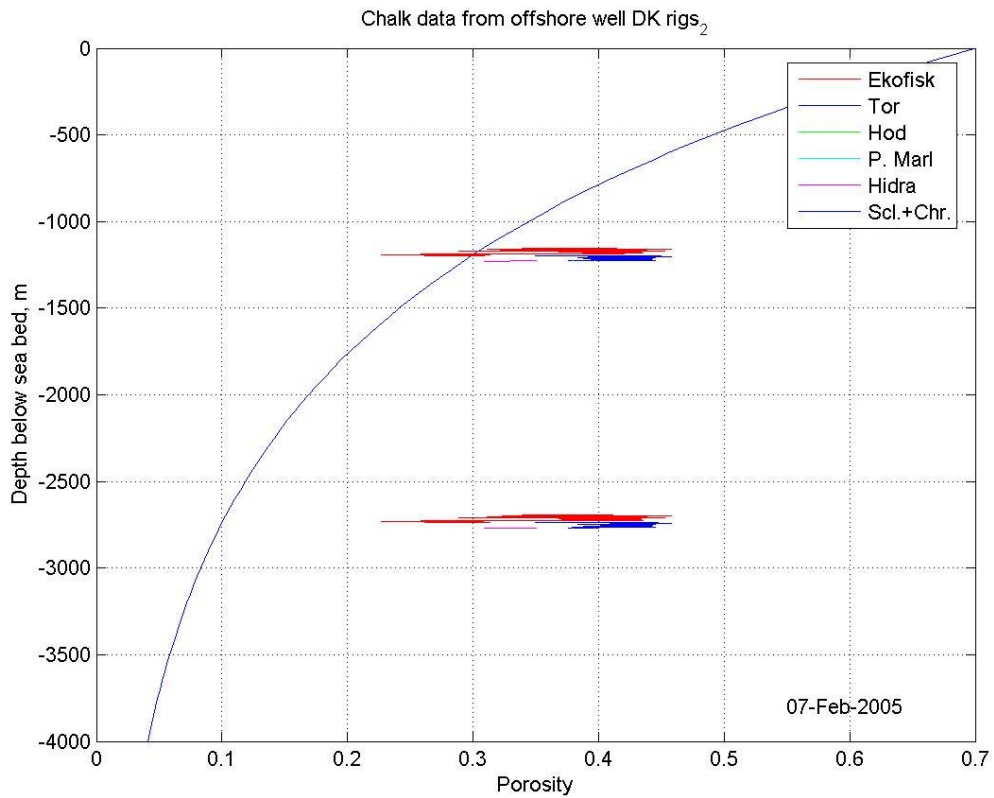
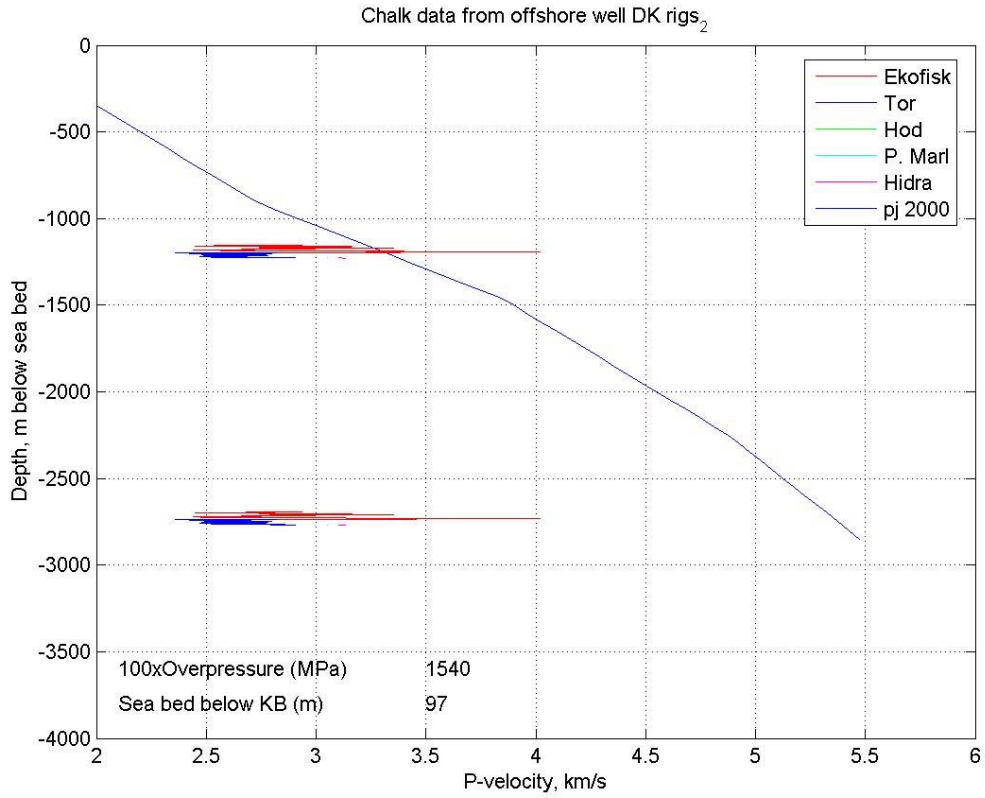
Ravn-2



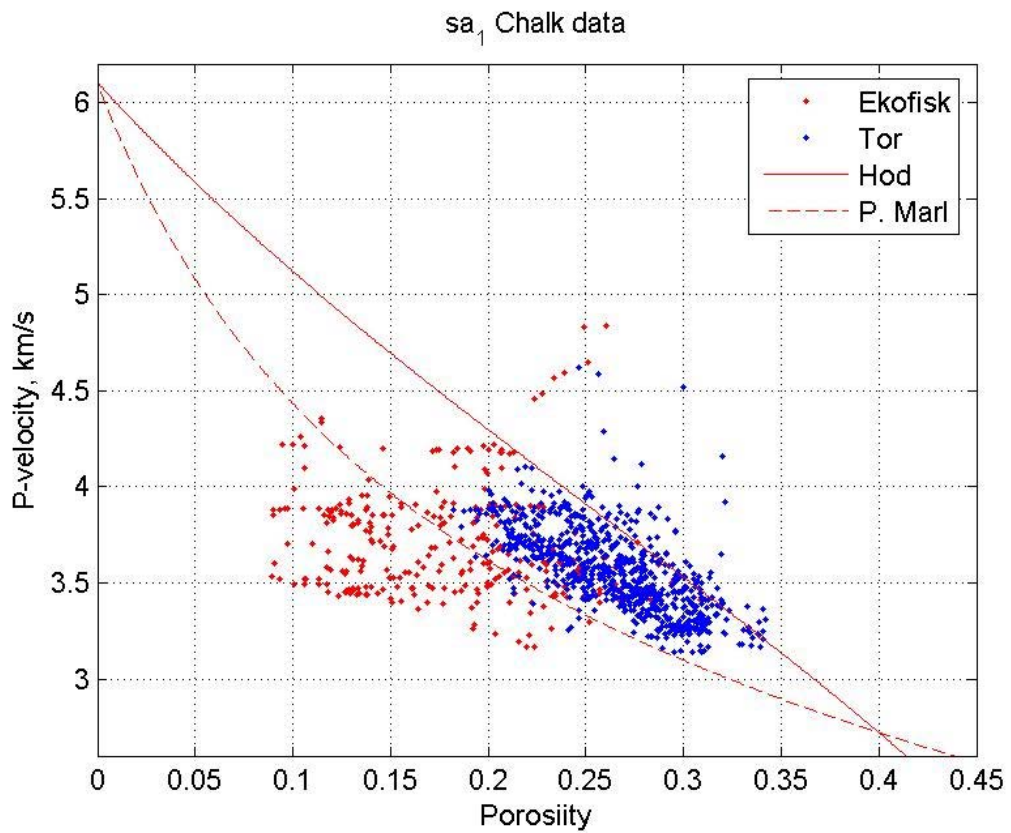
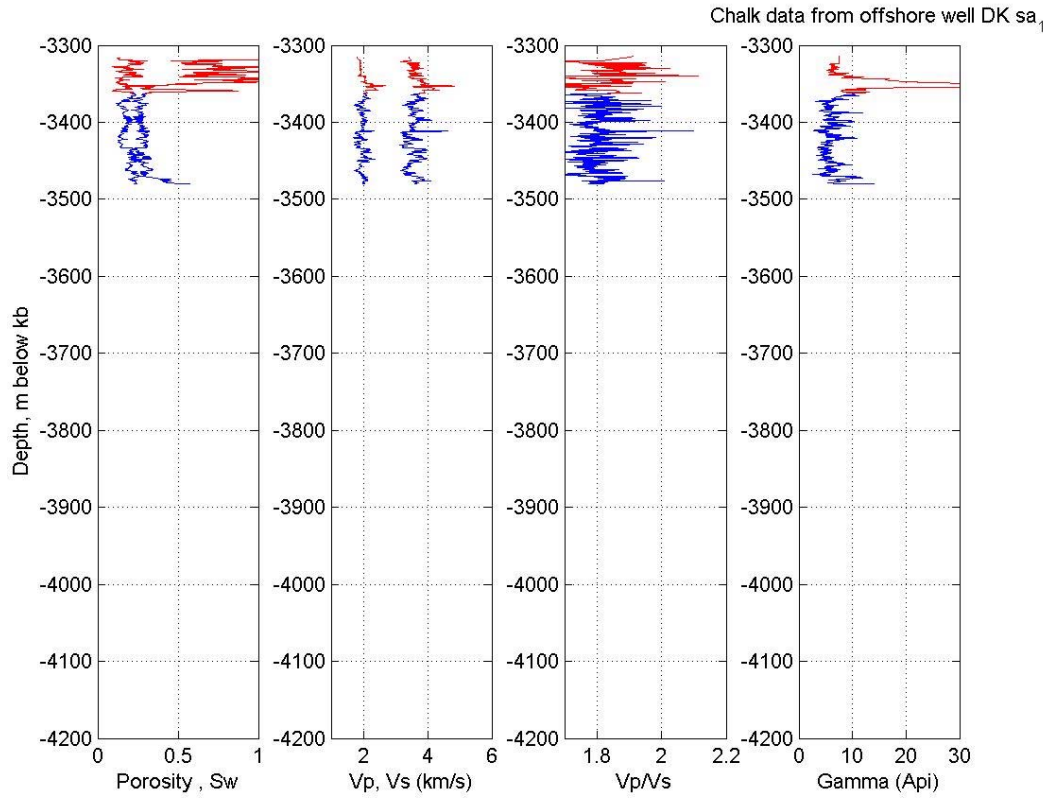
Ravn-2



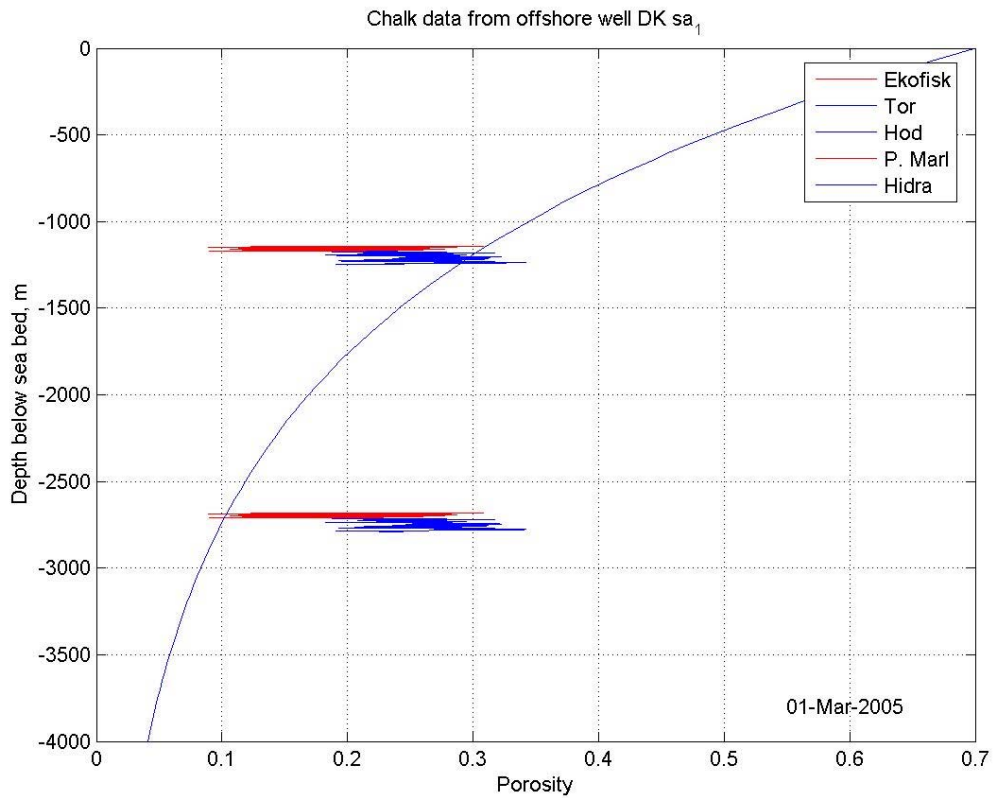
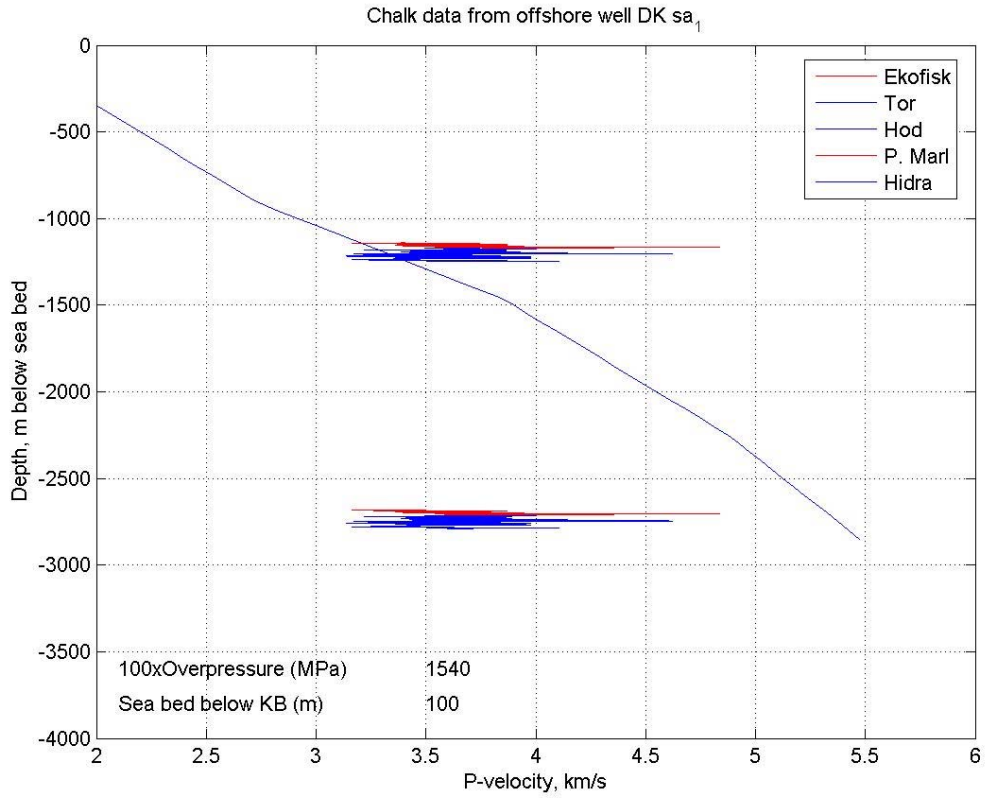
Rigs-2



Rigs-2

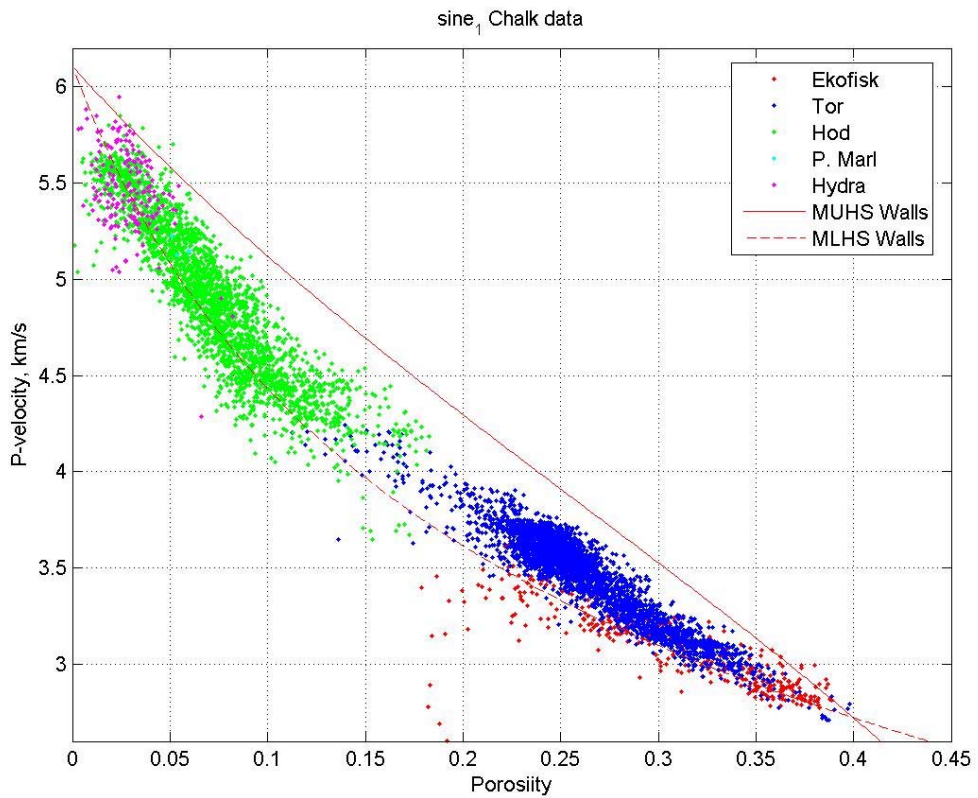
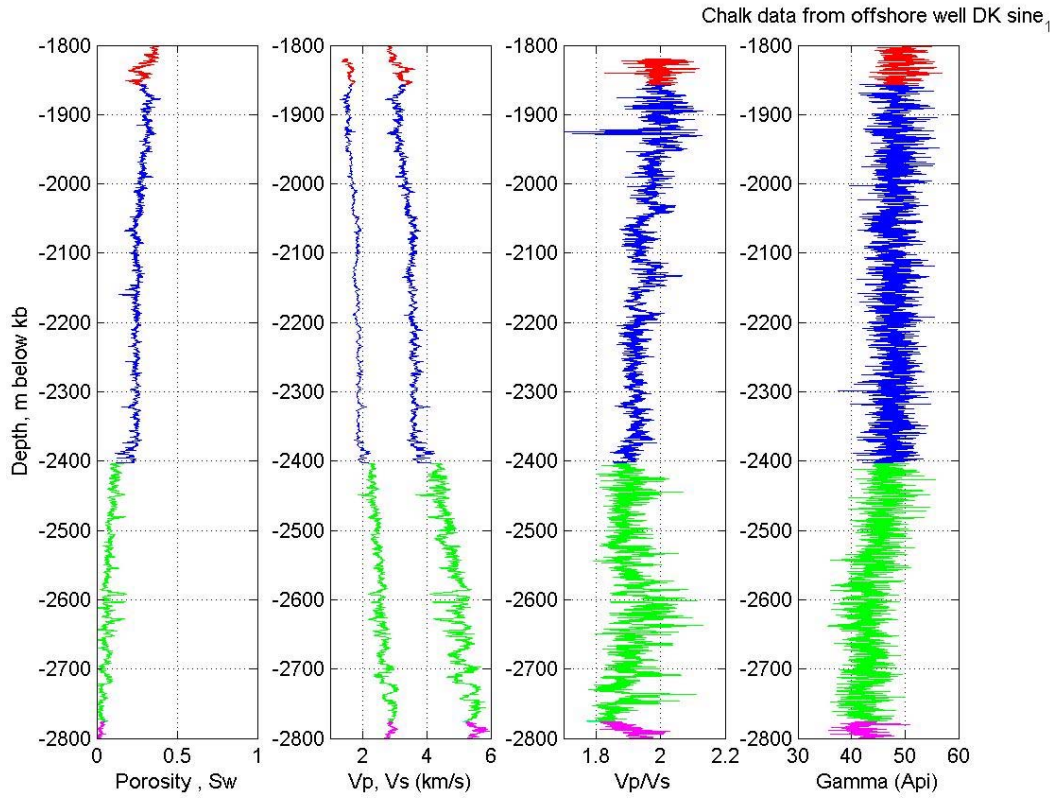


SA-1
Log plot in measured depths

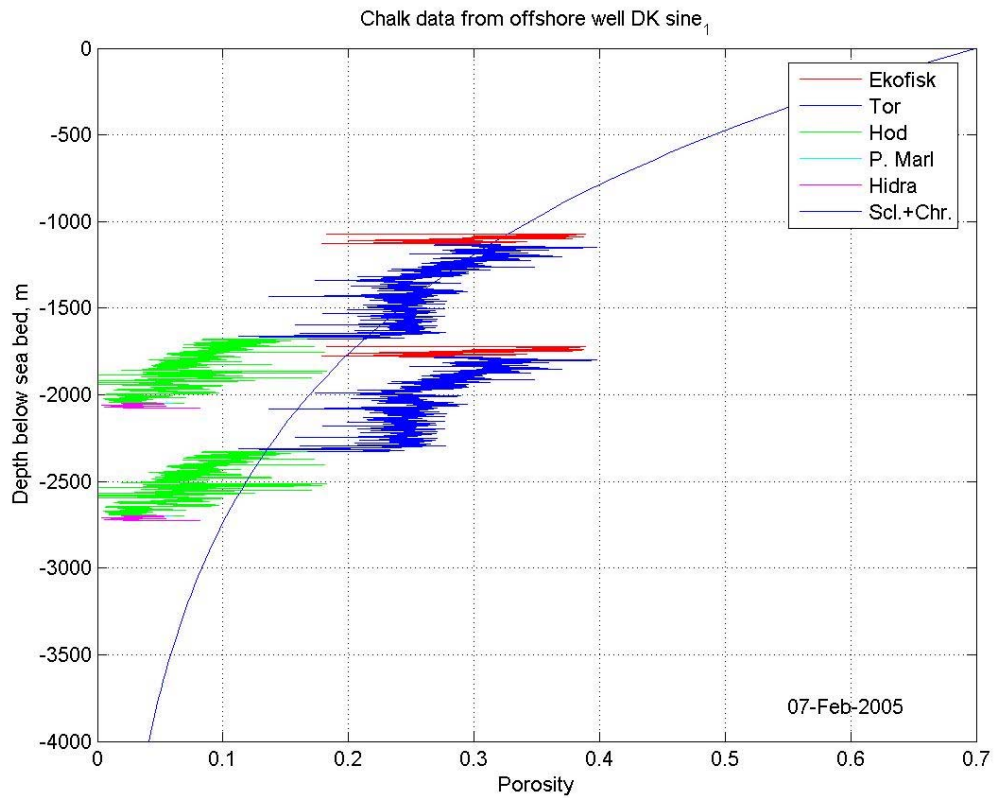
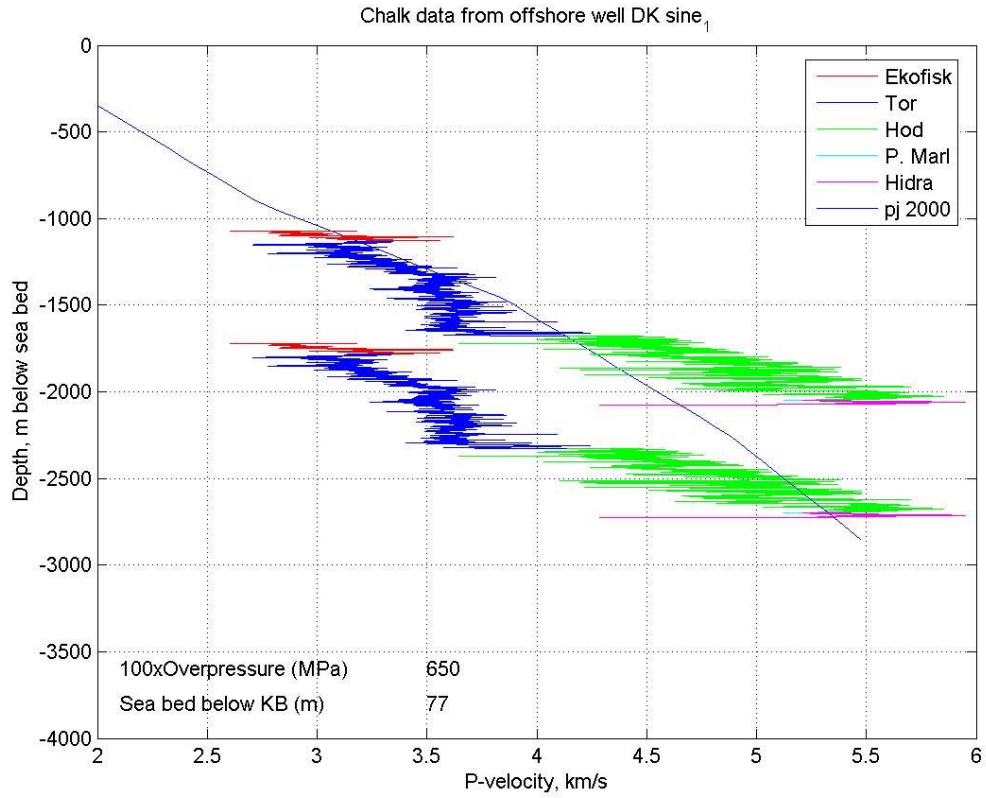


True vertical depths

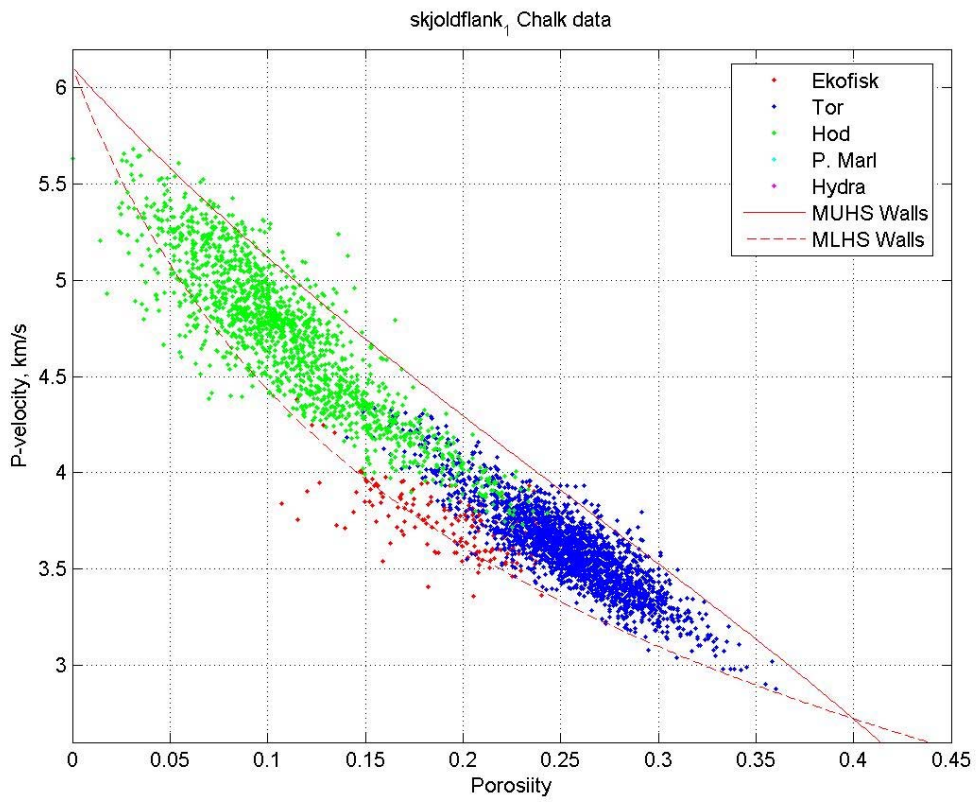
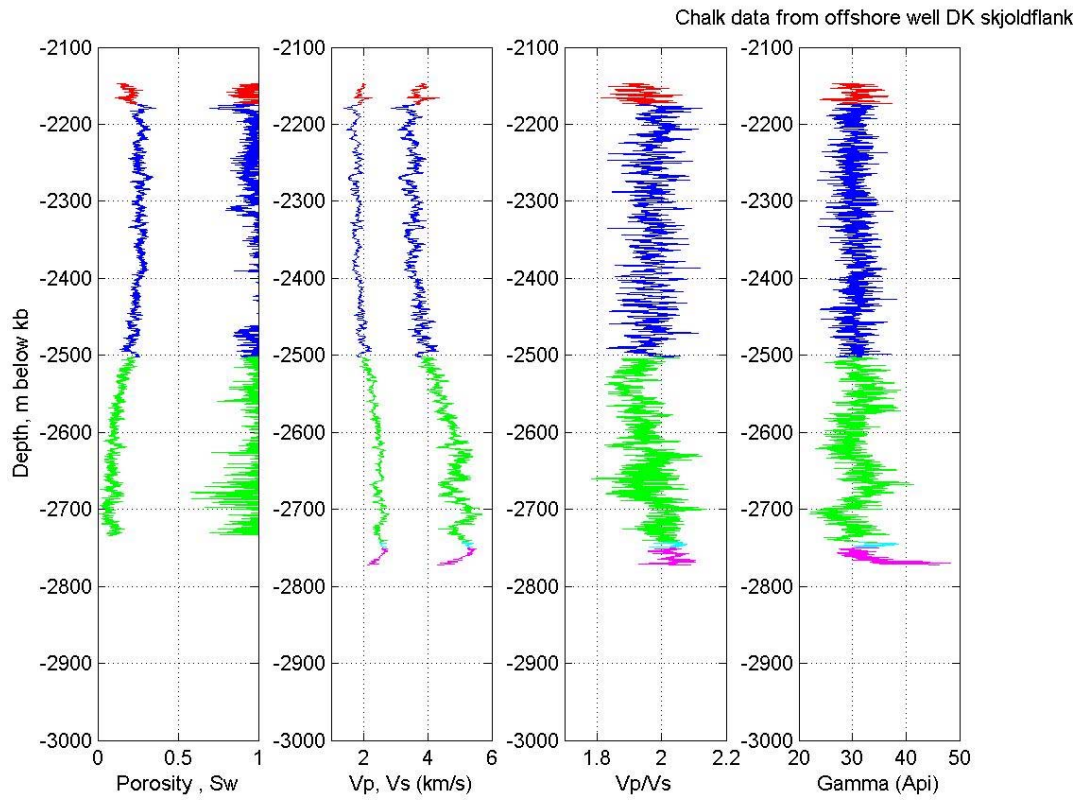
SA-1



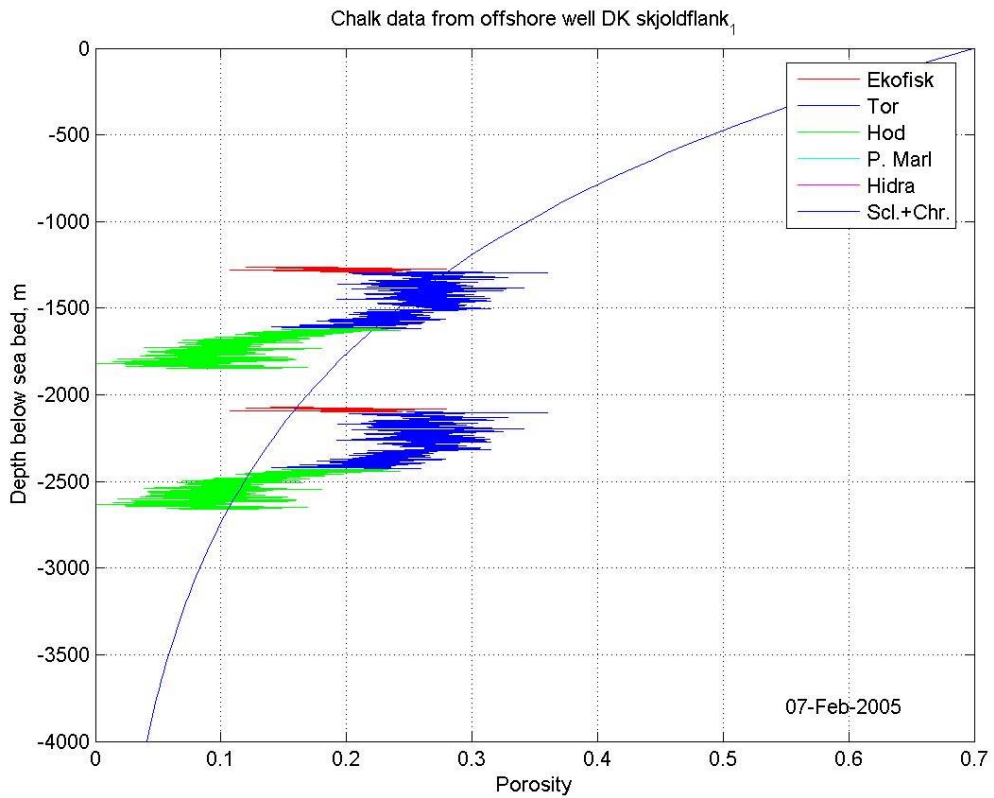
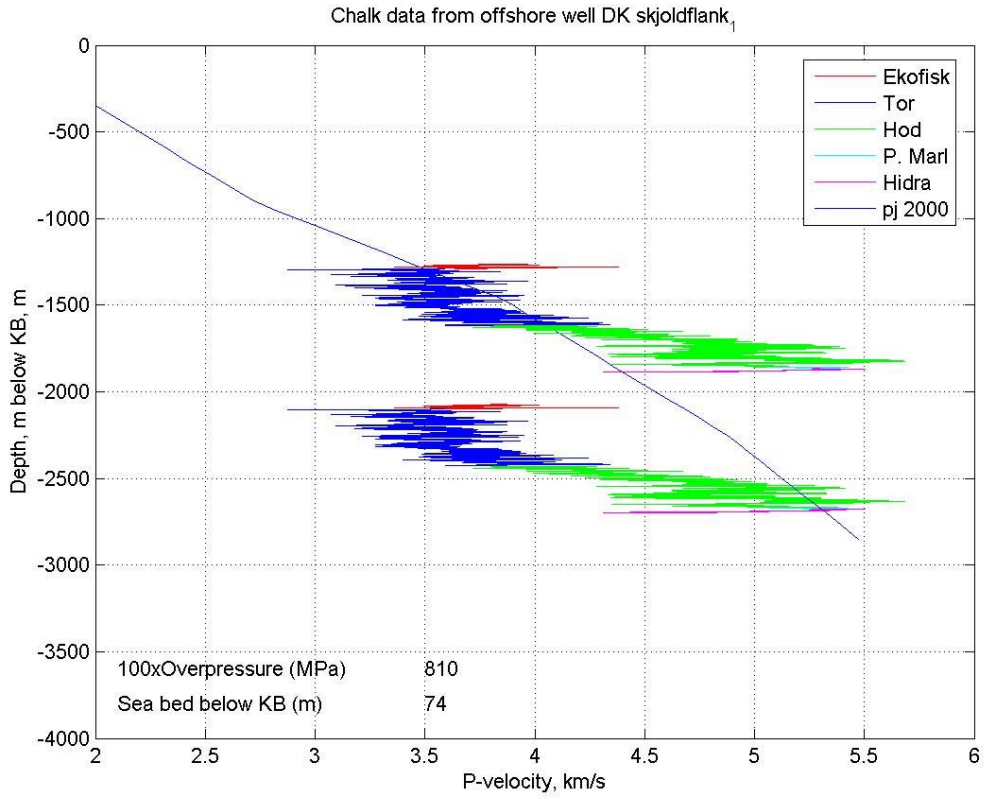
Sine-1



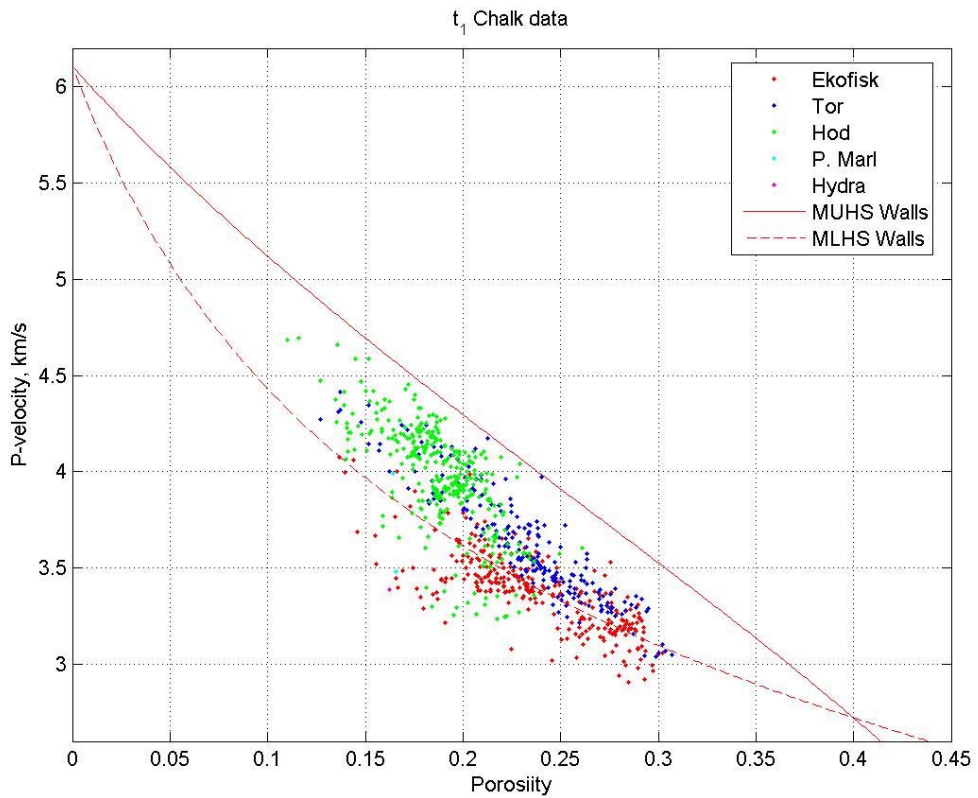
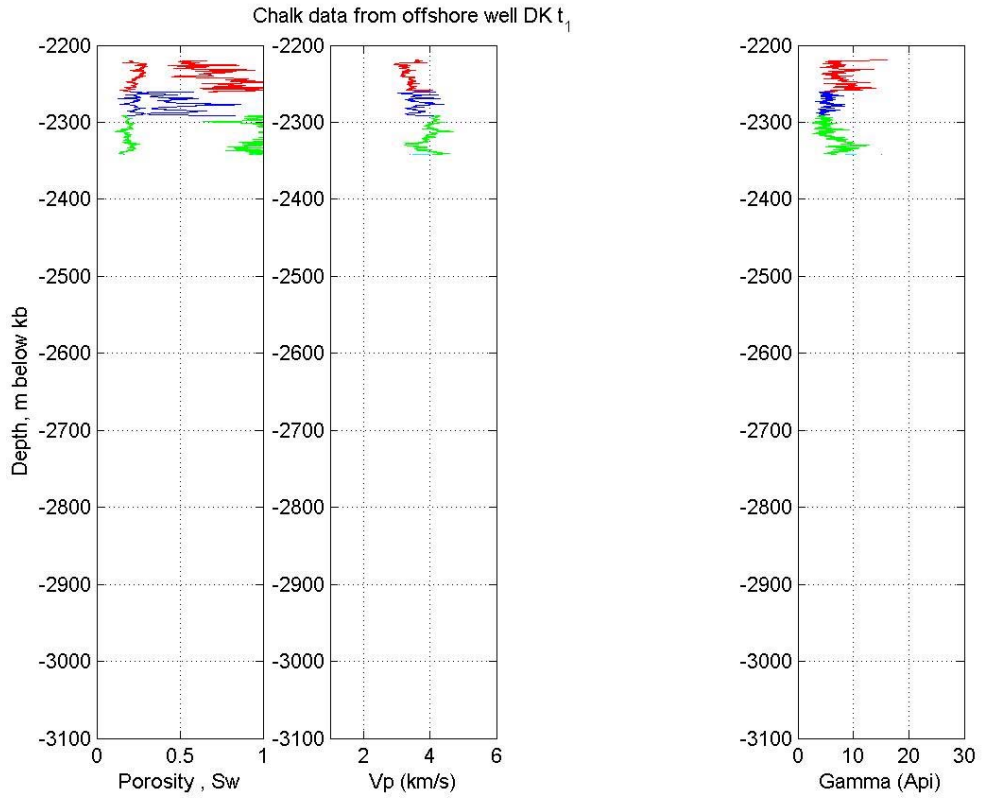
Sine-1



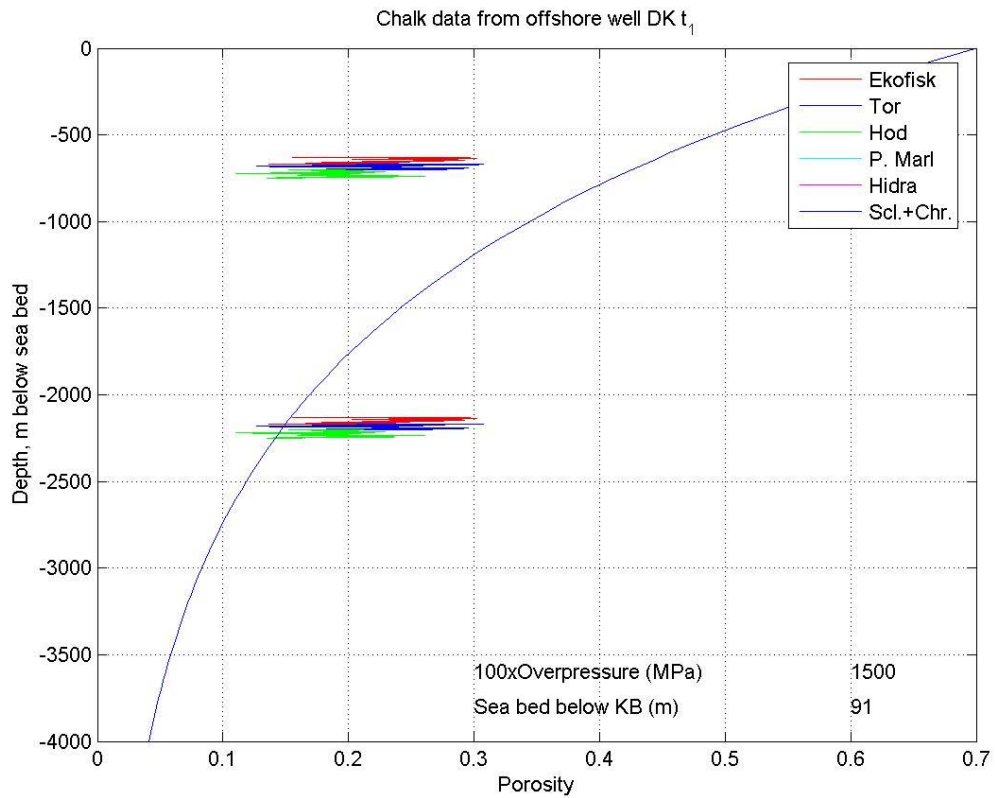
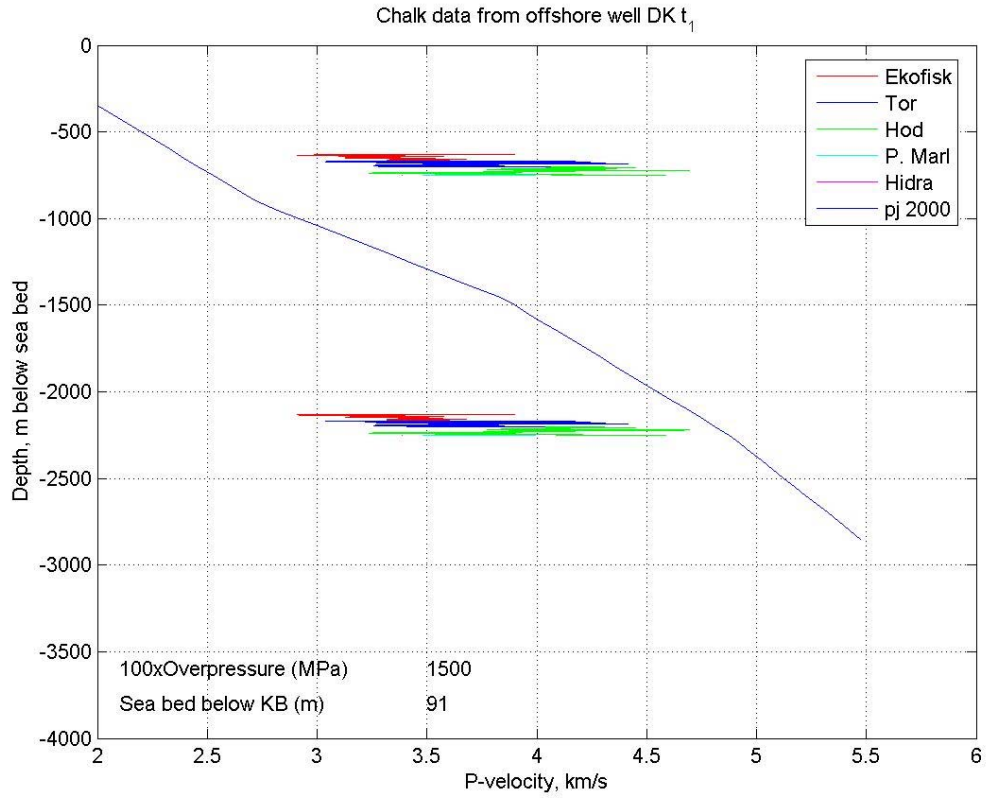
Skjold Flank-1



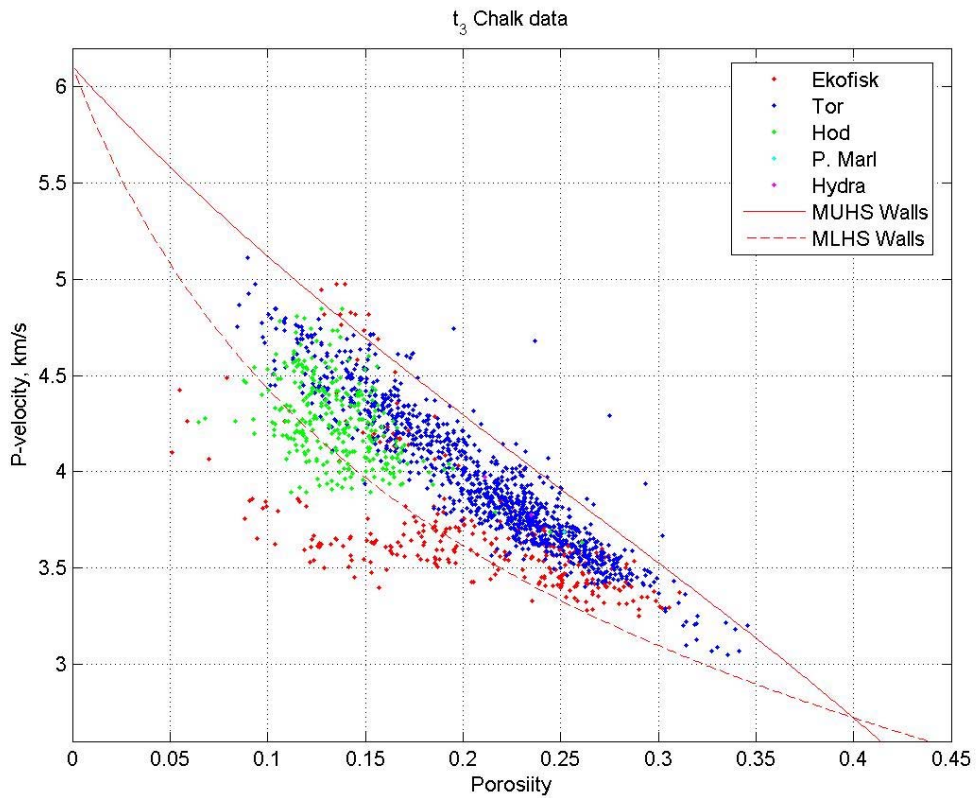
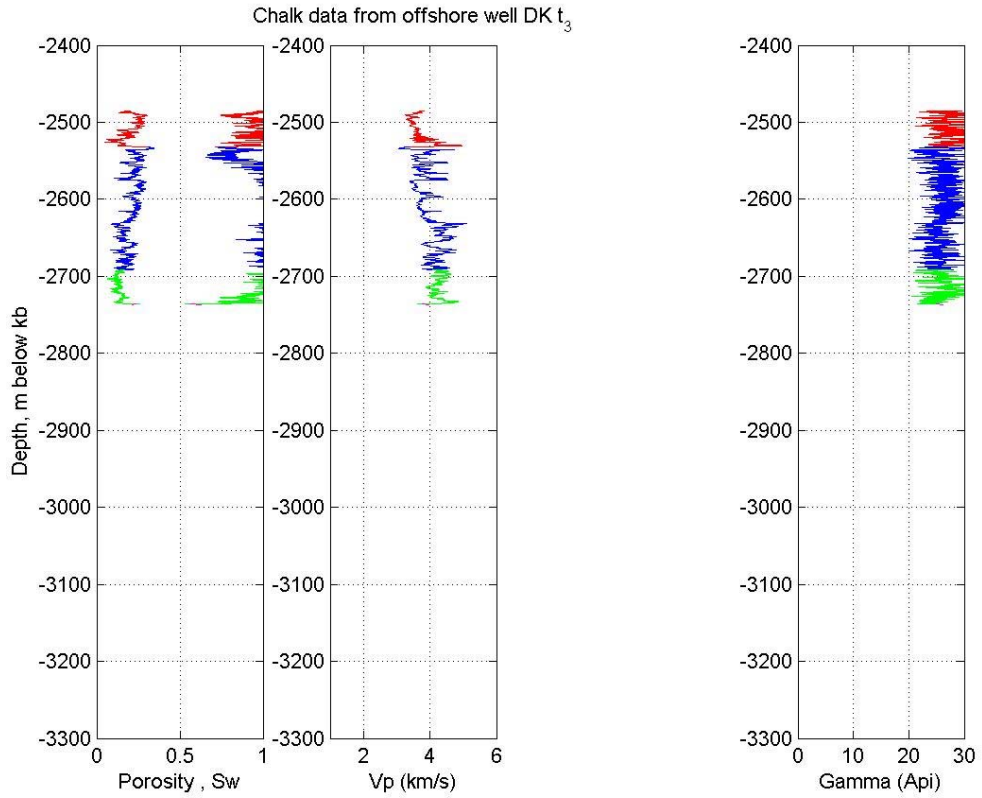
Skjold Flank-1



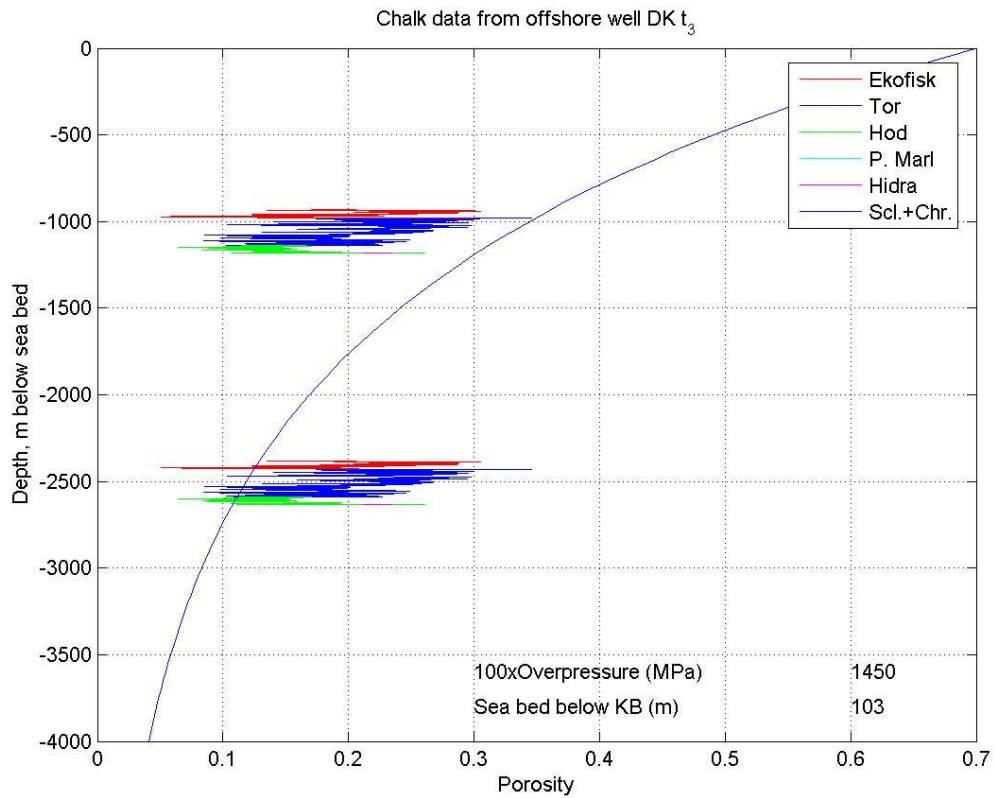
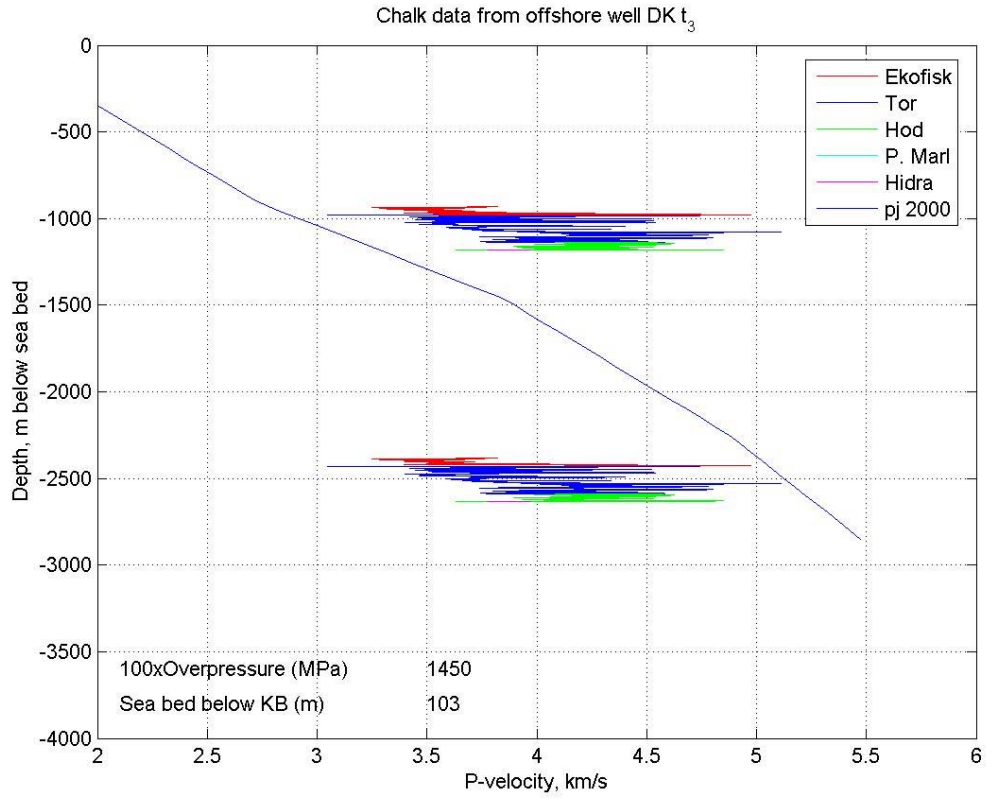
T-1



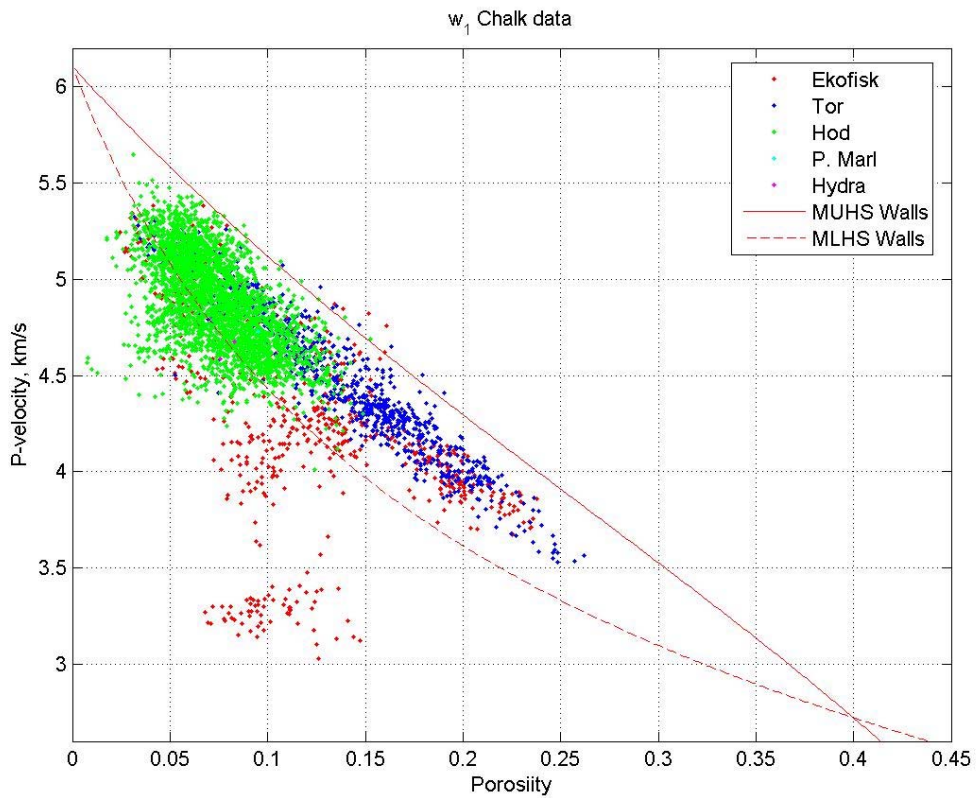
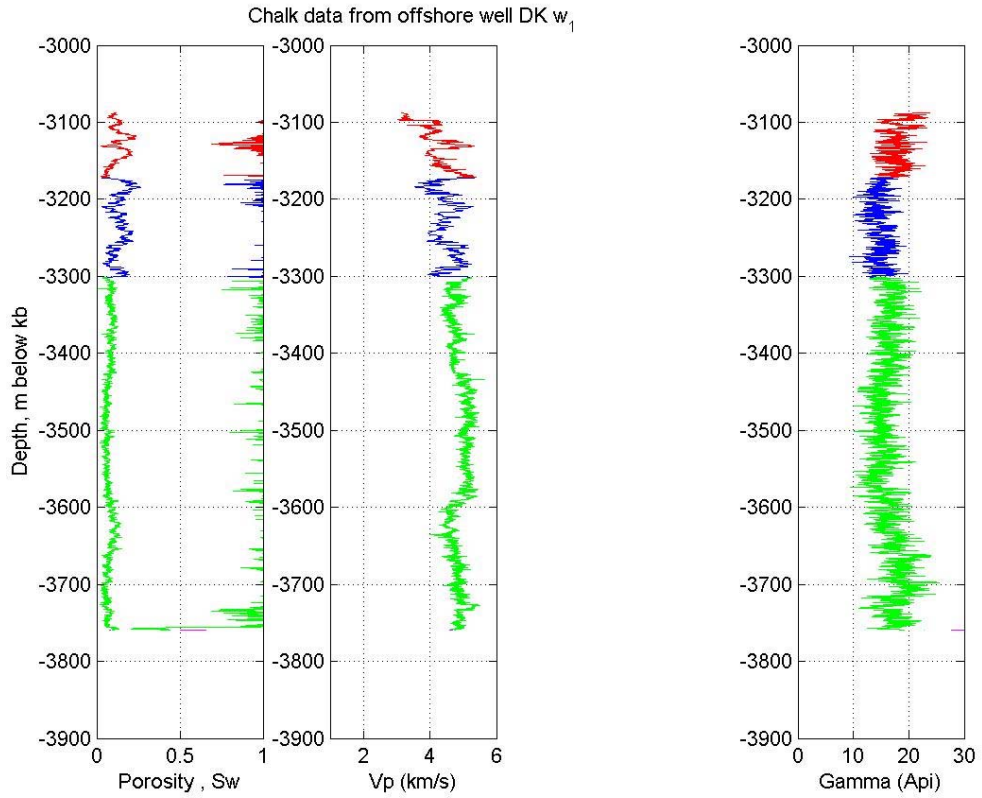
T-1



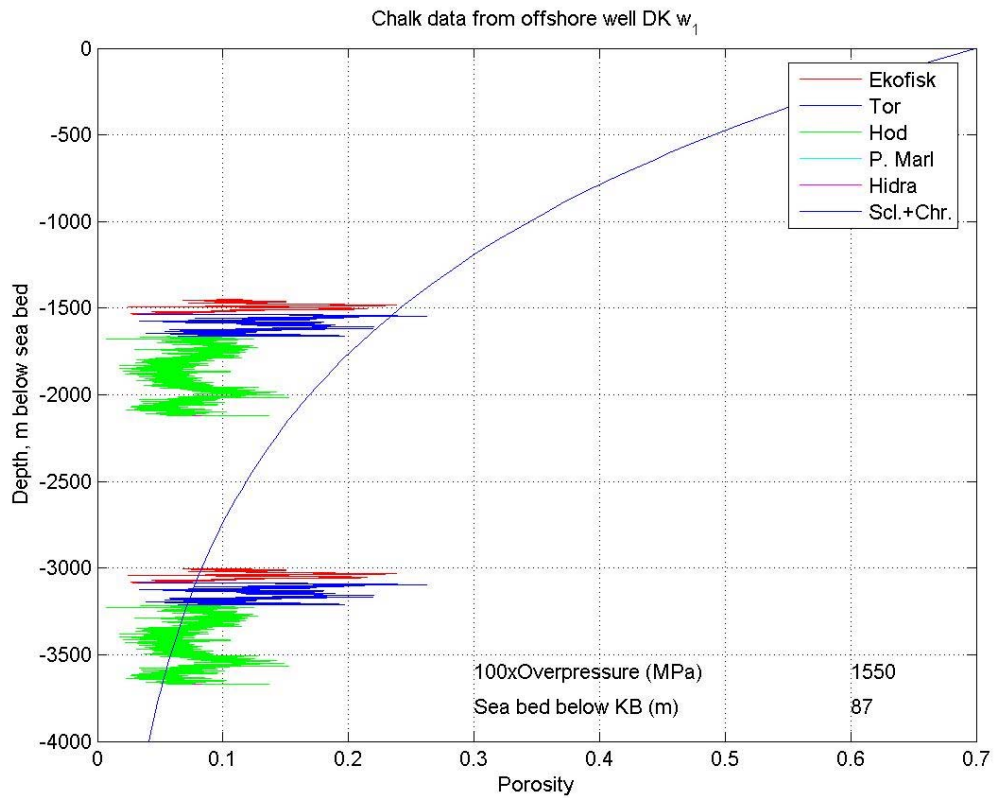
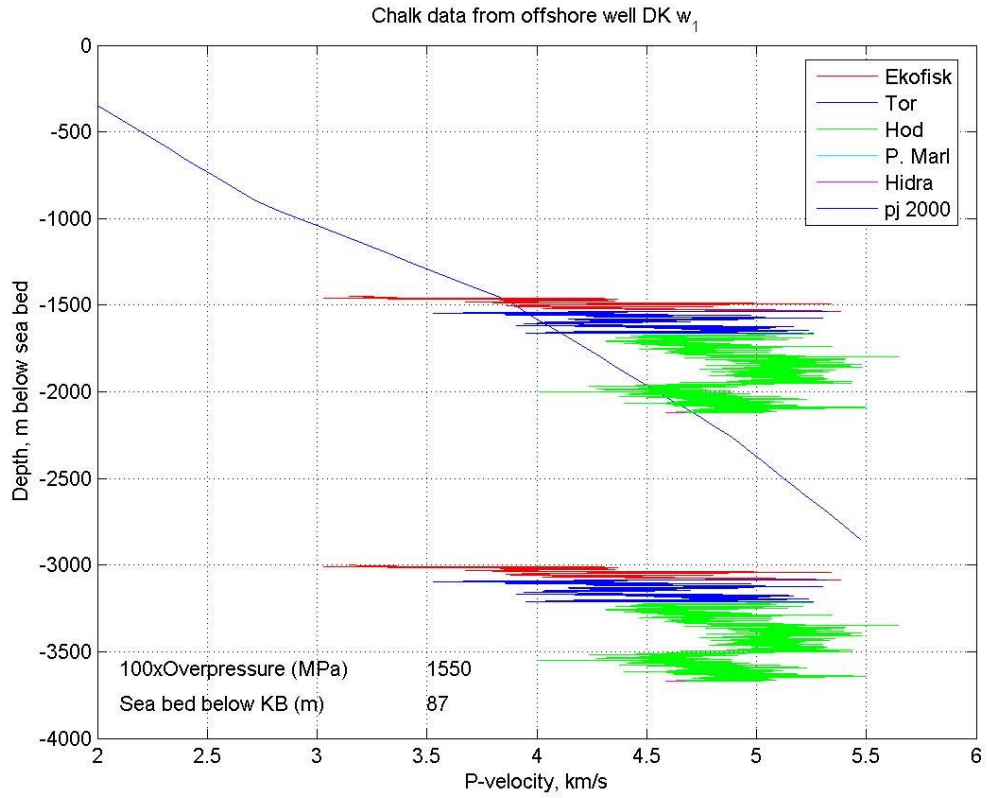
T-3



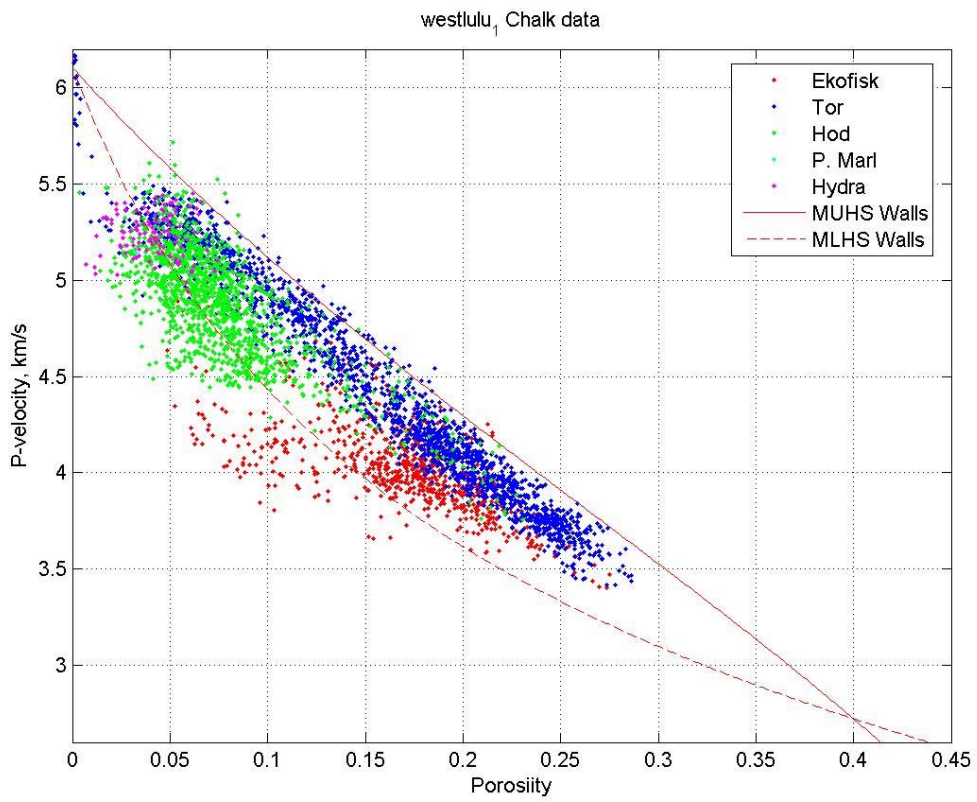
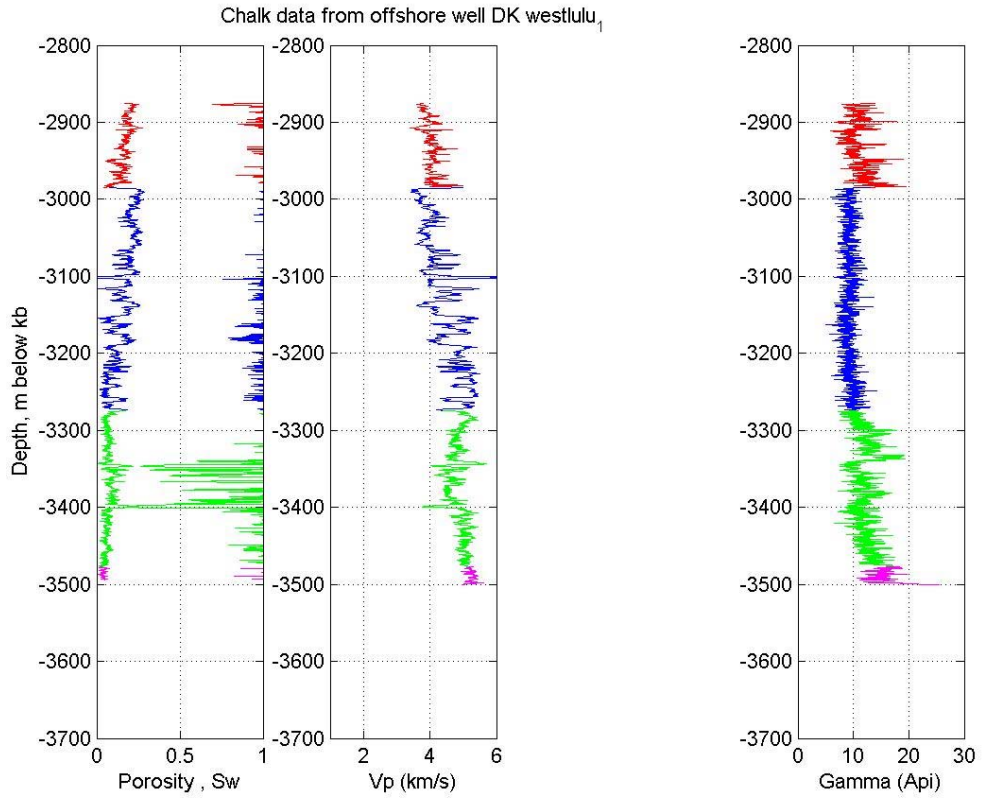
T-3



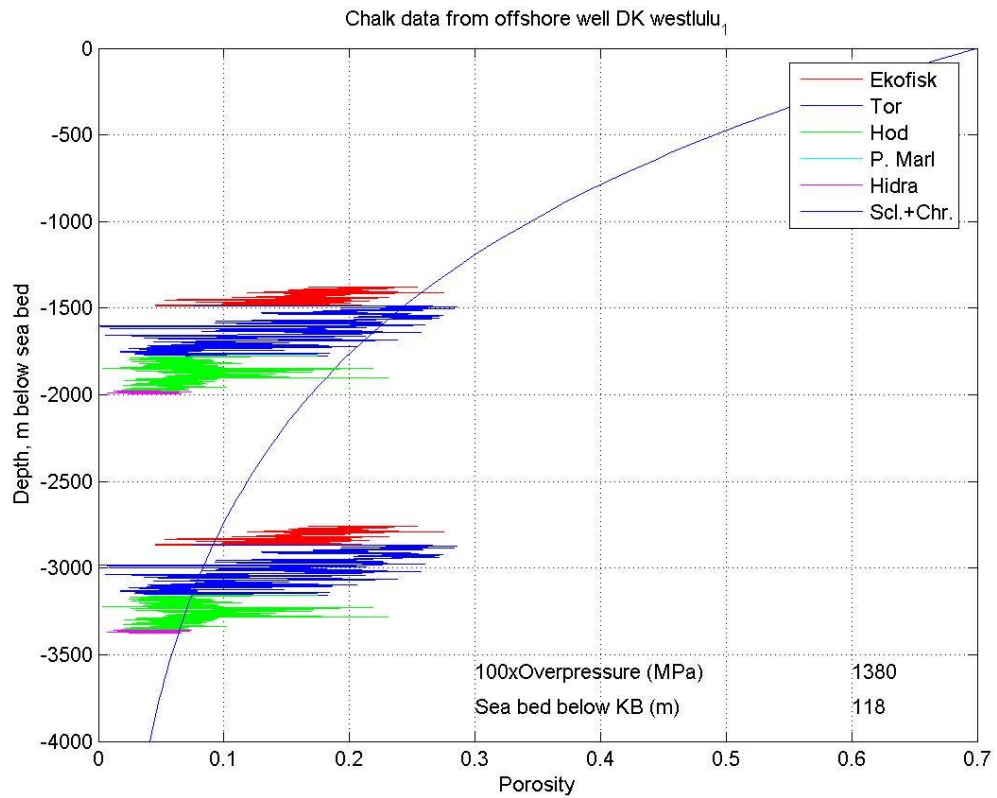
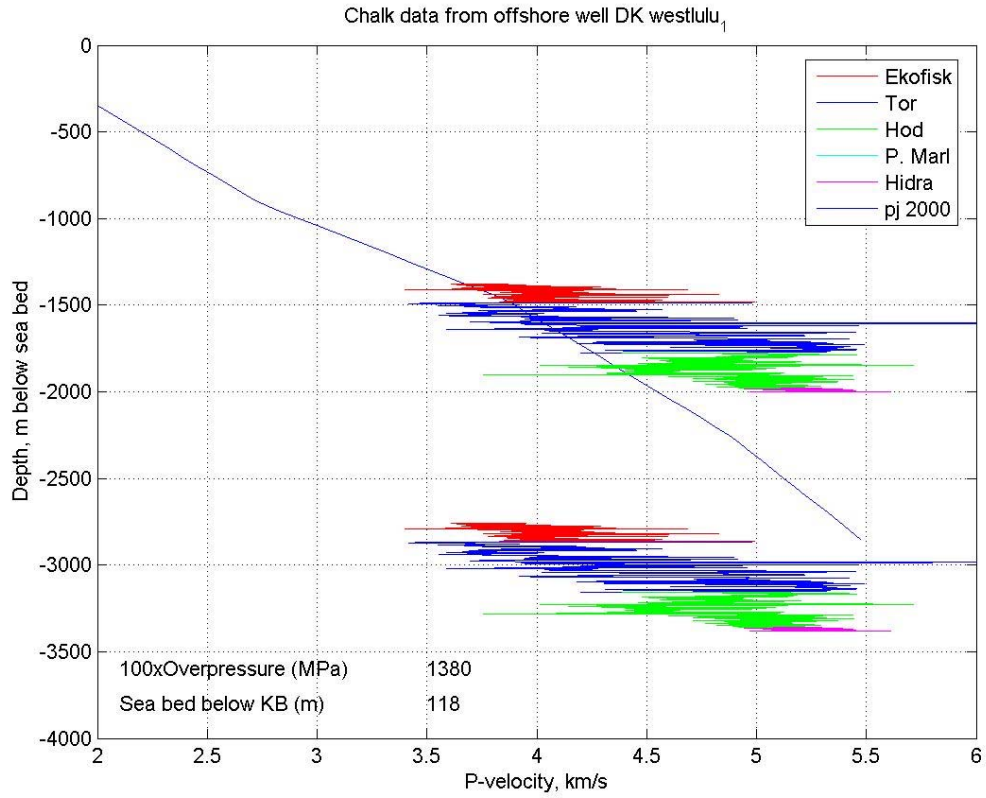
W-1



W-1

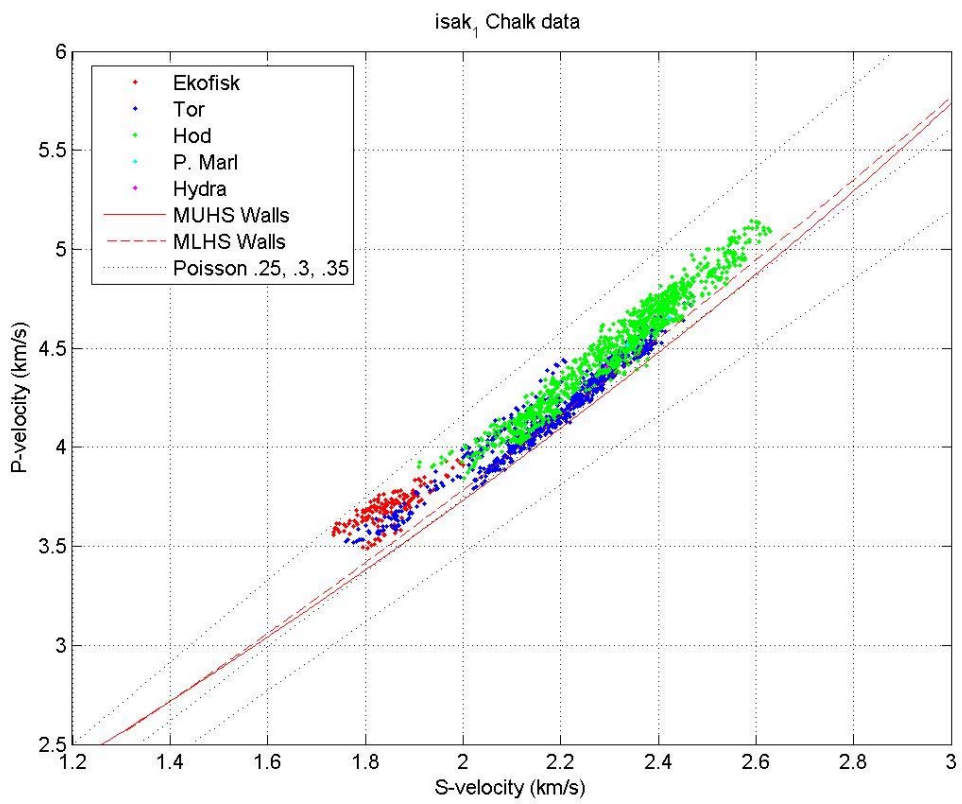
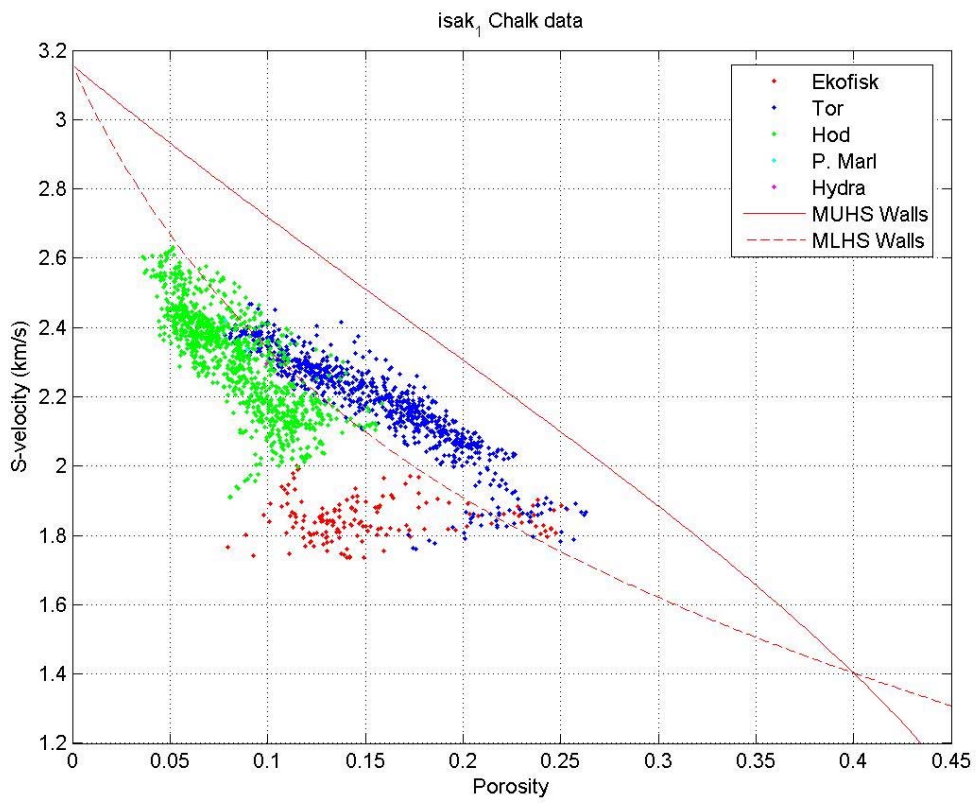


West Lulu-1

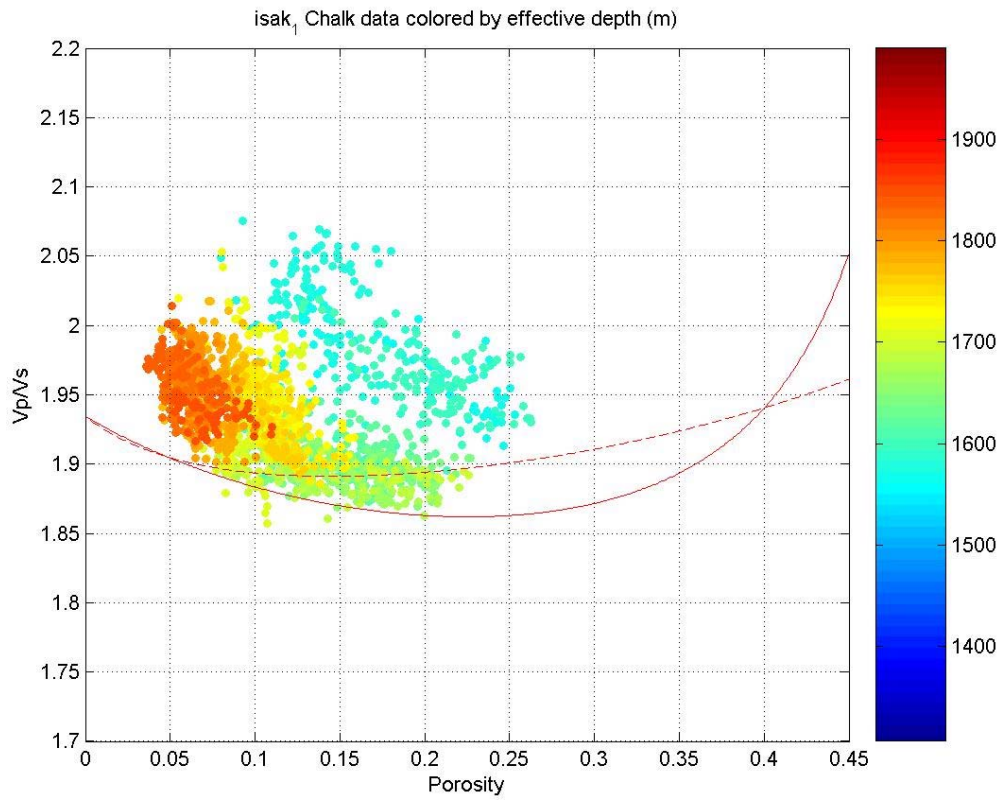
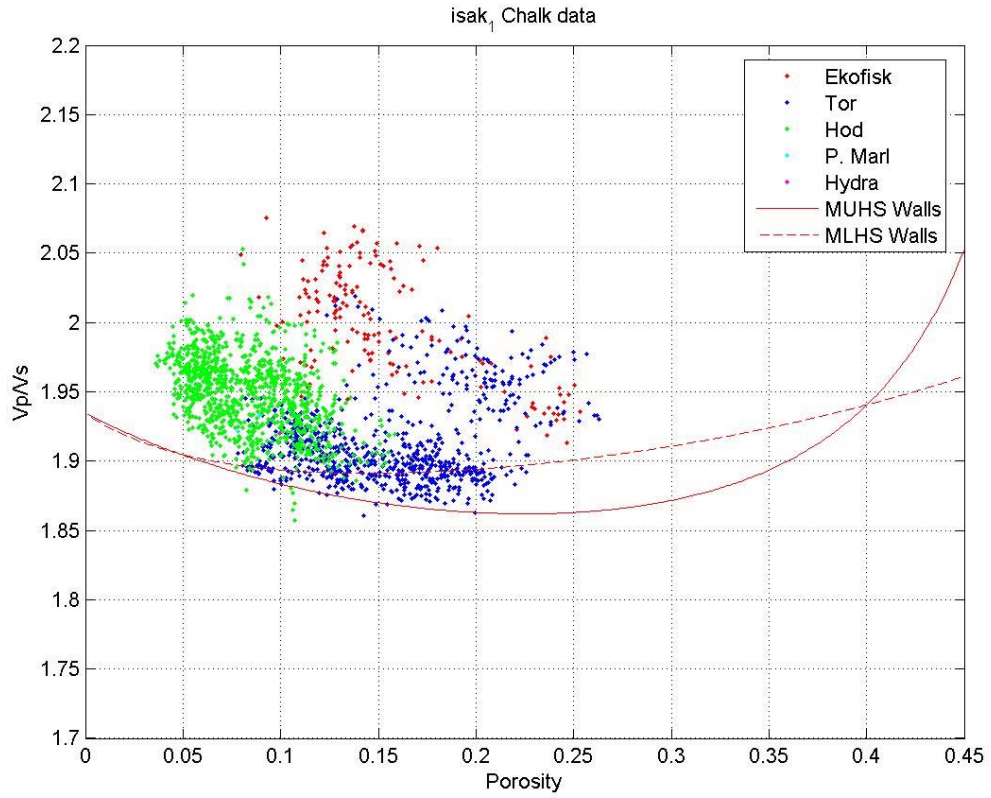


West Lulu-1

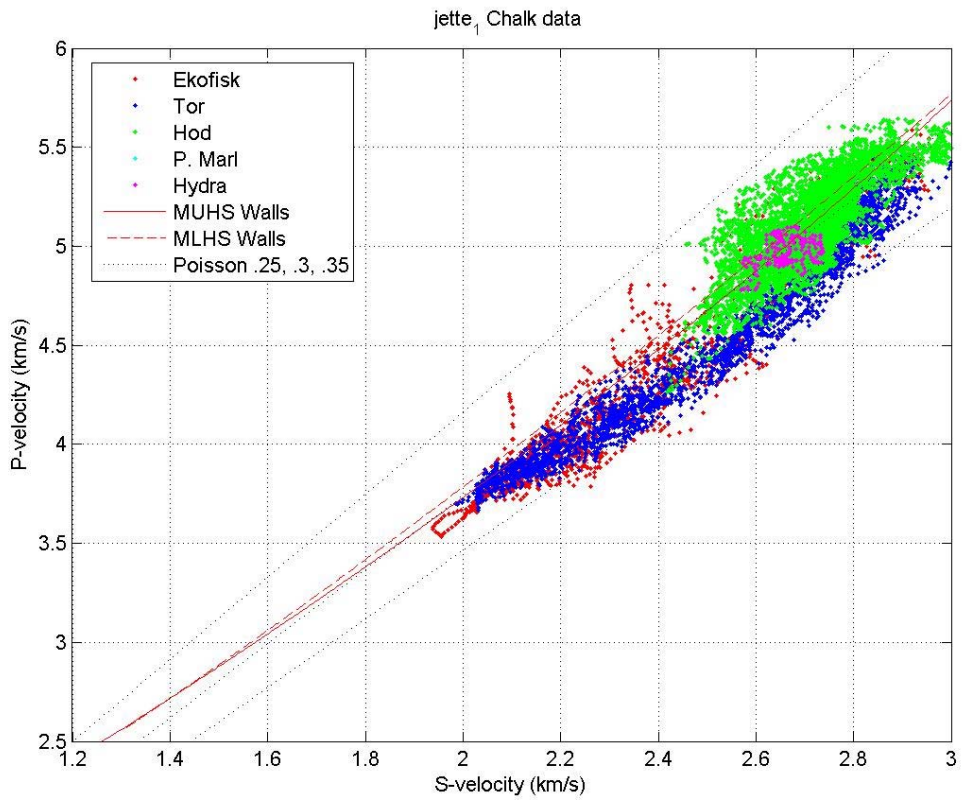
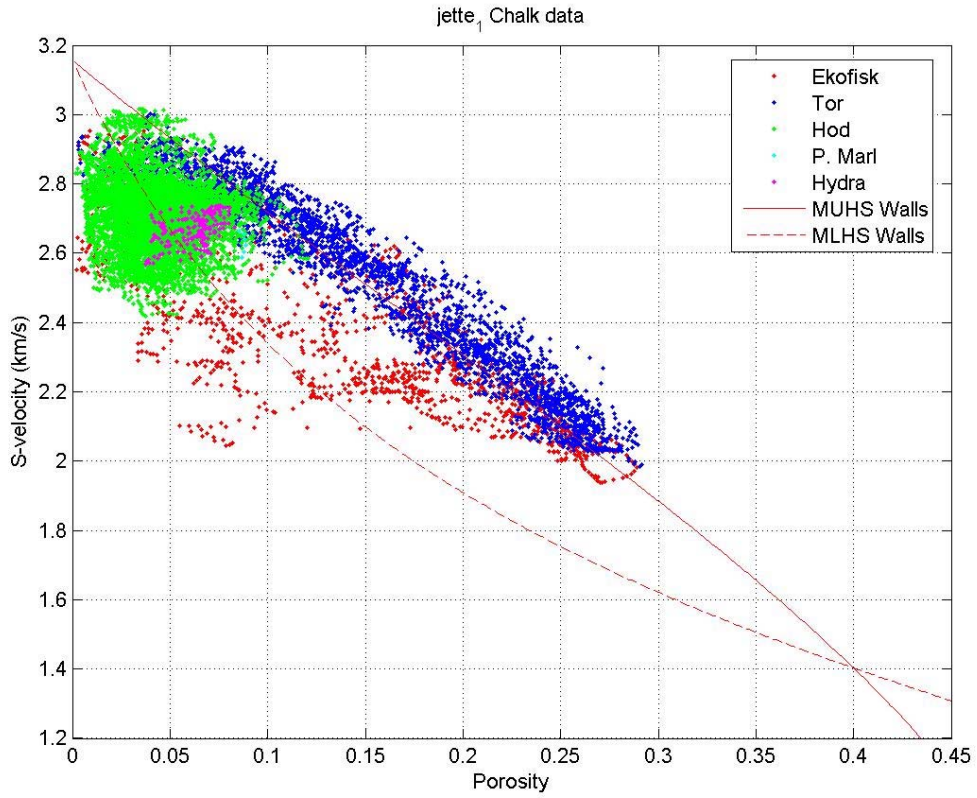
Vp-Vs plots



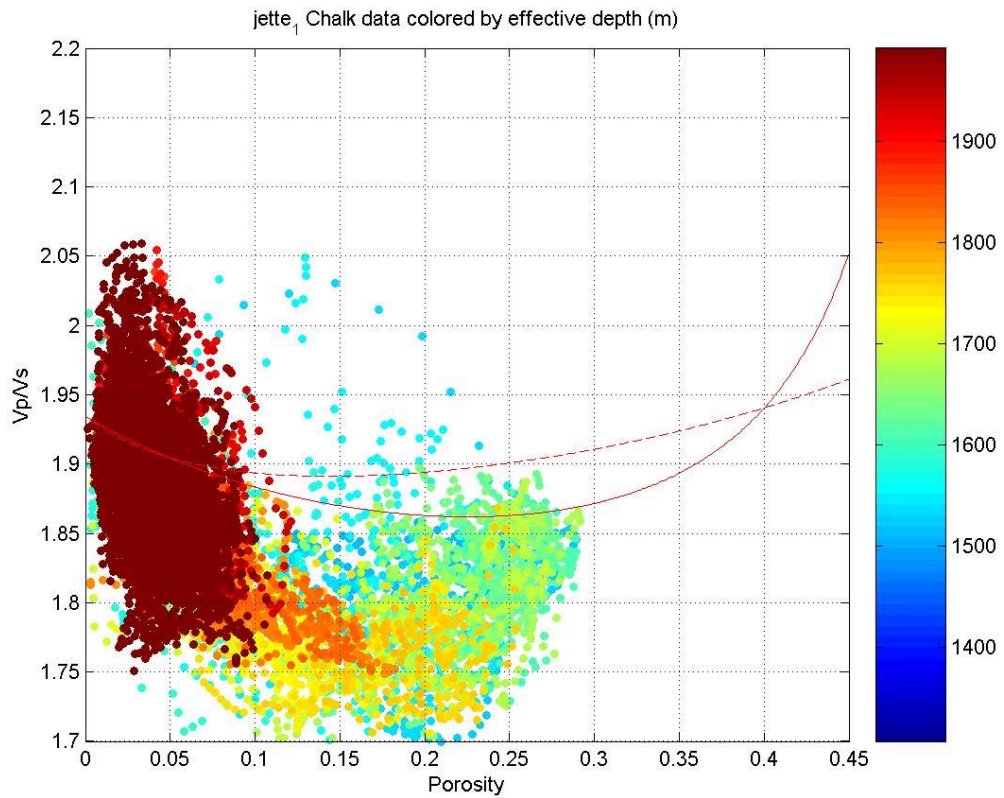
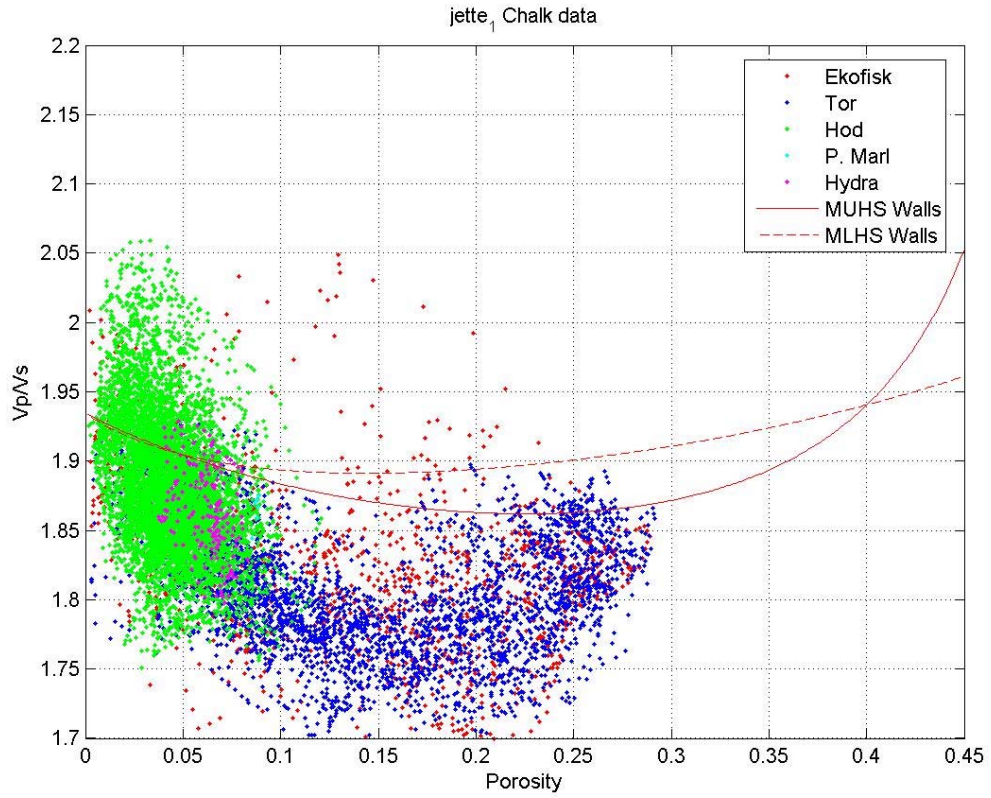
Isak-1



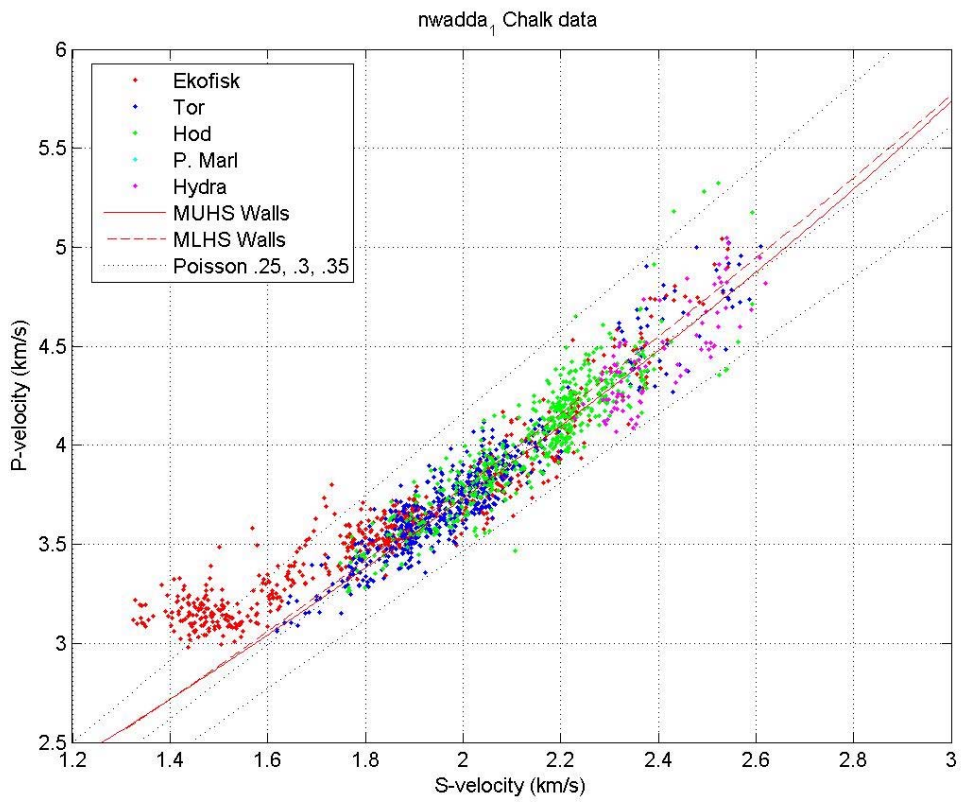
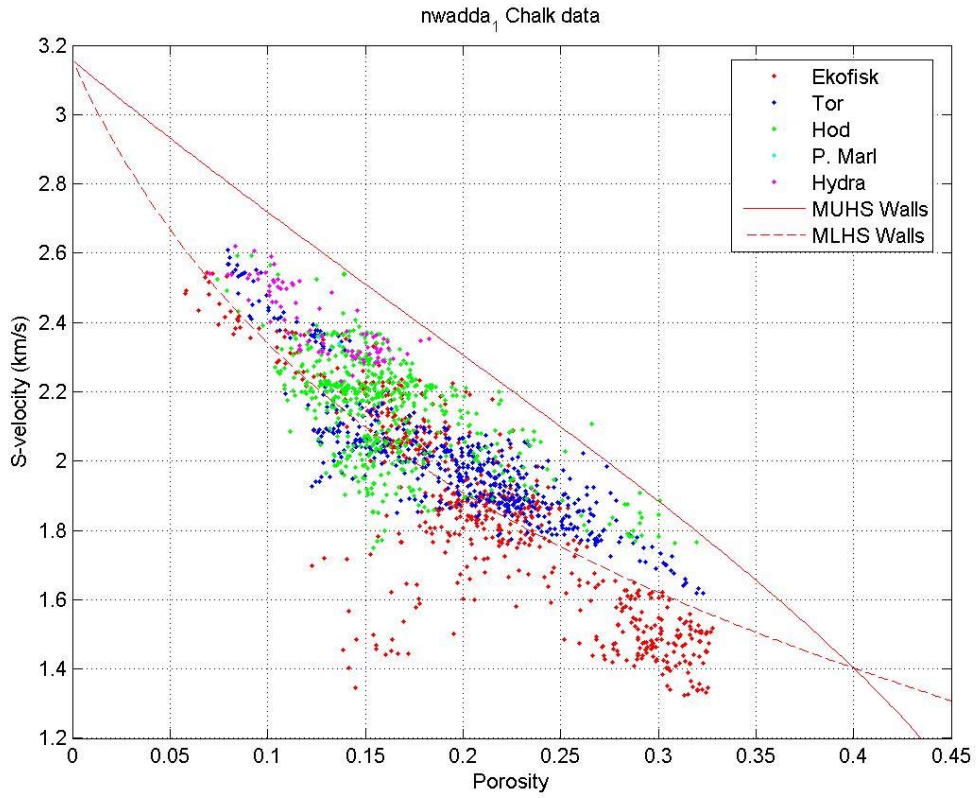
Isak-1



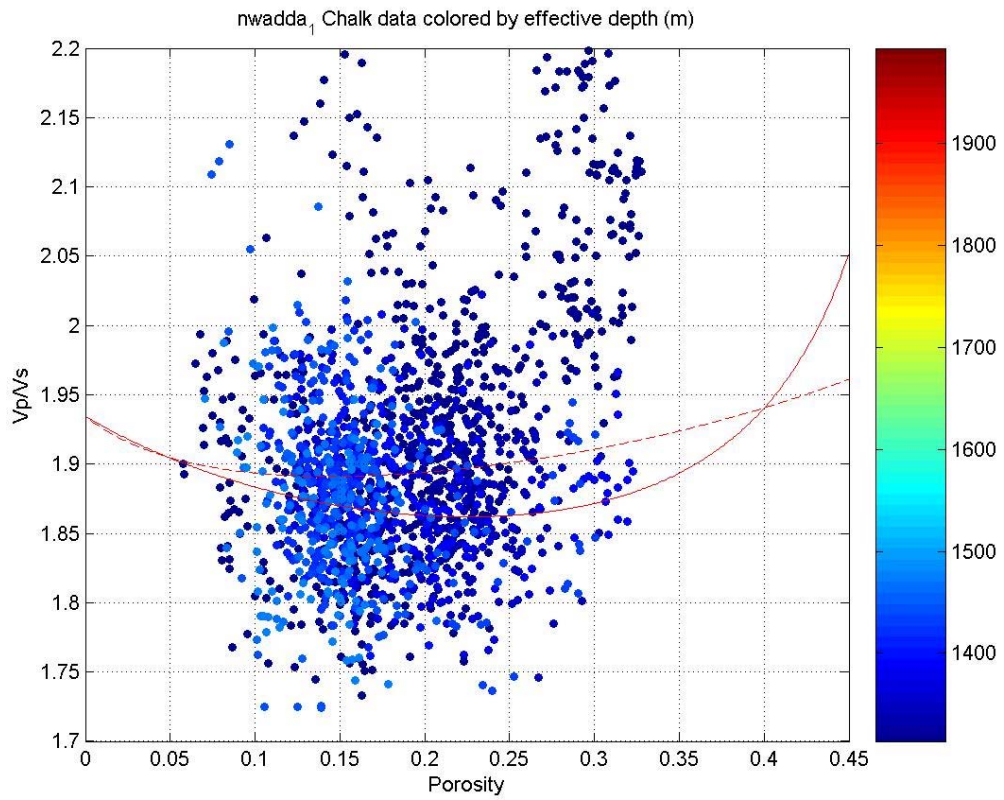
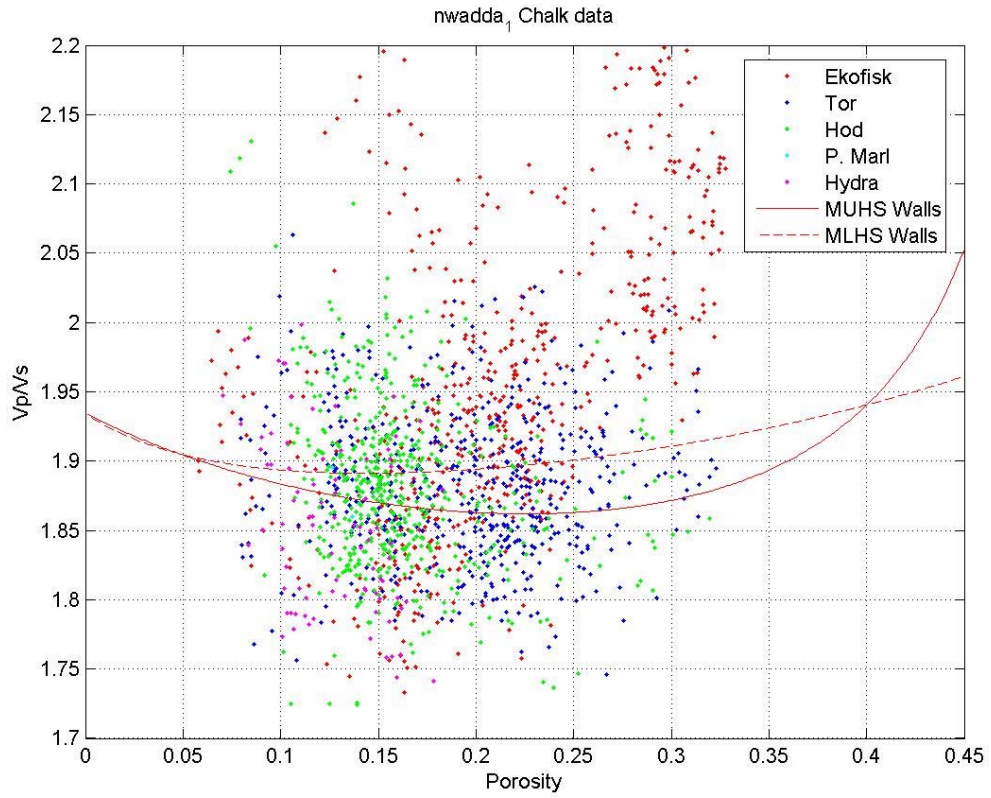
Jette-1



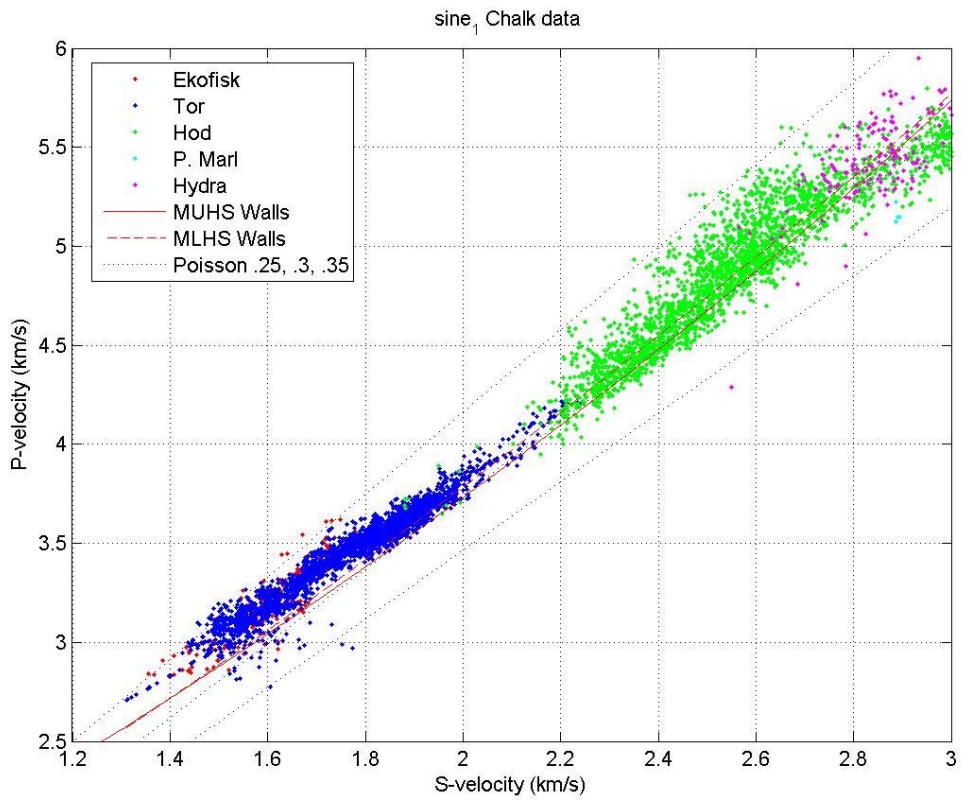
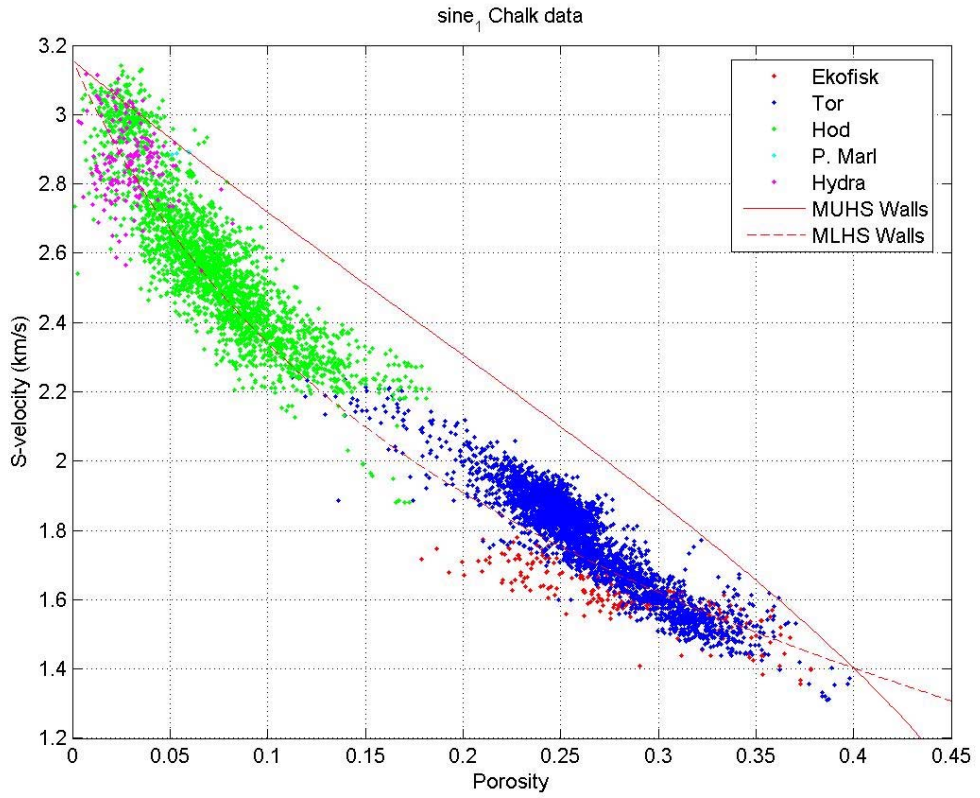
Jette-1



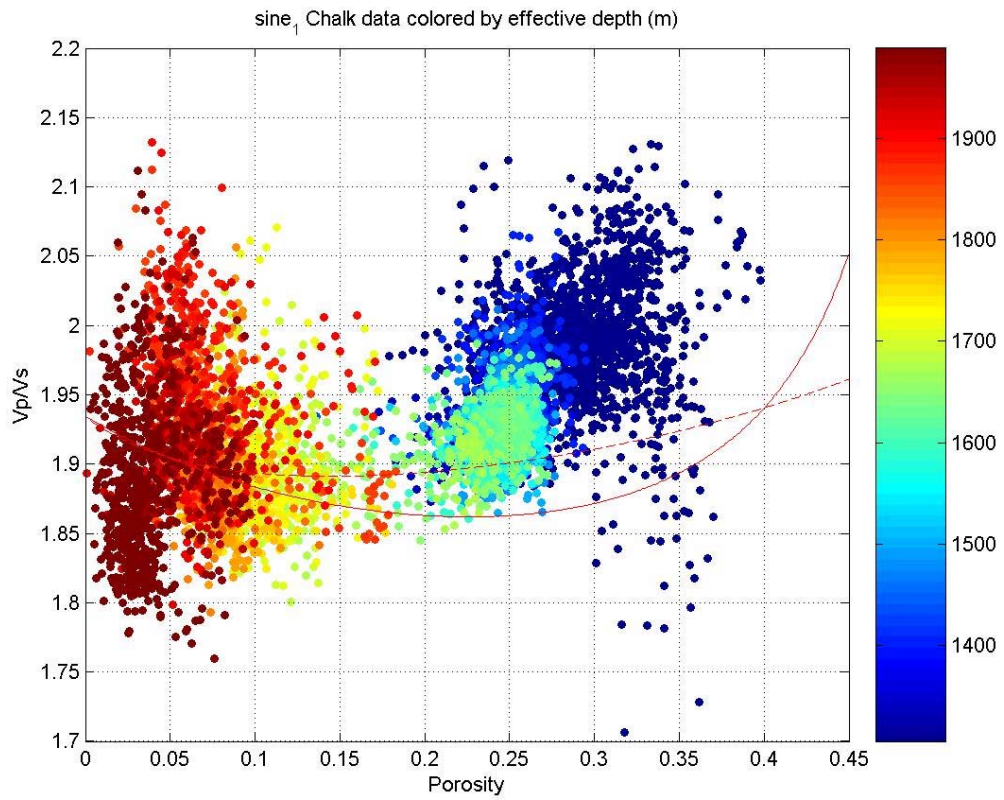
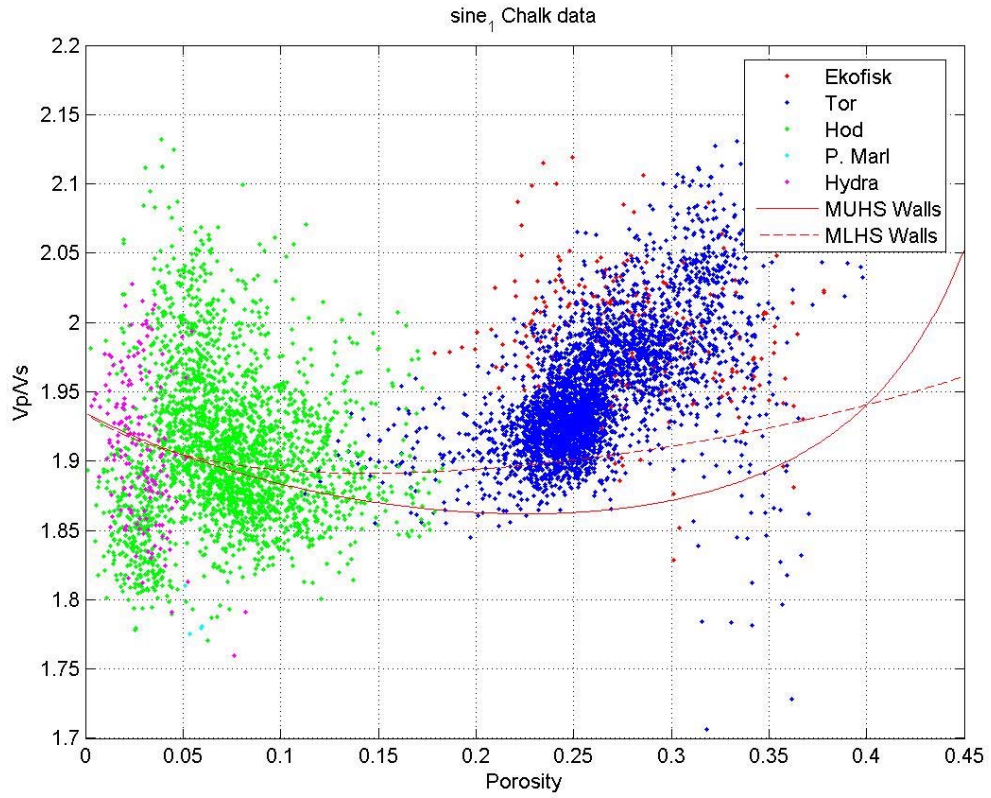
NW Adda-1



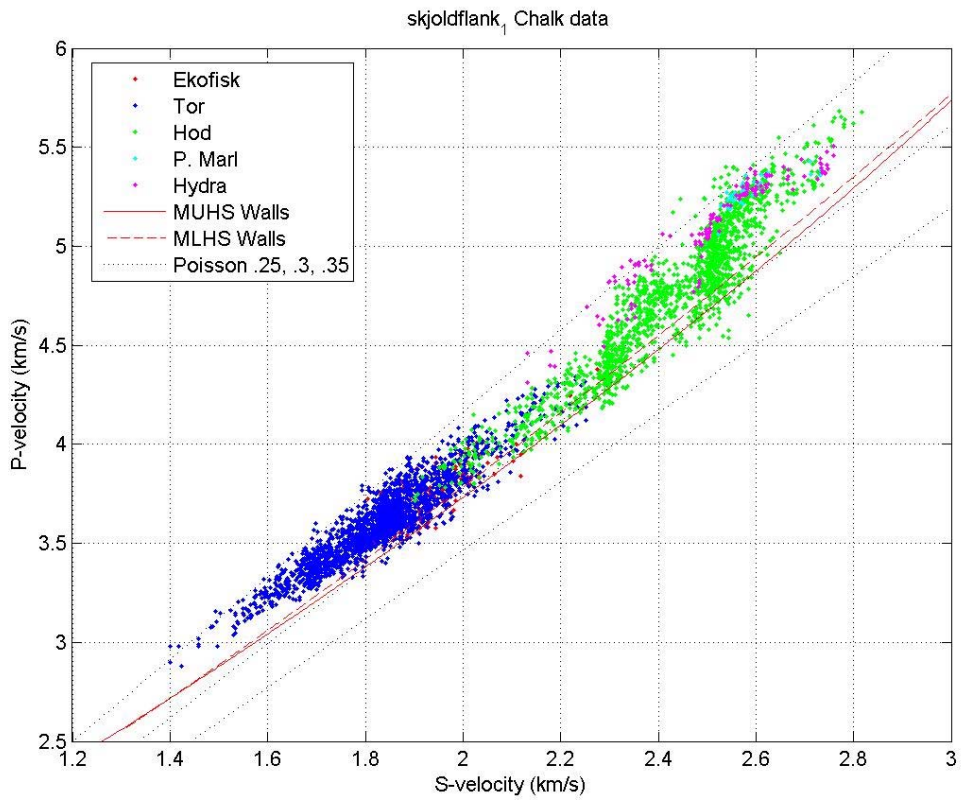
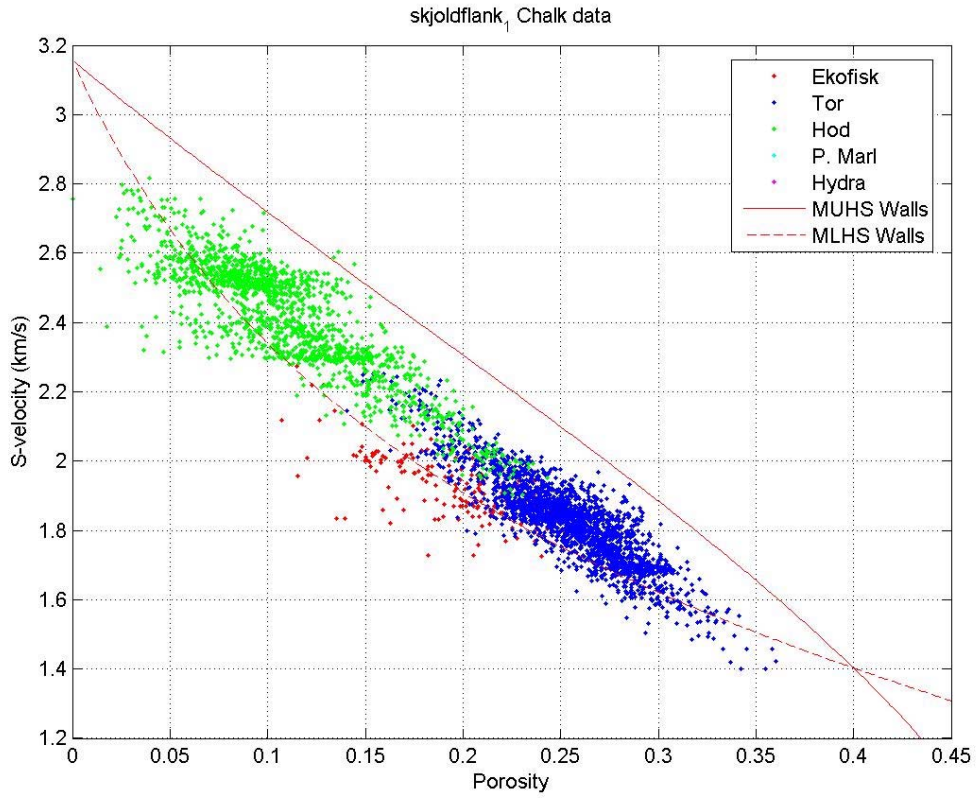
NW Ada-1



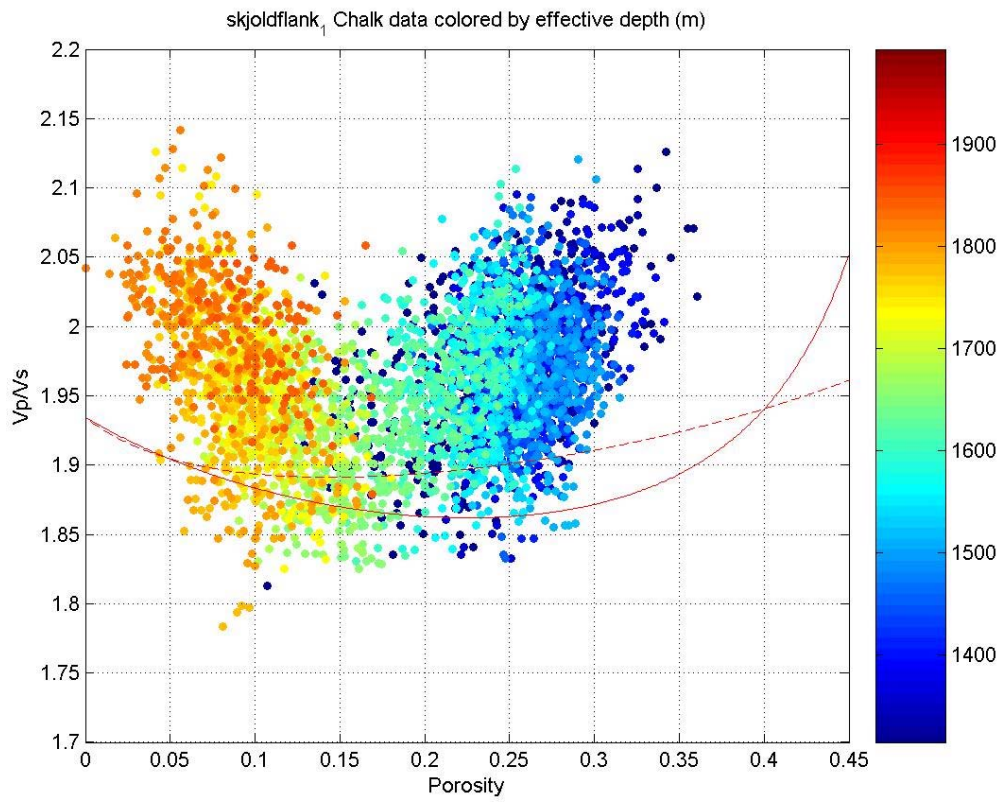
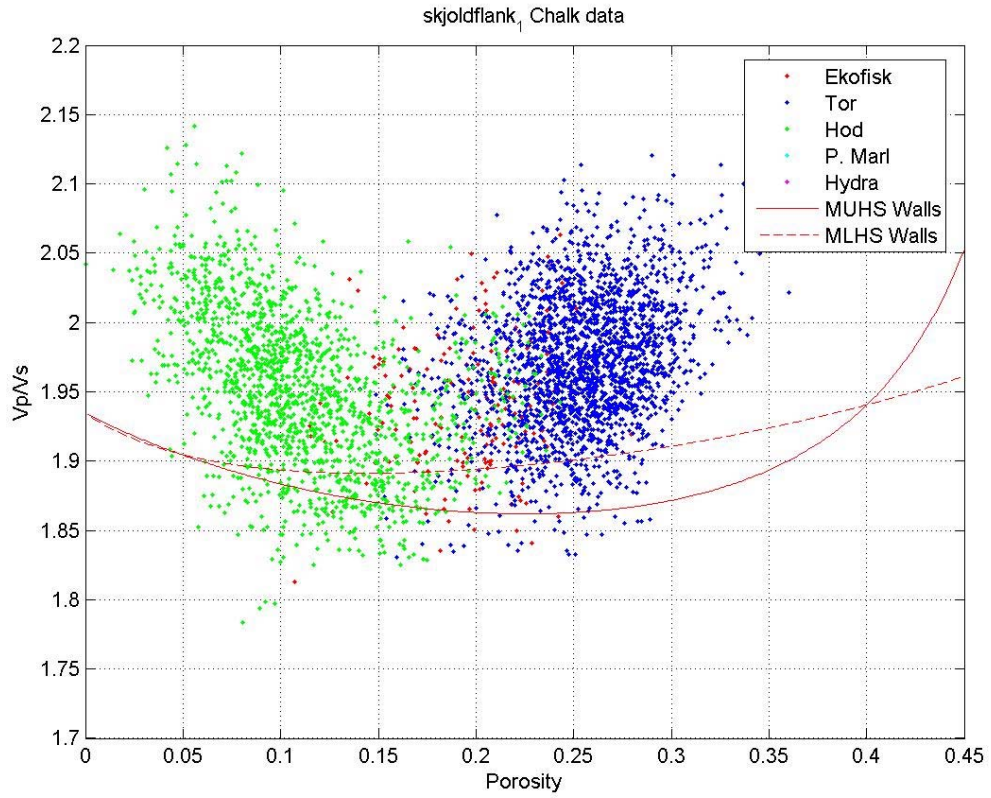
Sine-1



Sine-1



Skjold Flank-1



Skjold Flank-1